Elsevier Editorial System(tm) for Remote Sensing of Environment
Manuscript Draft

Manuscript Number: RSE-D-19-02086R1

Title: EVALUATING THE POTENTIAL OF LiDAR DATA FOR FIRE DAMAGE ASSESSMENT: A RADIATIVE TRANSFER MODEL APPROACH.

Article Type: Research Paper

Keywords: LiDAR, radiative transfer models, full waveform simulation, fire effects, severity, King Fire

Corresponding Author: Dr. Mariano Garcia Alonso, Dr

Corresponding Author's Institution: University of Leicester

First Author: Mariano Garcia Alonso, Dr

Order of Authors: Mariano Garcia Alonso, Dr; Peter North; Alba Viana-Soto; Natasha E Stavros; Jacqueline Rosette; Pilar Martin; Magí Franquesa; Rosario González-Cascón; David Riaño; Javier Becerra; Kaiguang Zhao

Abstract: Providing accurate information on fire effects is critical to understanding post-fire ecological processes and to design appropriate land management strategies. Multispectral imagery from optical passive sensors is commonly used to estimate fire damage, yet this type of data is only sensitive to the effects in the upper canopy. This paper evaluates the sensitivity of full waveform LiDAR data to estimate the severity of wildfires using a 3D radiative transfer model approach. The approach represents the first attempt to evaluate the effect of different fire impacts, i.e. changes in vegetation structure as well as soil and leaf color, on the LiDAR signal. The FLIGHT 3D radiative transfer model was employed to simulate full waveform data for 10 plots representative of Mediterranean ecosystems along with a wide range of post-fire scenarios characterized by different severity levels, as defined by the composite burn index (CBI). A new metric is proposed, the waveform area relative change (WARC), which provides a comprehensive severity assessment considering all strata and accounting for changes in structure and leaf and soil color. It showed a strong correlation with CBI values (Spearman's Rho = 0.9 ± 0.02), outperforming the relative change of LiDAR metrics commonly applied for vegetation modeling, such as the relative height of energy quantiles (Spearman's Rho = 0.56 ± 0.07, for the relative change of RH60, the second strongest correlation). Logarithmic models fitted for each plot based on the WARC yielded very good performance with R2 (± standard deviation) and RMSE (± standard deviation) of 0.8 (± 0.05) and 0.22 (± 0.03), respectively. LiDAR metrics were evaluated over the King Fire, California, U.S., for which pre- and post-fire discrete return airborne LiDAR data were available. Pseudo-waveforms were computed after radiometric normalization of the intensity data. The WARC showed again the strongest correlation with field measures of GeoCBI values (Spearman's Rho = 0.91), closely followed by the relative change of RH40 (Spearman's Rho = 0.89). The logarithmic model fitted using WARC offered an R2 of 0.78 and a RMSE of 0.37. The accurate results obtained for the King Fire, with very different vegetation

characteristics compared to our simulated data, demonstrate the robustness of the new metric proposed and its generalization capabilities to estimate the severity of fires.

Dear Editor,

Thank you for the opportunity you have given us to improve this manuscript. We are also very thankful for the reviewers' time and thoughtful comments as well as for highlighting weaknesses in our previous version. We considered their recommendations very seriously and revised the manuscript accordingly.

Reviewers #3-#5 were highly positive, and following suggestions by reviewer #5, we run new simulations to assess the impact of scan angle on the results. We have made more major changes in response to Reviewer #2. This reviewer was mainly concerned about the degree to which the new proposed metric WARC improved compared to other metrics over the King Fire, and to clarify the degree of novelty and implications for practical application. We have strengthen the evaluation of the metrics. As suggested by the reviewer, we have also compared WARC to a recently proposed metric (PAC) to estimate fire severity from discrete return, which demonstrated the superiority of WARC over this metric too. Comparison of WARC with PAC was only possible for the King Fire case study since the latter metric can only by computed from discrete return data. We have also highlighted the interest and novelty of the work; the interest of simulating LVIS data or the sensitivity of LiDAR to changes in color; which were some of the reviewer's concerns.

We have now discussed the limitations of using the King Fire case study, a concern also raised by other reviewers. Despite not being an ideal dataset, the availability of pre- and post-fire data along with concomitant GeoCBI measures, makes it a very unique dataset to assess the potential of LiDAR to estimate severity of fires and an opportunity to show the possibility of applying the method to not only full waveform data but to discrete return data as well.

We hope we have made the necessary amendments to the manuscript and addressed all questions of the reviewers to make it suitable for publication.

Next, we provide a detailed answer to the reviewer's comments. Their comments are in black and our answers in blue.

Reviewer #2: Comments on "Evaluating the Potential of Lidar Data for Fire Damage Assessment: A Radiative Transfer Model Approach" by García et al.

General comments

The authors present to using the relative change ratio of waveform area (WARC) from full-waveform lidar data to evaluate the fire severity. The authors first used a radiation transfer model (RTM) method to simulate full-waveform lidar data with different forest conditions and fire severities, and then tested the sensitivity of the proposed WARC index to fire severity compared to other normally used change metrics derived from lidar. The results showed that WARC significantly outperformed other lidar-derived metrics in depicting fire severity. Then, the authors further tested the proposed index by using real-word case, the King fire in Serra Nevada Mountain Range, California, USA. They simulated full-waveform lidar data from the pre- and post-fire discrete lidar data, and found that WARC was still the best index to fire severity, but the superiority was much smaller than other commonly used lidar metrics compared to the previous

experiment using RTM simulated data. Overall, the manuscript is easy to follow, although the writing and organization of the manuscript can be further improved. Moreover, the manuscript has its novelty in methodology, especially that it is one of few studies evaluating fire severity from lidar by both considering intensity (author claimed this as color information) and structure information. However, I have several major concerns from suggesting it being published in RSE in its current form.
First, although the methods presented here is interesting, the topic and novelty of this study might not be enough to be published in RSE in its current form. The current manuscript is more on the methodology side.

First of all, we would like to thank the reviewer for his/her in depth review of the manuscript and his/her comments and suggestions to improve it. The reviewer was concerned that the novelty of the manuscript lied mainly in its methodological aspect. However, as confirmed by the other reviewers, our research is highly innovative and of high interest for the RSE audience. Below are several examples of the least reasons to justify the value of our work and its relevance to RSE readers:

- Although we had outlined the timeliness of the research in our previous version, we have now emphasized relevance of the topic in lines 60-66 of the new version (lines refer to the tracked changes version):
    - “Fire managers require information on fire effects to support strategic planning before and during fires, to establish mitigation strategies aimed at reducing soil erosion, establishment of invasive species, as well as to evaluate the results of prescribed fires {Morgan, 2014 #26}. Therefore, accurately quantifying fire effects is necessary to improve our understanding of the impact of fires on ecosystem processes as well as the carbon cycle. This becomes especially important as with projected climate change an increase in forest fires is expected (Stephens et al. 2013).”
- We are not aware of any other papers published evaluating the potential of large footprint full waveform LiDAR to assess severity of fires. On top of this, we tested the novel metric on simulated data and validated our approach over real data.
- As we remarked in lines 474-475, the novelty of this work relies on using a radiative transfer model (RTM) approach to appraise the potential of LiDAR data for evaluating the impact of fires. The use of RTM allowed us to better understand factors affecting the recorded signal. This is relevant because we took into account not only the structural changes, as usually evaluated with LiDAR data, but also the impact of the proportion of foliage altered (change in color) on the LiDAR signal (intensity). We were able to simulate a wide range of scenarios impossible to capture in a single fire (e.g. the King Fire) and so, to analyze the sensitivity of different LiDAR metrics. Speaking differently, the use of LiDAR for environmental applications have been dominated by the use of empirical methods. There has long been a rising call from the communities to see more physics-based investigation of LiDAR applications. In this regard, our work adds positively to this direction.

- We proposed a new metric to quantify fire damage that was sensitive not only to structural changes but to fire induced tree mortality (scorched trees), which result in radiometric changes in the remotely sensed (LiDAR) signal and that we described as changes in leaf color following the CBI methodology. Moreover, the consistency of the metric under different scenarios, simulated and real, suggest the potential of broad applicability of the metric. We have highlighted this point in the discussion (lines 563-564, tracked changes version): "The WARC consistency for both, the simulated data as well as the King Fire case study, indicate the potential for the broad applicability of this metric."
- The availability of pre- and post-fire LiDAR data with concomitant field GeoCBI estimates for a real case study is also a unique aspect of this work. Previous studies having field-CBI values only had available post-fire LiDAR data (Montealegre et al., 2015) or only related height changes to a modified version of the CBI in a sagebrush ecosystem (Wang and Glenn, 2009). Furthermore, we estimated CBI values (0-3) whereas previous works just attempted to classify severity levels into broad classes (low-high). We stated this in lines 500-506:
    - "Montealegre et al. (2014) found good correlation between field measured CBI values and a set of post-fire LiDAR metrics, which were used to classify burn severity levels. Despite reporting a global accuracy of 85.5%, their results are not comparable to ours since they did not estimate CBI, but classified severity levels into three broad classes. Likewise, Wang and Glenn (2009) classified burn severity levels in sagebrush steppe rangelands based on vegetation height changes obtaining a global accuracy of 84%."
- Whereas previous studies using LiDAR just focused on the structural changes caused by fires in vegetation, we have demonstrated that LiDAR can also be sensitive to changes induced by fire heat (scorched vegetation) that result in radiometric changes.
- Our approach to compute the severity from LiDAR, based on a stratified change of the waveform, resembles the way CBI is computed in the field. We state this point in lines 494-496. "In addition to accounting for the changes in structure and leaf and soil color, the WARC considered all plot strata, computing the changes from the substrate to the upper canopy and averaging at the plot level, in the same way the CBI does."
- We would also like to make a clarification about the use of color information. We did not claim color as intensity. Change in color is the variable assessed in the field when measuring severity using the CBI. This change in color results in radiometric changes that in turn, changes the energy reflected off the target (intensity). We included the following clarification in the paper (lines 219-221):
    - "On the other hand, variation in color of scorched leaves results in changes in the spectral reflectance, affecting the returned LiDAR signal."

If the authors can further dig deeper on how the proposed method may benefit the scientists and managers on study fire behaviors and managing wildfires, it may make the manuscript have much broader impact.

Thanks for the suggestion. We have included additional sentences to highlight how the method can improve forest and fire management activities in lines 60-66 (see our previous comment).

Second, I have concerns on why the authors used simulated full-waveform lidar data to present the superiority of the proposed algorithm. Currently, the evaluation results in King Fire regime showed that the proposed WARC metric is not better (the improvement in R is very small) compared to other commonly used ldiar metrics, which is very concerning.

We think that the reviewer is missing a paramount point of the manuscript. The main advantage of using 3D RTMs is that they allow to evaluate the individual impact of instrument/survey characteristics (beam divergence, flying height, sampling density, etc) and environmental conditions (e.g. canopy structure, composition) on the LiDAR signal (e.g. Gastellou et al., 2016; Disney et al. 2010), by varying them within a wide range of values defining different survey configurations and vegetation scenarios. In our study, we were just interested in modifying the environmental conditions to represent different degrees of severity. This can help improving our understanding of the interactions between the LiDAR signal and the vegetation before and after the fire. The main objective of our manuscript was to assess the potential of LiDAR data for providing a comprehensive characterization of burn severity, beyond structural changes, considering all layers of a forest (page 6, lines 135-137 of the original submission). Furthermore, because the RTM allows to create what some authors called “virtual laboratories” (e.g. Disney et al., 2011), RTM approaches allow creating a broader range of scenarios than can be tested on a real case, thus offering better generalization than empirical approaches. We opted for simulating full waveform data because these data provide better description of the vertical vegetation volume distribution, from the top of the canopy to the ground, including the crown volume and understory layer, than discrete return data (Lim et al., 2003; Means et al., 1999), which do not sense the full vertical distribution of vegetation. This is very important to provide comprehensive analysis of the severity of fires as we need to evaluate the ecological change through different vegetation strata. To outline this point, we added the following sentence (lines 154-158): “Evaluation of fire effects requires analyzing changes over different strata, from the substrate to the upper canopy. Large footprint full waveform data provide better description of the vertical vegetation volume distribution, from the top of the canopy to the ground, including the understory layer, than discrete return data {Lim, 2003 #76}, thus making it ideal to evaluate severity of fires.”

Regarding the King Fire, it should be noted that it represents a rather unique case, where pre-, post- fire and concomitant field measures of GeoCBI were available; a common difficulty in estimating severity of fires from LiDAR data. Nevertheless, it just represents a particular example or more specifically, a narrow set of the simulated scenarios, not covering by far most of the simulated scenarios. Therefore, the RTM is the right approach to evaluate the superiority of the WARC metric as compared to other structural metrics. Moreover, the fact that WARC also outperformed other metrics in the King Fire case study, even if only slightly, just confirms the simulation results. Another aspect the reviewer missed to acknowledge is the consistency of the WARC metric, which offered the best results for our simulations and for the King Fire case study.

At least, the authors should present more detailed examples (waveform curves) from the real airborne lidar data to discuss the methodology.

We include now some examples of pseudo-waveforms and the point clouds of several plots with different GeoCBI levels. They have been included in the supporting information since from our point of view figure 3 shows our point on the impact of different fire effects on the LiDAR signal. We added the following sentence to the new version of the manuscript (lines 439-442):

"Pseudo-waveforms generated from discrete return intensity data also showed ability to discriminate different degrees of severity (Fig. S6-S9, supporting information). Nevertheless, the sensitivity analysis of the LiDAR metrics to the burn severity of the King Fire showed important differences with our previous simulations (Fig. 6)."

From the current results, I am not convinced that WARC is a better choice all the time, especially considering the fact that WARC needs full-waveform information, which is not available all the time (or needs more processing steps to be derived than common lidar metrics).

We disagree with the reviewer and to a lesser degree, we are puzzled by what the reviewer meant by "all the time", especially because the criticism was targeted at the use of full-waveform information to derive WARC—that is exactly what we propose to address. To explain further, first, our results showed that WARC offers better performance and much more consistency than other metrics (Fig. 4 & 6). Although it is a full waveform metric it can also be derived from discrete return data after creating the pseudo-waveforms as we demonstrated for the King Fire. The fact that it requires more processing steps to be derived (a weakness of our approach from the reviewer's point of view) should not be a limitation to apply a method; the few more processing steps are nothing compared to the whole LiDAR data processing flow. Moreover, the generation of pseudo-waveforms from discrete return data is quite common and many examples can be found in the literature (e.g. Popescu and Zhao 2008: Farid et al., 2008; Muss et al., 2011; Luo et al., 2019). In the King Fire case the improvement was small over the best performing metric, but in other cases it would be more significant, as shown by our simulations. It should be noted that the King Fire was a megafire, which produced large changes in structure. The common approach of deriving a set of LiDAR metrics and putting them into a given modeling framework, though simple, may not fully exploit the capabilities of LiDAR data. In addition will require additional steps than fitting a model to a single variable. WARC does a better job on this aspect and provides better generalization. This is now clarified on discussion and conclusion sections (lines 561-564 and lines 631-634):

"Moreover, our approach is based on a single simple metric, increasing its generalization capability, as opposed to previous studies that included multiple metrics. The WARC consistency for both, the simulated data as well as the King Fire case study, indicate the potential for the broad applicability of this metric."

“Application of the WARC metric to the real case study of the King Fire, California, with very different vegetation characteristics of those of our simulated plots, revealed the robustness and generalization capability of this metric. Although improvement over the best performing common LiDAR metrics was small in this case, the WARC still outperformed them.”

Third, the authors themselves mentioned a similar method proposed by Hu et al. (2019) as well, which is very similar to the idea of the WARC metric proposed by the authors. In my opinion, the profile area change (PAC) metrics seems to be much simpler metric than WARC, since it can be directly derived from discrete point clouds. It would be interesting to see a more detailed comparison in the manuscript with PAC.

In order to provide a comprehensive comparison between both metrics it would be necessary to compute PAC from our simulated data. This is not possible since PAC cannot be derived from large footprint full waveform data. Nevertheless, we tested the metric over the King Fire and found poorer performance of PAC compared to WARC. We included the results in the new version of the manuscript (lines 565-575): “Recently, Hu et al. (2019) also proposed a single metric to estimate burn severity from LiDAR data. The performance of this metric was evaluated against changes in LAI, canopy cover and tree height, but not against field measures of CBI or GeoCBI. Their metric shows similarities to WARC, as it is based on the change in the area of the height percentile profile (PAC), but their metric is computed from the height distribution of returns and thus only account for changes in structure. Contrary, WARC is derived from the intensity, which is affected by the radiometric changes resulting from the modification in soil and leaf color. A comprehensive comparison between PAC and WARC was not feasible over our simulated scenarios since PAC can only be derived from discrete return data. However, we tested PAC over the King Fire and found poorer performance compared to WARC, with R2= 0.55 and RMSE= 0.53.”

We present here the scatter plot of PAC vs GeoCBI measures for the reviewers’ information, but note that our point is made just including R^2 and RMSE in the paper.

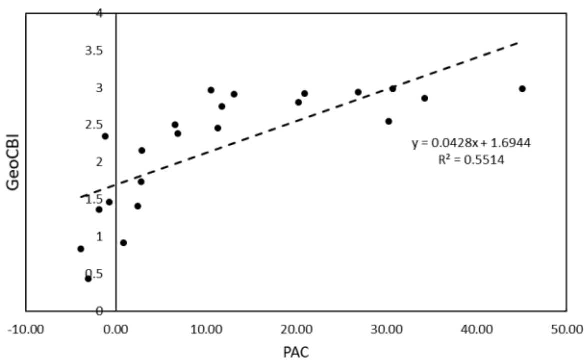

We also present here two examples which can help to understand the limitation of PAC.

Example 1: The GeoCBI value measured in the field was 2.35, representing high severity (low severity: 0.1 to 1.24; moderate severity: 1.25 to 2.24; and high severity: 2.25 to 3.0). GeoCBI measures of the plot showed low LAI reduction but high proportion of foliage altered (scorched trees). As we can see, the structure of the upper canopy remained largely unchanged, with most of structural change happening in the understory layer. We also present the pseudo-waveforms of the plot. The left panel shows the pre-fire point cloud, the central panel the post-fire point cloud, and the right panel the x-axis. The axis has been truncated to better show the change in the returned energy for understory and overstory layers. The PAC value for this plot was 1.2, whereas the WARC value was 0.46.

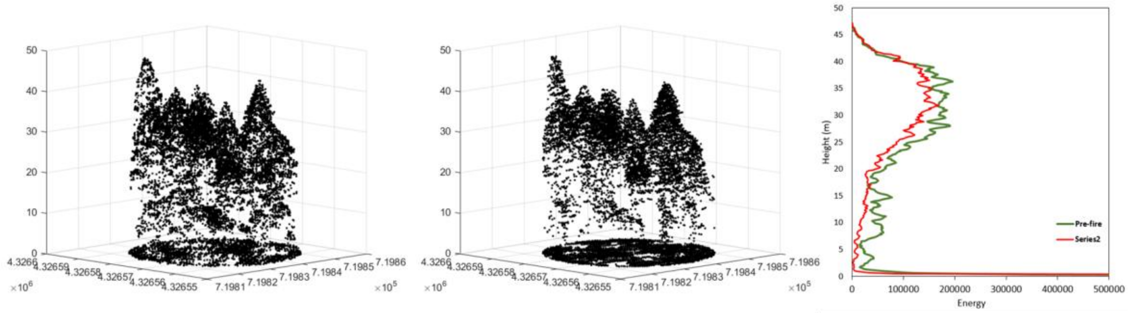

Example 2: The GeoCBI value measured in the field was 2.5, representing high severity. Likewise, according to the field measures, the plot showed low LAI reduction but very high proportion of foliage altered (scorched trees). As we can see, the upper canopy remained largely unchanged, with most of change happening in the understory layer. A much larger proportion of ground returns are observed in the post-fire plot. Pseudo-waveforms are also presented. The left panel shows the pre-fire point cloud, the central panel the post-fire point cloud, and the right panel the x-axis. The axis has been truncated to better show the change in the returned energy for understory and overstory layers. The PAC value for this plot was 6.5, whereas the WARC value was 0.77.

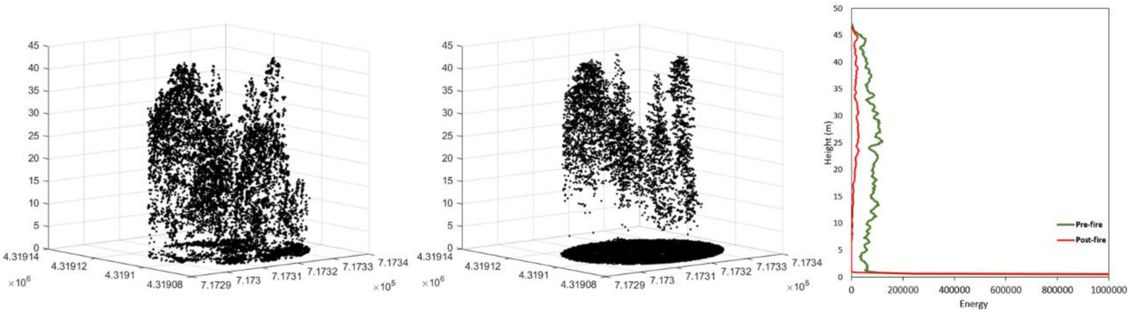

Fourth, I have concerns on the authors certain statements. 1) The waveform area change has actually been used before to indicate forest changes, as the authors claimed by themselves. In this case, I don't think it is appropriate to claim this method as a new method.

It seems that the reviewer misunderstood our statement. In García et al. (2017) work, the metric employed was the canopy area profile, which only considers the canopy energy to estimate biomass in a burned area, but it was not used to study forest changes as it was only a one time metric. However, we realized that the canopy area showed a spatial agreement with a Landsat derived burn severity map and therefore, we came up with the WARC metric which is computed using all waveform energy, from the ground to the top of the canopy, but requires pre- and post-fire LiDAR data as it computes the relative change. Besides, WARC is computed for each fuel stratum and subsequently averaged in a similar way as the CBI, which is an innovative aspect of the metric.

In order to avoid confusion, we have modified the paragraph (Lines 313-319): "García et al., (2017a) calculated the canopy waveform from a post-fire LiDAR campaign, and based on a qualitative analysis they observed a very good agreement between this metric and a severity map derived from Landsat data. Nevertheless, they only used the energy reflected by the canopy to compute the metric, thus missing the information from the ground and the vegetation below the height threshold used to separate the canopy. Therefore, in this study we modified the metric to account for the total energy of the waveform to compute the waveform area in order to include all vertical strata affected by the fire."

2) The authors claimed that they used the color information from lidar. I have concerns on this. It has been well-known the intensity information is problematic for lidar data to be used, even after normalization. Moreover, the change of waveform in pre- and post-fire lidar data is very likely to be caused by the structure of forests. The authors need to provide proofs on this statement.

In Figure 3 we show different scenarios and how changes in structure and 'color' affect the waveform. Specifically, figure 3d) corresponds to a scenario for which the main effect of the fire is a change in color (scorched trees).

We acknowledge the issues with the intensity, which is a function of many variables such as laser power, incidence angle, target reflectivity and area, atmospheric absorption and the range (sensor target distance). Despite the normalization of the intensity, it is not possible to derive reflectance from discrete return intensity values. However, this variable has proved to be useful for different applications such as estimating biomass fractions (García et al., 2010), classify vegetation (Korpela, et al., 2010), detect dead standing trees (snags) (Casas et al., 2016), etc. Furthermore, since we are not using intensity values of individual returns but at the plot level, we expect the noise in intensity to be smoothed (García et al., 2010).

We agree that pre- and post-fire LiDAR signal will be affected by forest structure. However, what we have shown is that in those cases in which structure has not been dramatically changed, but the impact of fire is still high, for example scorched trees, LiDAR data can detect high severity values. Obviously, in a fire structural and radiometric impacts are coupled, but in order to better capture this information, intensity data is required. We have outlined this aspect (also in our previous version in lines 484-488) "Therefore, the WARC considers not only structural, but also foliage alteration (change in color), although PCC has a higher impact on the signal than the PFA. Despite geometric variables may have a larger influence on intensity than reflectance (Korpela et al. 2010), these variables can also be modified as result of tree scorching, thus affecting the recorded intensity over burned areas."

Finally, the writing the manuscript can be improved. I have listed some specific comments for your reference.

Specific comments

Line 24: is critical to understanding --> is critical to understand or is critical for understanding

It is our view that the correct form is: “is critical to understanding” since “to” in this case is a preposition which should be followed by a gerund (-ing).

Line 26: generally-->usually or commonly.

Ok, changed

Line 26: "yet this is only" inaccurate expression. Maybe rephrased as they are less

Ok, we have rephrased the sentence to (lines 26-27): “…yet this type of data is only sensitive to the effects in the upper canopy.”

Line 27: on the upper canopy-->in the upper canopy.

OK, changed. See our comment above.

Line 27: evaluate-->evaluated.

We think the present tense in this sentence is correct.

Line 27: Please give the full name of LiDAR since this is the first time of using this abbreviation.

From our point of view LiDAR is a well-known term nowadays. In fact, many papers published in the last few years do not explain the LiDAR acronym.

Line 30: on the LiDAR signal-->from the LiDAR signal.

We we want to evaluate the impact that fire effects have on the signal recorded by the LiDAR sensor. Therefore, “on the LiDAR signal” is correct.

Line 37: LiDAR metrics? What metrics? You need to clarify this in the abstract.

We have changed the sentence, following the reviewer’s comment, to (lines 37-38): “outperforming the relative change of LiDAR metrics commonly applied for vegetation modeling, such as the relative height of energy quantiles”

Line 52: environmental-->environment.

From our point of view environmental is correct since we refer to a type of fire effect: environmental impacts. Nevertheless, we have added a comma to improve the reading of the sentence. The new sentence is (line 53-57): “The impact of fires encompasses a wide variety of effects, from environmental, such as vegetation pattern distribution, habitat quality and particulate and greenhouse gases emissions (Bond et al. 2005; Casas et al. 2016; Nikonovas et al. 2017; van der Werf et al. 2010), to socio-economic, including health issues related to air quality, property damage or even human casualties (Chuvieco et al. 2014; Fowler 2003).”

Line 57-58: The change of vegetation composition and vegetation structure caused by wildfires can also be a continental or global-scale impact. Please rephrase.

We think the examples are correct. It is true that fires contribute to the global vegetation pattern since it is a global phenomenon, while the effects of a single fire on vegetation composition and structure are local, its effect on the air quality for example can be a continental issue, for example.

Line 65: The use of the appropriate terminology-->The use of an appropriate terminology

Changed.

Lien 66: has been subject-->has been a subject

Changed.

Line 68: Delete therefore.

The sentence has been rephrased (lines 69-72): "Some authors advocate for the use of fire severity when considering immediate fire effects as a result of the combustion process and the term burn severity when considering longer-term effects, thus including therefore ecosystem response processes (Lentile et al. 2006)."

Line 128: Add and before founded.

We do not think "and" should be added before founded, as founded is used as synonym of based on.

Line 145: You have defined radiation transfer model as RTM.

Ok, changed to: "…the FLIGHT 3D RTM was…"

Line 180: Have you missed the rule to define layer D?

It has been corrected and now it reads (lines 195-199): These strata are: A) substrate (rock and soil, duff, litter, and downed woody fuels); B) herbs, low shrubs and trees ≤ 1 m tall; C) tall shrubs and trees ≤ 5 m; D) suppressed and intermediate trees (10 ≤ DBH ≤ 25 cm; 8 ≤ canopy height ≤20 m); and E) dominant and co-dominant trees (DBH > 25 cm; canopy height >20 m).

Line 189: miss a comma before the variables.

Corrected

Line 220-221: Can you simulate the ground conditions with different portions of bare earth (soil)?

We used soil proportions observed in the field for reference plots used to create our scenarios, which can be considered realistic in a Mediterranean environment. We have added the following sentence to clarify this point (Lines 241-243): "The proportion of soil, grass and litter was set based on our knowledge of the study area of the reference plots used to create the scenarios.”

Moreover, as we stated in line 259, our simulations correspond to an initial assessment (immediately to a few weeks after the fire), so we simulated expected proportions of charcoal and ash based on the pre-fire scenario.

Line 325-326: But you never used the imagery in the manuscript!

We have changed the sentence to (lines 347-348): “For this site an exceptional set of airborne data were collected (see Stavros et al., (2016) for detailed information on the available dataset) including pre and post-fire LiDAR”

Line 339: Will the normalization result change if you further smaller the radius of the plots?

Yes, the radius impacts the normalization as it affects the sampling. However, an analysis of the impact of the radius of the plot on the normalization is out of the scope of the paper. We made the plots as large as possible to have a significant sampling (number of returns within the plot), but small enough to avoid including returns from other covers, for example crowns at the edge of the roads.

Line 345: in what footprint you simulated the waveform lidar and compare the field measurements?

The simulated data were based on a typical Mediterranean scenario. The field data used to create the scenarios were collected in Spain (García et al., 2010). The King Fire occurred in California and there was no field data to validate waveforms. Nevertheless, the methodology used has been widely applied.

Line 345-349: Exactly! In your previous RTM-based simulation results, you keep a constant portion of soil in the simulation (a low number). If it is a pure bare ground, a total burn down of vegetation may actually increase the intensity of ground returns, even after intensity normalization. It is necessary to discuss this in the results and discussion.

The scenario described by the reviewer is not realistic, at least in a Mediterranean environment as the one used for our simulations, so there is no point in simulating such a pure bare ground scenario. Second, the reviewer is confusing the effect of canopy occlusion with the proportion of bare ground in the substrate (including soil, litter, duff, and in the post-fire situation, charcoal and ash). The situation we described in lines 379-383 happens when there is a dense canopy present reducing the number of returns from the ground due to the attenuation. After the fire, we may have many more returns (especially single returns) from the ground and that is why the amplitude of the ground peak in the pseudo-waveform can be larger than for the pre-fire situation. For that reason, we applied the constraint to avoid relative changes in the substrate > 1.

Line 354: How many field measurements have you used? How did they get measured? Details are needed.

We have now included the number of plots evaluated in the field, when describing the datasets available for the King Fire (lines 349-352): “In addition, a field assessment of severity was carried out between November 2014 and January 2015 over 52 plots, 22 of which were located within the pre- and post-fire LiDAR surveys. Plots were positioned using GPS measurements and the ecological damage caused by the fire was assessed using the GeoCBI index.”

Line 377-379: Again, the current assumption that the bare ground only accounts for a few of the ground composition. The ratio change of bare ground may lead to different response in the intensity of returns near ground. You need to discuss this here.

See our previous comment above.

Line 381-384: How did you determine the this? Moreover, the results of Figure 3 B and D are very similar to me.

From our LUT. For every scenario we defined the proportion of foliage altered (change in color) and the proportion of foliage consumed (LAI reduction). In 3B changes are structural and radiometric, yet in figure 3D they are mainly radiometric (with very low structural change). The fact that the results are similar, reinforces our assumption that we can use LiDAR to detect this kind of changes (change in color). This can only be observed if intensity is used.

Line 402-403: Maybe I misunderstood, but I still feel very confused on why the loss of lower canopy vegetation have a negative correlation with fire severity. It might have weak correlations, but should be still positive correlated to fire severity.

This is because lower percentiles only account for the substrate and part of the understory whereas fires can affect the whole vegetation strata. This point is stated in line 428-430. The reviewer should have in mind that the Spearman’s rank correlation was computed for all simulated scenarios.

Line 404: This information here, including Figure 5, is very similar to those in previous section. Maybe consider it to be merged with previous section.

Done

Line 412-417: this result is very troubling to me. The improvements of WARC on fire severity modelling is very tiny in real-word cases, especially considering the more computation requirement by the WARC method.

WARC showed the strongest correlation with the field measured Geo-CBI values as compared to the rest of the metrics. There was a wide dispersion in the other metrics, but it is true the best of these performed close to WARC in this instance. WARC also showed much more consistency than other metrics, with the strongest correlation for both the simulated as well as for the real data. Percentile metrics (RH25, RH50, RH75,…) are widely applied but they are not consistent, for example a given percentile/s can be used to model a biophysical variable for a given site and dataset, and for another dataset, a different model can be selected. Therefore, it is likely that for the

King Fire we found RH40 the second strongest predictor, but for other fires it would probably by another percentile the one to be selected.

Despite more processing is required when applied to discrete return data, since a pseudo-waveform has to be created, and additional processing is also required if intensity is to be used. However, our point is precisely that using intensity provides very useful information to characterize fire damage, better than only the distribution of returns. Moreover, some authors have reported that simulating pseudo waveform provide more information than just using the distribution of returns (e.g. Muss et al., 2011). If large footprint full waveform data is available, computation of WARC is as simple as any other metric, including PAC.

Line 425-429: Can you make more detailed analysis on your spatial map? For example, how does the proposed method perform in different vegetation conditions, terrain conditions, etc.

We have added the following information (lines 462-471 and lines 600-609):

"The LiDAR data covered the Rubicon Valley, which was characterized by high severity levels (estimated GeoCBI ≥2.25). Moderate severity is observed near the edge of the burn area, as well as the bottom of the valley, and a low severity patch at the north east part of the fire (Fig. 8). The topographic characteristics of the valley, with a concave shape and steep slopes that favored strong winds and fire spread {Coen, 2018 #62}, explained the high severity observed. Our results show good agreement with the Monitoring Trends in Burn Severity (MTBS) product (Fig. S10, supporting information), downloaded from https://mtbs.gov (last access on 20th February 2020). The MTBS product showed lower severity at the edge of the fire, as well as some larger patches of moderate severity in the north west Rubicon Valley than our LiDAR-based estimates."

"Although a thorough comparison between the LiDAR and Landsat-products is out of the scope of our study, differences between the two products could be explained by the different acquisition time of the post-fire LiDAR and Landsat data. The LiDAR data was collected shortly after the fire, thus representing an initial severity assessment. Meanwhile, the Landsat image was acquired nearly a year after the fire and so, it corresponded to an extended assessment, which could be influenced by vegetation recovery processes. Moreover, the inability of Landsat data to capture fire damage to the understory and substrate, particularly under unaffected dense canopies, can result in higher uncertainties in moderate severity areas {Chuvieco, 2007 #34;Miller, 2015 #36}, contributing also to the differences between the two products."

Line 482-487: I don't quite agree with the explanation here. If the authors want to make this point, the authors have to present results on the differences in accuracy between the WARC method and common lidar metrics under fire severities.

The reviewer probably thinks only about discrete return LiDAR data. We haVE already compared the performance of WARC with other metrics commonly used from full waveform LiDAR. In addition, we have now included the performance of PAC, as suggested by the reviewer, and found much better performance of WARC, probably because PAC only considers the distribution of returns not taking into account intensity. See also our prior response on the results of PAC

Line 492-499: It would be interesting to include PAC into your comparison, especially considering that it is very easy to implement.

Done. See our previous response.

Figure 8: Can you show a comparison with the results derived from WARC and other commonly used satellite imagery index (such as dNBR).

Done, see our previous comment on the discussion about the severity map.

Reviewer #3: General:

This is an excellent paper! I say this as a frequent critic of CBI, because of the way it discards much of the useful information contained in all the component biophysical measures that get collapsed into it. But I also acknowledge its utility as a ground-based severity metric, in large part due to its simplicity, especially for managers. The authors do a great job acknowledging the many specific fire effects that comprise the CBI, as an aggregated metric of severity. I especially appreciate the thorough awareness of how fire causes complex ecological changes to vegetation (all strata) and the ground surface. In other words, the reasoning for why WARC surpasses other remote sensing of fire (or burn) severity metrics is well founded. That said, they should not go quite so far as to say that this is "proven", which they do twice in this paper, by my count.

I anticipate that this paper will be highly cited, as another application of lidar, specifically waveform lidar. It will have relevance for the utility of GEDI data. Given that the FLIGHT model has been parameterized for photon-counting lidars also (L148), I wonder if ICESAT-2 may also have some utility for severity assessments also, albeit diminished because of the lack of intensity information. Some comment on that in the Discussion would be warranted.

Thank you. We greatly appreciate the reviewer's comments and encouragement on the manuscript. We have considered his comments, especially the insufficient evidence of the manuscript to use the word "proved". Regarding ICESat-2, it is our view that given the different characteristics of the sensor (photon counting) would require further analysis and so, discussion on the potential of this sensor it is out of the scope of our paper. Nevertheless, this is a very interesting avenue for future research. Our answer to each of his comments follows (lines refer to the tracked changes version):

Specific comments:

Last highlight. Supporting evidence from this one paper is insufficient to use the word "proved".

We have changed "proved" to "showed".

L451. I would expect charcoal to greatly decrease the intensity at 1064 nm, but white ash should conversely increase it. However, rarely does the proportion of white ash cover approach the proportion of black char cover, let alone exceed it. Thus, an overall decrease. This sentence therefore needs to be rephrased.

The sentence has been rephrased (Lines 488-493): “The effect on the LiDAR signal of the change in soil color, as result of charcoal and ash deposition, was evident in the amplitude of the ground peak, showing a clear reduction as the proportion of change in soil color increased. In our simulations the proportion of charcoal, with lower reflectance than the unburned substrate, was much higher than ash, with higher reflectance than the unburned substrate but rather ephemeral, thus reducing the substrate reflectance.”

L483. "Proved". Same comment as my first specific comment above.

Done. See our previous comment. We have also changed the word proved in:

Lines 621-622 of original submission: The new sentence reads: “The potential of LiDAR data to perform comprehensive evaluations of the severity of wildfires has been evaluated.”

“the metric proved to be able” has been changed to “LiDAR was able to capture” (Line 624).

“proved the robustness and generalization capability of this metric” has been changed to “revealed the robustness and generalization capability of this metric” (line 632-633).

“In this study we have proved” has been changed to “The potential of LiDAR data to estimate severity as measured by integrated indices such as the CBI and the GeoCBI was evaluated” (Line 635-636).

Fig. 3. Change the units on the x axes so you don't have to express the numbers in exponential notation; it really clutters the figure.

Done

Fig. 5. The x and y axes are all identical, so eliminate all of the white space between the component graphs, and they will all fit on a single page and be easier to read/interpret.

Done

Reviewer #4: This is a very interesting and well written paper that brings together a wide range of ideas about remote sensing of fire severity. The paper is easy to follow and well presented but there were a few things that were unclear to me:

Thank you for your encouraging comments and suggestions, which have helped to correct the flaws of the previous version. Detailed information on the changes made follows (lines refer to the tracked changes version).

1. I don't think the general audience will be familiar with the terms 'snags' - this needed some explanation

The term has been explained. Line 131 of the track-changes version: “to vegetation regrowth or presence of dead standing trees, so-called snags (Goetz et al. 2010).”

2. Please explain and justify the use of Spearmans Rho - this bypasses examining the form of the relationships, which may or may not have been informative. Ie linear, non-linear, monotonic, non-monotonic

We have explained the reason to select Spearman’s rank correlation. Lines 340-342: “To assess the sensitivity of each metric to severity we computed the Spearman’s rank correlation between the relative change of the metrics and the CBI since the variables did not fulfil the assumptions to compute Pearson’s correlation coefficient”.

3. There is reference to change in the color of leaves and understory, which may be true for the visual estimates of CBI, but a 1064 lidar does not see color, it sees differences in scattering (ie spectral reflectance). This could be reviewed and revised.
We agree with the reviewer on the fact that LiDAR does not see color but changes in spectral reflectance at the wavelength the sensor operates. We have tried to make this point clearer in the new version of the manuscript (lines 216-221): “In order to use remote sensing data, and more specifically LiDAR data, to evaluate the severity of fires, it is important to have in mind how the ecological changes observed in the field translate into the remotely sensed signal. Hence, changes in cover represent structural changes that LiDAR data can accurately capture. On the other hand, variation in color of scorched leaves results in changes in the spectral reflectance, affecting the returned LiDAR signal.”

In addition, in lines 405-407, we have modified the text. Now it reads: “The second moderate severity scenario (CBI=1.83; Fig. 3D) demonstrates the sensitivity of the LiDAR waveform to damage due to changes in color, resulting in changes in the spectral reflectance, rather than changes in the vegetation structure.”

Lines 594-596 have also been changed: “Contrary, WARC is derived from the intensity, which is affected by the radiometric changes resulting from the modification in soil and leaf color.”

4. My major criticism is that the simulations were of LVIS data but the Kings data sets were from two different sensors. This makes the comparisons rather untidy. Furthermore since the before and after ALS data for the Kings fire were very different, this make it a slightly weak test case. I do not suggest any reanalysis of the data sets, but a much stronger critical reflection on these points is really needed.

We acknowledge that the King Fire case may not be the ideal to validate our simulations. Nevertheless, it is also an opportunity to test the applicability of the method to not only LVIS (or large footprint full waveform data) but to airborne discrete LiDAR data, which are more common. In addition, creating pseudo-waveforms from airborne discrete data has been done in some other studies and allowed to apply the WARC metrics. We have now discussed the weakness and strengths of the King Fire example in Lines 545-554

“The King Fire case study has its limitations to test the robustness of the metrics since the LiDAR data has different pre- and post-fire survey configurations and sensors and the data were not full waveform. This issues require further research to draw more definitive conclusions. Nevertheless, the application of the WARC metric to the King Fire, with different vegetation characteristics than those of our simulated plots, showed the robustness and generalization capabilities of this metric to estimate severity. The availability of pre- and post-fire LiDAR data along with concomitant field measures of the GeoCBI, makes it a unique dataset to evaluate the potential of LiDAR data for the assessment of fire severity. Furthermore, it also allows to demonstrate the possibility of applying the method to the more frequent airborne LiDAR discrete return data by generating pseudo-waveforms.”

Reviewer #5: This manuscript presents an interesting approach to evaluate the suitability of the proposed LiDAR metric WARC to assess severity levels in terms of CBI index values using the radiative transfer model (RTM) Flight. This research is novel as there exist not many example in literature of the use of 3D RTM that simulate the LiDAR signal to assess severity. In addition, the authors propose the use of a new metric not commonly used. However, there exists some concerns about the methodology that should be met before publication.

First of all, form my point of view the tittle is too generic and should give more detailed information on the work performed and the main objective of the research, to assess the sensitivity or behavior of LiDAR waveform to fire damage. Besides, the authors claim that "The approach represents the first attempt to evaluate the effect of different fire impacts, i.e. changes in vegetation structure as well as soil and leaf color, on the LiDAR signal". There exist several studies that relate LiDAR metrics to the CBI index measured in the field, as mentioned by the authors, and this index accounts for soil and leave color. Accordingly, I suggest that the authors reformulate this statement. I will go deeper on this topic later.

We are very thankful for the useful and interesting points raised by the reviewer. We have made the necessary changes to comply with the reviewer suggestions (lines refer to the tracked changes version).

Regarding the title, though it may seems generic, since we applied the method to both, full waveform and discrete return data, we decided to maintain the original title.

1. Introduction.

Line 127, "These previous studies have been based on a set of structural metrics derived from the height distribution of returns, founded on the changes in vegetation structure produced by fires. However, they fail to provide a complete characterization of the severity as they focus only on structural changes rather than considering tree mortality or change in leaf color (scorched leaves) or soil (charred soil)". I do not agree with this sentences. As I mentioned before, the studies cited relate CBI, that accounts for not only structural changes but also changes in leave color and soil, to LiDAR metrics related to the distribution of heights in the returns in the case of discrete sensors.

To the best of our knowledge there are only two studies evaluating severity of fires from LiDAR and using CBI as field measure. The first one (Wang and Glenn 2009) used a modified version of CBI to measure severity in a sagebrush environment. These authors only evaluated changes in height, yet while useful in a sagebrush environment, it clearly does not fully characterize the ecological damage of the fire in a forest environment. The second study (Montealegre et al 2014) compared LiDAR metrics to a broad classification of severity levels based field measure CBI. Nevertheless, this paper only used post-fire LiDAR data within the burned area. Moreover, the metrics were derived from the height distribution of return above 1m, therefore, they did not fully characterize the fire impact either, regardless if field measured CBI does it. There is obviously a relation between the impact of the fire in the upper canopy, and the impact in the understory and substrate layers, but it is indirect. Moreover, in low to moderate burn severity areas, their approach would fail to estimate fire damage, as it happens from optical data. Our approach provides a more comprehensive evaluation of the fire damage.

These metrics are not only structural metrics as the distribution of returns depend on the energy scattered back in both types of sensors, discrete and full-waveform. From my point of view this sentence should also be reformulated or softened.

Although the energy reflected back to the sensors obviously determines whether a return is recorded or not, the distribution of returns depends on: canopy structure, triggering threshold, survey and sensor characteristics (flying height, pulse width, beam divergence…), target reflectance, among other factors. We should bear in mind that two objects with different spectral properties (reflectance) can be detected if the illuminated area is big enough (see Baltavias, 1999: minimum detectable object). This means that as long as the backscattered energy is above the triggering threshold, we would have a return but no information of the spectral characteristics unless the intensity is also recorded and used. Note that intensity is a function of reflectance of the target but it is not possible to derive reflectance from discrete return data. So in the case of fire caused damages, if intensity is not used, we would be just focusing on the impact of fire on the vegetation structure (change in cover as measured by CBI) but not changes related to leaf color, which translate into changes in the spectral reflectance and so in the intensity recorded by the LiDAR system.

Besides, the introduction lack a through revision of approaches devoted to 3D RTM with capabilities to simulate the LiDAR response.

We have added the following information in this regards in the new version of the manuscript (Lines 120-127): "Assessments of fire impacts using LiDAR data have been based so far on empirical relationships. Although RTM approaches have been applied to LiDAR data, they focused on the retrieval of biophysical information such as LAI, canopy height or fractional cover {Bye, 2017 #65}, assessment of the impact of sensor and survey characteristics on canopy height estimation {Disney, 2010 #78}, or to generate a fuel type LiDAR library {Lamelas-Gracia, 2019 #77}, but no research has been done yet on the simulation of LiDAR data to assess fire impacts, which can help improving our understanding of the capabilities of LiDAR systems to assess the severity of wildfires."

Why the flight model was selected? was this model previously tested to simulate the LiDAR response of forest environments?

The suitability of the 3D RTM FLIGHT to simulate full waveform and photon counting LiDAR data has been previously proved (e.g. North, 2010: Bye et al., 2018: Montesano et al.,2015, Morton et al.,2014). We included this sentence to support the selection of FLIGHT RTM in our simulations (lines 164-167): "The suitability of the FLIGHT 3D RTM to simulate full waveform and photon counting LiDAR data in forest environments have been widely demonstrated {Bye, 2017 #65;Montesano, 2015 #69;Morton, 2014 #79;North, 2010 #47;Rosette, 2013 #81}."

2.1. LiDAR full waveform simulations.
Lines 158-159. From the information included in Table 1 it follows that all simulations were performed with an azimuthal view. However, previous research that simulated the LVIS response to fuel types (see Lamelas et al. 2019) concluded the importance of this sensor parameter. Do you think this parameter may have influence the difference of results between the simulations and the king Fire case study? At least this should be mentioned in the discussion section.
Lamelas, M.T., Riaño, D., Ustin, S.L. (2019). A LiDAR signature library simulated from 3-dimensional Discrete Anisotropic Radiative Transfer (DART) model to classify fuel types using spectral matching algorithms. GIScience and Remote Sensing, 56 (7), 988-1023. https://doi.org/10.1080/15481603.2019.1601805.

Lamelas et al., 2019 simulated off-nadir observations of up to 20º, which is wider than the scan angle of the LVIS sensor (https://lvis.gsfc.nasa.gov/Home/instrumentdetails.html), and far beyond the expected scan angle of LVIS operations, normally not exceeding 6º (Hancock et al., 2019). We have run simulations at 3º and 6º and evaluated the impact of scan angle on the observations and observed no consistent bias in most of the metrics. Correlation between metrics remained above 0.9 for all metrics but RH25, RH20, RH10 and HTRT. In the case of WARC, correlation was higher than 0.99.

We added the following sentences in this regard (lines 526-538): "Lamelas et al., {, 2019 #83} reported the impact of scan angle on fuel type classification using the spectral angle mapper (SAM) classifier over an LVIS LiDAR signature library created from simulated waveforms. Although these authors found scan angle an important source of error in the classification, it was probably due to the large scan angles tested up to 20º, beyond the scan-angle limit of the LVIS sensor (https://lvis.gsfc.nasa.gov/Home/instrumentdetails.html; last access on 14th March 2020), and the sensitivity of the SAM algorithm to even small changes in the shape of the waveform. We tested the impact of off-nadir observations, up to 8 º {Hancock, 2019 #84; table 1}, on the metrics and found no consistent bias on most of them. Correlation between the nadir and off-nadir metrics remained above 0.9 for all metrics but RH25, RH20, RH10 and HTRT. In the case of WARC, correlation was higher than 0.99. These results agrees with Hancock et. {, 2019 #84}, who also found no impact of scan angles less than 8º on the metrics derived from simulated LVIS waveforms."

Lines 168-169 and 220. The substrate stratum was modeled as a plane with slope <5°. May the presence of steeper slopes have influenced the results? This should at least be mentioned or discussed. This could be the cause of differences between simulation and King Fire results.

Although slope can affect the filtering of ground returns, the data had been gone through a quality check and the effect of small errors in the filtering, on the generated pseudo waveform can be neglected. Therefore, we do not think this is the cause of the differences between simulation and King Fire results.

We added the following sentence in the discussion for clarification (lines 518-522): “Our simulations considered relatively flat terrain, with slope <5º, reducing the impact of slope on the signal. Therefore, further research is needed to assess the influence of this parameter in the results. In the case of pseudo-waveforms created from discrete return data, although slope can affect ground filtering algorithms {Montealegre, 2015 #82}, the convolution of ground and understory over steep terrain would be less problematic.”

2.2. Definition of postfire effects scenarios.
Line 215. "For this study we assumed that understory was composed of the same species as the overstory". May this assumption have influence the results? Also requires a short discussion. More over considering the main objective formulated "assess the sensitivity of LiDAR data for fire Damage assessment.

Obviously, assuming that the understory was composed of the same species as the overstory is a simplication of the real world. Nevertheless, this approximation do not have a significant impact in the method as we evaluated the relative change of the waveform. Using reflectance data for common shrub species in Mediterranean environments could result in a more accurate representation of the real world, but this would also require more complex parameterization and eventually it could reduce the generalization power of the approach. Moreover, using the same species for the understory and overstory layer is quite common in simulating severity of fires from remote sensing data (Chuvieco et al., 2006; Chuvieco et al., 2007; de Santis et al., 2010)

We added the following sentence in the discussion for clarification (Lines 523-525): “Additionally, we assumed the same species for the understory and the overstory layers. This assumption should not significantly affect the results since our approach to estimate severity is based on the relative change of the waveform, this assumption should not affect the results.”

2.4. Modeling severity from LiDAR
Line 315, "In the case of the WA metric, the relative change of each stratum was derived and the average of the three was computed to provide a plot value; the CBI at the plot level is computed in the same way". Did the authors try to calculate the change in WA for the whole waveform? This may have solved the problems encountered with the use of different thresholds, improving generalization.

Although this could solved the problems of using different thresholds, computing the area of the whole waveform would imply the loss of an important characteristic of the WARC metric, which attempts to evaluate damage at different strata and average them, like CBI does. Moreover, in the case of the pseudo-waveform by computing the change per stratum and averaging we reduced the impact of occlusion (we applied a constraint to the lower layer limiting the change in area to 1). Lines 378-379: “This can result in a relative change > 1, which could result in an overestimation of severity at the plot level; therefore, in these cases the relative change was constrained to 1.”

2.5. The King Fire case study

Line 321. "In order to validate our method over a real scenario, we used as a case study the King Fire". What are the authors validating, the assessment of severity with RTM (main objective) or the new metric proposed (second objective)? From my point of view with the methodology proposed for validation and the results presented (see comments to section 3.4.), the authors only can validate the proposed metric and this should be also discussed due to the slightly better results obtained from the correlation of WARC with CBI in comparison to the other metrics, summed up to the differences in sensor parameters, field measure of severity and environmental conditions.

The main objective of the study is to evaluate the potential of LiDAR data to assess severity of fires. To do so, we used an RTM approach which allowed to simulate a wide variety of fire scenarios, unfeasible to test from actual data. Severity is assessed from changes in LiDAR metrics.

We have rephrased the sentence (lines 344-345): “The King Fire served to evaluate the potential of the LiDAR metrics to estimate severity over a real scenario.”

We also discussed the limitations of our case study for example lines 545-554: “The King Fire case study has its limitations to test the robustness of the metrics since the LiDAR data has different pre- and post-fire survey configurations and sensors and the data were not full waveform. This issues require further research to draw more definitive conclusions. Nevertheless, the application of the WARC metric to the King Fire, with different vegetation characteristics than those of our simulated plots, showed the robustness and generalization capabilities of this metric to estimate severity. The availability of pre- and post-fire LiDAR data along with concomitant field measures of the GeoCBI, makes it a unique dataset to evaluate the potential of LiDAR data for the assessment of fire severity. Furthermore, it also allows to demonstrate the possibility of applying the method to the more frequent airborne LiDAR discrete return data by generating pseudo-waveforms.”

Regarding the slightly better results of WARC compared to other metrics we modified the text (Lines 555-564): “Contrary to the simulation results, structural metrics showed almost the same sensitivity as the WARC for the King Fire, most probably due to large fuel amounts consumed by the fire (Coen et al. 2018). Although structural metrics have shown significant differences between burned and unburned areas in boreal forests (Goetz et al. 2010; Wulder et al. 2009), and can be useful to evaluate specific impacts of fires, such as biomass consumed, the ability of these metrics to provide an integrated measure of severity, such as the CBI or the GeoCBI, which also accounts for tree mortality, may be limited. Moreover, our approach is based on a single simple metric, increasing its generalization capability, as opposed to previous studies that included multiple metrics. The WARC consistency for both, the simulated data as well as the King Fire case study, indicate the potential for the broad applicability of this metric."

Line 327. "In addition, a field assessment of severity was carried out using the GeoCBI index". How many plots? Environmental characteristics? CBI range? Date of acquisition? This information may have influence the results as mentioned before.

This information has been included lines 349-352: "In addition, a field assessment of severity was carried out between November 2014 and January 2015 over 52 plots, 22 of which were located within the pre- and post-fire LiDAR surveys. Plots were positioned using GPS measurements and the ecological damage caused by the fire was assessed using the GeoCBI index."

Line 332. "Based on the intensity of the returns, the discrete return data was converted into a pseudo waveform as described in García et al., (2017b). As mentioned before the influence of the difference in sensor between simulation and validation should be discussed.

Done. See our previous comment

3.1. Sensitivity of full waveform LiDAR to severity
Fig. 3 is very illustrative, however I would have expected to have also information on the values of the relative change of the metrics in different CBI values. In addition, to illustrate the importance of WA computation in different strata, it would have been interesting to include this value in Fig.3 where the value of CBI by strata is also included.
The purpose of figure 3 is to show the influence of different severity scenarios, including structural and change in color effects, on the LiDAR signal (waveforms), not the metrics derived from them. Moreover, adding the information suggested by the reviewer would have cluttered the figure. Therefore, we have kept figure 3 as it was.

3.3. Lidar-Based severity modeling.
This should be part of methodology and not results.

Done. The section has been removed and merged into section 3.2.

3.4. The king fire case study
I would have expected to see also the values of the metrics and graphs in Fig .3 in different severity values for the real data of King Fire. This would allow to assess the behavior of the RTM.

We include now some examples of pseudo-waveforms and the point clouds of several plots with different GeoCBI levels. However, we have not included these examples in the main text but in the supporting information since figure 3 shows our point on the impact of different fire effects on the LiDAR signal. We added a sentence to the new version of the manuscript (lines 439-442): "Pseudo-waveforms generated from discrete return intensity data also showed ability to discriminate different degrees of severity (Fig. S6-S9, supporting information). Nevertheless, the sensitivity analysis of the

LiDAR metrics to the burn severity of the King Fire showed important differences with our previous simulations (Fig. 6).”

Finally, there are some minor comments:
Line 3, number 4 in Martín and not Pilar.

Corrected
Line 97-98, NBR reference required.

Done
Line 335, the terms of the equations should be explained.

Done

Line 715, reference incomplete.

Done
Line 725 reference incomplete.

Done
In general in tables acronyms should be defined to better understanding.

All parameters are described in the second column of table 1. In table 2, the only acronym is LAI, defined in the main text. In table 3, CBI, PFA and PCC are also defined in the main text. Furthermore, their meaning is explained in brackets.

EVALUATING THE POTENTIAL OF LiDAR DATA FOR FIRE DAMAGE ASSESSMENT: A RADIATIVE TRANSFER MODEL APPROACH.

Mariano García[1], Peter North[2], Alba Viana-Soto[1], Natasha E. Stavros[3], Jackie Rosette[2], M. Pilar Martín[4], Magí Franquesa[1], Rosario González-Cascón[5], David Riaño[4,6], Javier Becerra[4], Kaiguang Zhao[7,8]

[1] Environmental Remote Sensing Research Group, Department of Geology, Geography and the Environment, Universidad de Alcalá. Calle Colegios 2, Alcalá de Henares, 28801, Spain.

[2] Global Environmental Modelling and Earth Observation (GEMEO), Department of Geography, Swansea University, SA2 8PP, United Kingdom.

[3] Jet Propulsion Laboratory, California Institute of Technology, 4800 Oak Grove Drive, Pasadena, CA 91109, USA.

[4] Environmental Remote Sensing and Spectroscopy Laboratory (SpecLab), Spanish National Research Council (CSIC), Albasanz 26-28, 28037, Madrid, Spain.

[5] Department of Environment, National Institute for Agriculture and Food Research and Technology (INIA), Ctra. Coruña, Km. 7,5, Madrid, 28040, Spain.

[6] Center for Spatial Technologies and Remote Sensing (CSTARS), University of California, 139 Veihmeyer Hall, One Shields Avenue, Davis, CA 95616, USA.

[7] School of Environment and Natural Resources, Ohio Agricultural Research and Development Center, The Ohio State University, Wooster, OH 44691, USA.

[8] School of Environment and Natural Resources, Environmental Science Graduate Program, The Ohio State University, Columbus, OH 43210, USA.

ABSTRACT

Providing accurate information on fire effects is critical to understanding post-fire ecological processes and to design appropriate land management strategies. Multispectral imagery from optical passive sensors is ~~generally~~ commonly used to estimate fire damage, yet this ~~is~~ type of data is only sensitive to the effects ~~o~~in the upper canopy. ~~In t~~This paper~~, we~~ evaluates the sensitivity of full waveform LiDAR data to estimate the severity of wildfires using a 3D radiative transfer model approach. The approach represents the first attempt to evaluate the effect of different fire impacts, i.e. changes in vegetation structure as well as soil and leaf color, on the LiDAR signal. The FLIGHT 3D radiative transfer model was employed to simulate full waveform data for 10 plots representative of Mediterranean ecosystems along with a wide range of post-fire scenarios characterized by different severity levels, as defined by the composite burn index (CBI). A new metric is proposed, the waveform area relative change (WARC), ~~that~~ which provides a comprehensive severity assessment considering all strata and accounting for changes in structure and leaf and soil color. It showed a strong correlation with CBI values (Spearman's Rho = 0.9 ± 0.02), outperforming the relative change of LiDAR metrics commonly applied for vegetation modeling, such as the relative height of energy quantiles (Spearman's Rho = 0.56 ± 0.07, for the relative change of RH60, the second strongest correlation). Logarithmic models fitted for each plot based on the WARC yielded very good performance with R^2 (± standard deviation) and RMSE (± standard deviation) of 0.8 (± 0.05) and 0.22 (± 0.03), respectively. ~~This approach was~~LiDAR metrics were evaluated over the King Fire, California, U.S., for which pre- and post-fire discrete return airborne ~~pre- and post-fire~~LiDAR- data ~~was~~ were available. Pseudo-waveforms were computed after radiometric normalization of the intensity data. The WARC showed again the strongest correlation with field measures of GeoCBI values (Spearman's Rho =

0.91), ~~although~~ closely followed by the relative change of RH40 (Spearman's Rho = 0.89). The logarithmic model fitted using WARC offered an R^2 of 0.78 and a RMSE of 0.37. The accurate results obtained for the King Fire, with very different vegetation characteristics compared to our simulated data, demonstrate the robustness of the new metric proposed and its generalization capabilities to estimate the severity of fires.

Keywords: LiDAR, radiative transfer models, full waveform simulation, fire effects, severity, King Fire.

1. INTRODUCTION

The impact of fires encompasses a wide variety of effects, from environmental, such as vegetation pattern distribution, wildlife habitat quality and particulate and greenhouse gases emissions (Bond et al. 2005; Casas et al. 2016; Nikonovas et al. 2017; van der Werf et al. 2010), to socio-economic, including health issues related to air quality, property damage or even human casualties (Chuvieco et al. 2014; Fowler 2003). Fire impacts also vary spatially, from landscape (e.g. changes in vegetation composition and structure) to continental or global scales (e.g. biomass burning emissions); and over time, including the fire environment, post-fire environment and the response phases of the so-called fire continuum (Jain et al. 2004). Fire managers require information on fire effects to support strategic planning before and during fires, to establish mitigation strategies aimed at reducing soil erosion, establishment of invasive species, as well as to evaluate the results of prescribed fires {Morgan, 2014 #26}. Therefore, accurately quantifying fire effects is necessary to improve our understanding of the impact of fires on ecosystem processes ~~as well as to develop appropriate forest and fire management~~

~~strategies~~as well as the carbon cycle. This becomes especially important as with projected climate change an increase in forest fires is expected (Stephens et al. 2013).

Fire damage is generally described in terms of its severity, which represents the ecological change caused by fire (Lentile et al. 2006). The use of ~~the~~ an appropriate terminology to describe post-fire effects has been a subject of discussion. Some authors advocate for the use of fire severity when considering immediate fire effects as a result of the combustion process and the term burn severity when considering longer-term effects, thus including ~~therefore~~ ecosystem response processes (Lentile et al. 2006). On the other hand, Keeley (2009) recommend not including ecosystem response in fire or burn severity measures since some of the ecosystems response processes are not related to the severity of the fire event, and in such a case the interchangeable use of both terms would not be problematic. Similar to French et al. (2008) and Morgan et al. (2014), hereinafter we will use the generic term severity to generally describe the ecological change produced by fires.

A plethora of field measures has been designed to quantify severity according to the particular objectives of the fire damage assessment. These measures include changes in soil characteristics such as color, structure or hydrophobicity (Lewis et al. 2006; Neary et al. 1999), tree mortality (Hood et al. 2018; Whittier and Gray 2016) or biomass consumed (Garcia et al. 2017a). Key and Benson (2006) proposed the composite burn index (CBI), which integrates different post-fire effects into a single semi-quantitative index ranging from 0 (unburned) to 3 (completely burned). The CBI was designed to serve as a field validation of remotely sensed estimations of burn severity. De Santis and Chuvieco (2009) proposed a modified version of the CBI, the GeoCBI, that improved severity estimations from remote sensing by accounting for the fractional cover and leaf area index (LAI) changes of the intermediate and upper canopy strata. Despite the generalized acceptance and application of the CBI/GeoCBI, particularly in remote sensing studies, they are highly subjective. Morgan et al. (2014) recommend to directly measure fire effects, which can be later integrated according to an objective severity measurement instead of collapsing them into a single integrated severity index, such as the CBI.

The heterogeneity of fire effects both in space and time make remote sensing techniques a suitable alternative to field measures given their comprehensive and systematic view of the Earth. Most attempts have been based on the use of multispectral imagery due to the spectral changes associated with vegetation removal, soil exposure, decrease in moisture content of soil and vegetation, or carbon and ash deposition that result from fires (Jakubuaskas et al. 1990). The potential of remotely sensing data, particularly Landsat imagery, for mapping wildfire severity has been demonstrated across the world from boreal forests to savannas (Boer et al. 2008; Landmann 2003; Viana-Soto et al. 2017; Whitman et al. 2018). The most common approach to derive severity from optical remote sensing develops empirical relations between the normalized burn ratio (NBR) {Key, 2006 #27} or some of its derivatives, namely the differenced NBR (dNBR) (Miller and Thode 2007) or the relative dNBR (RdNBR) (Miller et al. 2009), with the CBI or the GeoCBI. More recently, methods based on radiative transfer models (RTM) have been developed to improve the retrieval of severity estimates from the spectral information recorded by spaceborne sensors (Chuvieco et al. 2007; De Santis et al. 2010; Disney et al. 2011). RTM approaches can help improving our understanding of the factors modifying reflectance and offer better universality than empirical approaches, yet their performance is subject to an appropriate model parameterization. Performance of the different severity retrieval approaches using optical data varies widely in terms of R^2 and RMSE but in general, low and high severity values are accurately predicted while larger errors are found for intermediate severity values

(Chuvieco et al. 2007; De Santis and Chuvieco 2007). This can be explained by the inability of Landsat data to accurately capture the actual fire damage to under- and mid-story vegetation in low and moderate severity areas, especially under high canopy cover (Miller and Quayle 2015).

LiDAR data provide detailed 3~~d~~D information on forest structure ~~and~~, so it can evaluate the severity on different strata. Specific fire caused damage such as changes in vegetation structure (McCarley et al. 2017; Wulder et al. 2009), biomass consumption (Garcia et al. 2017a), LAI changes (Hu et al. 2019) or habitat suitability (Casas et al. 2016), have been generally estimated from LiDAR data, rather than an integrated measure of severity as that provided by CBI. While only changes in the overstory layer are generally assessed, LiDAR has potential to separate biomass consumption at different canopy levels (Alonzo et al. 2017). Assessments of fire impacts using LiDAR data have been based so far on empirical relationships. Although RTM approaches have been applied to LiDAR data, they focused on the retrieval of biophysical information such as LAI, canopy height or fractional cover {Bye, 2017 #65}, assessment of the impact of sensor and survey characteristics on canopy height estimation {Disney, 2010 #78}, or to generate a fuel type LiDAR library {Lamelas-Gracia, 2019 #77}, but no research has been done yet on the simulation of LiDAR data to assess fire impacts, which can help improving our understanding of the capabilities of LiDAR systems to assess the severity of wildfires. The simplest approach to burn assessment consists of evaluating vegetation height changes. Although this successfully correlated to field measures in a sagebrush ecosystem (Wang and Glenn 2009), over forest areas this variable alone may not capture severity appropriately due to vegetation regrowth or presence of dead standing trees, so-called snags (Goetz et al. 2010). Differences between LiDAR derived digital elevation models (DEMs) have been also utilized to estimate soil consumption in peat swamps (Reddy et al. 2015). So far, only a study in a Mediterranean forest in Spain applied LiDAR data to classify the severity of fires using a logistic regression between LiDAR and field measured CBI values (Montealegre et al. 2014). Nevertheless, the metrics only considered returns above 1 m not completely evaluating fire effects on the ecosystem.

These previous studies ~~have been~~were based on a set of structural metrics derived from the height distribution of returns, founded on the changes in vegetation structure produced by fires. However, they fail to provide a complete characterization of the severity, as they focus only on structural changes rather than also considering tree mortality or change in leaf color (scorched leaves) or soil (charred soil). This is particularly relevant for scorched trees that may retain leaves at the moment of the LiDAR survey, thus preserving the pre-fire structure. On the other hand, LiDAR has proved successful to detect snags using intensity data (Casas et al. 2016; Wing et al. 2015). Therefore, further research is required to assess the utility of LiDAR data for providing an integrated estimation of the severity of wildfires. The main goal of this research was to assess the potential of LiDAR data for providing a comprehensive characterization of the ~~burn~~ severity of fires, beyond structural changes, considering all layers of a forest. The specific objectives were to: 1) assess the sensitivity of LiDAR data to different severity degrees as measured by CBI using a 3D RTM; 2) develop a new integrated LiDAR metric that better captures severity of a forest plot; 3) evaluate the proposed metric over an actual fire occurrence in a fire prone environment using pre- and post-fire airborne LiDAR data.

2. Methods

2.1. LiDAR full waveform simulations

Evaluation of fire effects requires analyzing changes over different strata, from the substrate to the upper canopy. Large footprint full waveform data provide better description of the vertical vegetation volume distribution, from the top of the canopy to the ground, including the understory layer, than discrete return data {Lim, 2003 #76}, thus making it ideal to evaluate severity of fires.

In order to evaluate the sensitivity of LiDAR data to different degrees of severity, the FLIGHT 3D ~~radiative transfer model~~RTM was selected to simulate LiDAR waveforms under different severity levels, including an unburned scenario representing the pre-fire conditions. FLIGHT was originally developed to model vegetation bidirectional reflectance (North 1996) and later extended to model LiDAR waveforms (North et al. 2010) and photon counting LiDAR returns (Chen et al. 2020~~; Montesano et al. 2015~~). The suitability of the FLIGHT 3D RTM to simulate full waveform and photon counting LiDAR data in forest environments have been widely demonstrated {Bye, 2017 #65;Montesano, 2015 #69;Morton, 2014 #79;North, 2010 #47;Rosette, 2013 #81}. The model is based on Monte Carlo evaluation of photon transport within a 3D representation of the vegetation, and can be configured for both airborne and satellite instruments. Waveforms are simulated by uniformly sampling the path of photons within the instantaneous field of view of the LiDAR sensor at a given position, accumulating the path length (equivalent to the time of signal) and energy from both laser and solar sources. Multiple orders of scattering are accounted for and the contribution of successive orders of scattering is reduced using an exponential function until contributions approach zero. The energy is binned into m bins, the width of which is defined by the sensor model temporal sampling. For this study the set of parameters defining the LiDAR sensor corresponded to the Land, Vegetation and Ice Sensor (LVIS) (Blair et al. 1999), listed in Table 1.

Insert Table 1

A forest plot or stand representation in FLIGHT can be generated statistically using fractional cover and crown size range values. Alternatively, if field measurements or airborne LiDAR data enabling tree delineation are available, a more realistic representation can be realized. Tree crowns are modeled using ellipsoidal or conical geometric primitives of given horizontal and vertical dimensions. The overlap between neighboring crowns is limited using a simple growth model. Within each crown, vegetation is represented as a turbid medium described by leaf area density, leaf-angle distribution, and the optical properties of the scene components, namely leaves, branch, shoot and ground. The ground is approximated using a planar surface with defined slope angle. In order to be able to simulate post-fire effects on different forest strata, including cases in which there is a tree canopy and understory vegetation both with various levels of fire damage, the FLIGHT model was modified to allow definition of different properties for understory and overstory vegetation.

2.2. Definition of post-fire effects scenarios

Simulation of fire effects first required the selection of a reference measure of fire damage. We used the CBI, which has been previously applied in other remote sensing simulation approaches for burn severity estimation from passive optical data (Chuvieco et al. 2007; Chuvieco et al. 2006; De Santis et al. 2010). The CBI consists of a visual assessment of fire effects on up to five vertical strata of the field plot under consideration. These strata are: A) substrate (rock and soil, duff, litter, and downed woody fuels); B) herbs, low shrubs and trees ≤ 1 m tall; C) tall shrubs and trees ≤ 5 m; D) suppressed and intermediate trees (10 ≤ DBH ≤ 25 cm; 8 ≤ canopy height ≤20 m); and E) dominant and co-dominant trees (10 ≤ DBH ≤ > 25 cm; 8 ≤ canopy height ≤>20 m). Fire effects are evaluated by analyzing soil charring, organic matter consumption, proportion of fuel consumed (change in cover), altered foliage (proportion of brown leaves), canopy mortality and char height. CBI also accounts for ecosystem response processes such as presence of colonizers or percentage of resprouting. All these changes are expressed relative (%) to the pre-fire situation (Key and Benson 2006). Each stratum is evaluated individually and rated between 0 and 3, and finally averaged to provide an estimate of the burn severity at the plot level. Although the CBI was initially designed to validate severity estimates derived from Landsat imagery, the variables considered to assess the ecological change caused by the fire makes it suitable also for LiDAR data.

With the purpose of simulating scenarios showing diverse degrees of post-fire severity using FLIGHT, we made some simplifications of the CBI taking into account those variables that LiDAR can actually measure. Similarly to Chuvieco et al. (2007), the first simplification consisted in reducing the five strata of the CBI to three by grouping strata B and C into the understory vegetation stratum, and strata D and E into the overstory stratum. The CBI variables considered for the simulations included charcoal and ash proportion for the substrate (soil charring); whereas for the understory and overstory layers, the percentage of foliage altered (PFA), i.e. change in leaf color~~,~~; and percentage of cover change (PCC) were evaluated. In order to use remote sensing data, and more specifically LiDAR data, to evaluate the severity of fires, it is important to have in mind how the ecological changes observed in the field translate into the remotely sensed signal. Hence, ~~C~~changes in cover represent structural changes that LiDAR data can accurately capture~~;~~. On the other hand, variation in ~~leaf~~ color of scorched leaves results in changes in the spectral reflectance, affecting the returned LiDAR signal~~ intensity~~.

Because severity is measured in relation to the vegetation conditions before the fire event, a pre-fire scenario was simulated for 10 plots representing typical Mediterranean vegetation (Table 2). Further details about vegetation in these plots can be found in Garcia et al., (2010).

Insert Table 2

Field measurements of tree height, diameter at breast height (DBH), crown size and LAI defined the structural characteristics of the overstory vegetation. Likewise, measurements of LAI, height and diameter of shrubs described the understory vegetation. Because tree location was not measured in the field, each individual was randomly set within the plot of 25 m diameter, equivalent to the LVIS footprint. Regarding the optical properties of leaves, reflectance was measured using an ASD Fieldspec® 3 spectroradiometer (Analytical Spectral Devices Inc., Boulder, CO, USA), with a spectral resolution of 2–10 nm in the range of 400–2500 nm. Transmittance values were estimated using Prospect-5D (Féret et al. 2017) for oak leaves and the LIBERTY model (Dawson et al. 1998) for pine needles (see supporting information). For this study we assumed that understory was composed of the same species as the overstory; therefore, the optical properties of the overstory were applied. In addition to leaf properties, FLIGHT requires tree-bark reflectance factor which was measured in the field using an ASD Fieldspec® 3attached to an ASD Plant Probe based on 25 measurements collected over three different individuals (Melendo-Vega et al. 2018). The substrate stratum was modeled as a plane with slope <5° and its optical properties defined by a mixture of soil (≤10%), grass (20-30%) and leaf litter (60-40%). The proportion of soil, grass and litter was set based on our knowledge of the study area of the reference plots used to create the scenarios. Grass and soil reflectance values, measured over a medium-moisture sandy soil, were provided by Melendo-Vega (personal communication, 2019). Leaf litter corresponding to dry leaves and needles of holm oak (*Quercus ilex* L.) and black pine (*Pinus nigra* Arn.) were measured using an ASD FieldSpec® 3 spectroradiometer (see supporting information for more details). Despite measuring the reflectance of each cover in the range of 400-2500 nm, we use here only the 1064 nm wavelength, at which the LVIS sensor operates.

In order to simulate post-fire scenarios representing a wide range of severity levels, CBI values resulting from changes in color and cover for each of the three strata considered were combined in the range [0, 3] at 0.5 step values. Tables 3 and 4 show the relative change of each variable and stratum associated with each CBI value, and their combination to yield the CBI of the understory and overstory strata.

Insert Table 3

Insert Table 4

The substrate stratum of the post-fire scenarios was comprised of soil, charcoal and ash. Bearing in mind the low persistence of the ash signal, which is usually blown away by the wind shortly after the fire, the ash cover was limited to a maximum of 15% of the plot. This would represent a situation of up to a few weeks after a fire, i.e. an initial assessment (Key and Benson 2006). Soil reflectance values were the same for the pre-fire scenario whereas the spectra for charcoal and ash were measured in the field with a GER-2600 spectroradiometer (Geophysical & Environmental Research Corporation, Millbrook, NY) and provided by Chuvieco et al., (personal communication, 2019). The final spectrum for the post-fire substrate layer was a linear combination of the reflectance of the three components weighted by their proportion according to the CBI values as specified in Table 3.

As for the changes in understory and overstory strata the same two variables were considered, PCC and PFA. PCC was simulated as a reduction in the LAI. Based on the reference values of the CBI definition we assigned CBI values of 1, 2 and 3 to relative LAI reductions of 15%, 70% and 100% (Key and Benson 2006), whereas all intermediate values in Table 3 were linearly interpolated. With regards PFA, simulations were realized as a linear combination of green and scorched leaves/needles weighted by their proportion according to the CBI values (Table 3). Although in previous studies the spectral characteristics of scorched leaves were assimilated to senescent leaves (Chuvieco et al. 2007; Chuvieco et al. 2006), in this work we measured the spectra of scorched leaves in the laboratory using an ASD FieldSpec® 3 spectroradiometer attached to a ASD plant probe and leaf clip (Analytical Spectral Devices Inc., Boulder, CO, USA) provided with a low-intensity bulb specially designed for collecting non-destructive data from vegetation and other heat-sensitive targets. Samples of holm oak leaves and black pine needles were scorched to different degrees (see supporting information) and averaged to provide a single post-fire value for holm oak and black pine, respectively. Transmittance values were simulated using leaf level simulation models. Reference values of the CBI definition assigned CBI values of 1, 2 and 3 to relative changes in leaf color of 25%, 80% and 100% respectively (Key and Benson 2006), and intermediate values in Table 3 were obtained by linear interpolation. After the proportion of green and brown leaves was set, FLIGHT distributed them randomly within each tree crown.

Once the variables for each CBI scenario and stratum were defined, they were all combined to represent the CBI at the plot level. Considering the seven scenarios for the substrate and the 49 possibilities for each of the vegetation strata (Tables 3 and 4), 16807 simulated scenarios were possible. However, in order to avoid unrealistic simulations such as high overstory CBI with low understory CBI values, we applied the same set of filters as Chuvieco et al., (2007, 2006 #48): 1) CBI (understory) > CBI (substrate); 2) CBI (understory) > CBI (overstory); 3) CBI (understory) < 4 * CBI (substrate); 4) (PCC-PCC_e) ≤ PCC ≤ (PCC+PCC_e). The last filter was applied to avoid unrealistic combinations of PCC and PFA. PCCe was calculated applying the following equations (Chuvieco et al. 2007):

$$PCC_e = 0.2858 + 0.9188 * PFA, \text{ for the understory} \quad (1)$$

$$PCC_e = 0.0008 + 0.8912 * PFA, \text{ for the overstory} \quad (2)$$

These filters were considered adequate for this study since they were based on field observations carried out in the same study area as the field data used to characterize our plots. After filtering out unrealistic scenarios, 1348 simulations were run for each of the 10 plots considered.

2.3. Derivation of LiDAR metrics to estimate severity

A common pre-processing procedure of the waveform was applied prior to computing the LiDAR metrics from the simulated waveforms for each of the pre- and post-fire scenarios. First, the waveform was smoothed by applying a Gaussian filter with a width size of 5 bins. Second, a background noise threshold was applied to identify the signal beginning and end, that is, the first and last height bins where the returned energy is detected above the noise threshold, thus representing the interaction of the laser with surface elements. Subsequently, we derived a set of metrics previously applied for the estimation of structural attributes of vegetation and to assess forest disturbances and therefore, were expected to capture the changes caused by fire on vegetation. From the total waveform energy, the 1^{st} to 9^{th} deciles of the energy relative to the ground elevation, identified as the last Gaussian peak fitted to the waveform, were computed as well as the 25^{th} and 75^{th} percentiles. The height/median ratio (Drake et al. 2002) was computed and from the canopy height profile (CHP) we derived the quadratic mean canopy height (QMCH), the mean canopy height (MCH), representing the average height of the CHP (Lefsky et al. 1999), and the coefficient of variation of the CHP (Bouvier et al. 2015). García et al., (~~Garcia et al.~~ 2017a) calculated the canopy waveform ~~area to account for the biomass consumed by a wildfire in California~~from a post-fire LiDAR campaign, and based on a qualitative analysis they observed a very good agreement between this metric and a severity map derived from Landsat data. Nevertheless, they only used the energy reflected by the canopy to compute the metric, thus missing the information from the ground and the vegetation below the height threshold used to separate the canopy. Therefore, in this study we modified the metric to account for~~used~~ the total energy of the waveform to compute the waveform area ~~(WA)~~ in order to include all vertical strata affected by the fire. Moreover, since the plot CBI is the average of the CBI values of the strata considered, three in our simulations, we divided the waveform into three parts corresponding to the substrate, the understory and the overstory strata, and the area of each part was calculated. Because the ground signal is convolved with the energy reflected from low vegetation, even for flat surfaces, we applied different height thresholds from 0.3 to 1.2 m at 0.15 intervals, to separate the ground and the understory parts of the signal. Regarding the separation of understory and overstory vegetation, although the CBI establishes a threshold of 5 m, we reduced this threshold to 2 m, based on the characteristics of the vegetation used to model the 10 simulated plots.

2.4. Modeling severity from LiDAR

Severity is estimated as the change occurred relative to the pre-fire conditions, therefore it was estimated from LiDAR data as the relative change of the metrics computed from the pre-fire and post-fire~~s~~ simulated waveforms. Since the post-fire magnitude of the metrics was generally smaller than the pre-fire magnitude, we computed the absolute value of the difference to avoid negative values (eq.3):

$$RC_{LM} = \frac{\left|LM_{post-fire} - LM_{pre-fire}\right|}{LM_{pre-fire}}, \qquad (3)$$

where RC_{LM} is the relative change of a given LiDAR metric, and $LM_{pre\text{-}fire}$ and $LM_{post\text{-}fire}$ represent the value of the metric before and after the fire, respectively. In the case of the waveform area relative change (WARC) metric, the relative change of each stratum was derived and the average of the three was computed to provide a plot value; the CBI at the plot level is computed in the same way.

To assess the sensitivity of each metric to severity we computed the Spearman's rank correlation between the relative change of the metrics and the CBI since the variables did not fulfil the assumptions to compute Pearson's correlation coefficient.

2.5. The King Fire case study

~~In order~~The King Fire served to ~~validate our~~ evaluate the potential of the ~~method~~LiDAR metrics to estimate severity over a real scenario~~, we used as a case study the King Fire, which~~. The King Fire started in July 2014 and was controlled in October 2014 burning over 50000 ha in Eldorado National Forest located in the Sierra Nevada Mountain Range, California, U.S. For this site an exceptional set of airborne data were collected (see Stavros et al., {, 2016 #85} for detailed information on the available dataset) including pre- and post-fire LiDAR~~, as well as Airborne Visible/Infrared Imaging Spectrometer (AVIRIS) and the MODIS/ASTER airborne simulator (MASTER) imagery~~. ~~Detailed information can be obtained from Stavros et al., (2016).~~ In addition, a field assessment of severity was carried out between November 2014 and January 2015 over 52 plots, 22 of which were located within the pre- and post-fire LiDAR surveys. Plots were positioned using GPS measurements and the ecological damage caused by the fire was assessed using the GeoCBI index. ~~In addition, a field assessment of severity was carried out using the GeoCBI index.~~ Table 5 shows the characteristics of the available LiDAR data and ~~figure~~ Fig. 1 shows the study area.

Insert Table 5

Insert Figure 1

Based on the intensity of the returns, the discrete return data was converted into a pseudo-waveform as described in García et al., (2017b). Previously, the intensity was normalized to eliminate the impact of the range on the intensity values as follows (García et al. 2010):

$$I_n = I_{raw} \frac{R}{R_{std}}, \quad (4)$$

where I_n is the normalized intensity, I_{raw} is the intensity value before normalization, R is the range (sensor-target distance) and R_s is the standard range, which was set to 1000 m. This normalization removed the dependence of intensity on the sensor-target distance. ~~; however~~ However, due to the differences in the sensors used for the pre- and post-fire surveys, such as the radiometric resolution, it was necessary to carry out a between-sensors normalization. We selected 500+ plots over pseudo-invariant features encompassing roads and bare-soil across the study site. The radius of these plots was set to 2 m to avoid including other covers, particularly at the edge of the roads. Consequently, a linear model was fit (Fig. 2) and the pre-fire intensity values were normalized by applying the following equation:

$$I_{sensor\_n} = 1373.6 + 14.479 * I_n, \quad (5)$$

where I_{sensor_n} is the pre-fire sensor intensity normalized to the post-fire sensor and I_n is the range normalized intensity values of the pre-fire data.

Insert Figure 2

After generating the pseudo-waveforms, the set of metrics previously described were derived and their relative change computed. Due to the signal attenuation through the canopy, particularly in areas of dense cover, ground returns can be missed if the amount of energy reflected is lower than the triggering threshold of the sensor, resulting in a smaller amplitude of the ground and understory signal in the pseudo-waveform. After the fire, when the canopy is removed and most of the returns come from the ground, the amplitude of the ground peak can be much larger than that of the pre-fire waveform, despite the lower reflectance of the charcoal. This can result in a relative change > 1, which could result in an overestimation of severity at the plot level; therefore, in these cases the relative change was constrained to 1.

The Spearman's rank correlation between the derived variables and the field measured GeoCBI was computed, and a model was calibrated using a jackknife approach, based on the variable showing the strongest correlation. The model fit was evaluated in terms of its R^2 and the RMSE, and subsequently applied to the part of the study area covered by the bi-temporalpre- and post-fire LiDAR data to generate a LiDAR severity map.

3. Results

3.1. Sensitivity of full waveform LiDAR to severity

The sensitivity of LiDAR waveforms to different degrees of severity was first qualitatively evaluated according to the changes observed in the post-fire waveform relative to the pre-fire waveform one for the different scenarios simulated (Fig. 3).

Insert figure 3.

For the low severity scenario (CBI=1.0; Fig. 3A), only the understory and the substrate are affected. The waveforms show a reduction in the amplitude of the lowest peak as well as ~~some~~ a reduction for the understory part of the waveform (enlarged window). It should be noted that part of the effect of the understory change is reflected in the substrate section of the waveform due to the convolution of the ground and the low vegetation energy. The overstory part of the waveform remains unchanged since this stratum was unburned in this scenario. For the first moderate severity scenario (CBI= 2.0; Fig. 3B) a greater difference can be observed between the unburned and the burned signals. The largest effect occurs in the substrate and understory strata, which had a large~~r~~ proportion of charcoal on the ground as well as a large reduction of the understory LAI, with the remaining leaves totally scorched. A smaller change occurred in the overstory given the lower severity of this stratum, with only a small reduction in LAI and partial scorching of the leaves. As expected, ~~The~~the high severity scenario (CBI=2.42; Fig. 3C) showed~~, as expected,~~ the largest change in the waveform given the large proportion of charcoal in the substrate as well as the large reduction in LAI for both vegetation strata. The second moderate severity scenario (CBI=1.83; Fig. 3D) demonstrates the sensitivity of the LiDAR waveform to damage due to changes in color, resulting in changes in the spectral reflectance, rather than changes in the vegetation structure. Thus, a smaller amplitude is observed in the upper part of the waveform of the burned scenario, which is the result of a canopy that has been scorched but retains most of its leaves. Likewise, the lower part of waveform showed a significant reduction as result of the substrate charring and the scorching of the understory vegetation.

3.2. LiDAR metrics assessment

LiDAR metrics were computed using different height thresholds to separate the understory from the substrate part of the waveform. The best results were obtained for a 0.45 m height threshold, although differences with a 0.6 m threshold were negligible~~;~~. ~~therefore~~Therefore, the results shown throughout the rest of the text correspond to the former threshold. Fig. 4 shows the Spearman's rank correlation coefficient values between the relative change of the metrics derived from the waveforms and the CBI of the simulated scenarios.

Insert figure 4.

The WARC presented the strongest correlation with the CBI values, with a mean Spearman's Rho value of 0.9. This metric also showed a very good consistency among the 10 different simulated plots, with a standard deviation of 0.02 and a range of variation comprised between 0.86 and 0.93. The relative change of the structural metrics commonly derived from LiDAR data showed a moderate correlation with the CBI, with a mean value of approximately 0.55 and a much larger dispersion than the WARC. For instance, the relative height of the 60th percentile of the energy, which was ranked second, showed a mean Spearman's Rho value of 0.56, with a standard deviation of 0.07 and a range of variation between 0.49 and 0.69. A similar behavior was observed for the other structural metrics although negative correlations were found for the lower percentiles, since they just represent the lower part of the signal, i.e. the substrate and the understory layers.

~~3.3. LiDAR-based severity modeling~~

After identifying the best LiDAR-based metric to estimate CBI we fitted a logarithmic model for each of the forest plots simulated (Fig. 5).

Insert figure 5.

The models showed very good performance with a mean R^2 of 0.8 (± 0.05) and values ranging between 0.73 and 0.86. The mean RMSE was 0.22 (± 0.03) and values that varied between 0.18 and 0.26.

~~3.4.~~3.3. The King Fire case study

Pseudo-waveforms generated from discrete return intensity data also showed ability to discriminate different degrees of severity (Fig. S6-S9, supporting information). Nevertheless, ~~The~~ the sensitivity analysis of the LiDAR metrics to the burn severity of the King Fire showed important differences with our previous simulations (Fig. 6). The WARC once again showed the strongest correlation with field measured GeoCBI values (Spearman's Rho = 0.91); however, the structural metrics derived from the pseudo-waveforms showed much stronger correlation than that obtained for the simulated data. Thus, the RH40, the relchp_cv, the RH90, the MCHP and the QMCH yielded a Spearman's Rho value of 0.89, 0.87, 0.86, 0.81 and 0.8, respectively. The weakest correlation was obtained for the HTRT variable, with a Spearman's Rho correlation of 0.19.

Insert figure 6.

The height thresholds used to separate the three strata considered had a significant impact on the estimation of severity from the LiDAR data, obtaining the best results using a height threshold of 0.45 m to separate the understory from the substrate, and a height threshold of 5 m to separate the overstory from the understory strata.

The model fitted (Fig. 7) to the estimate GeoCBI values from the WARC using the jackknife approach was: $GeoCBI = 1.6 * \ln(WARC) + 3.03$, with a standard deviation of the parameters of 0.05 and 0.02, respectively. This model offered an R^2 of 0.78 and a RMSE of 0.37. This model was subsequently applied to the part of the King Fire for which pre- and post-fire LiDAR data were available to produce the LiDAR-based severity map shown in Fig. 8.

Insert figure 7.

Insert figure 8.

The LiDAR data covered the Rubicon Valley, which was characterized by high severity levels (estimated GeoCBI ≥2.25). Moderate severity is observed near the edge of the burn area, as well as the bottom of the valley, and a low severity patch at the north east part of the fire (Fig. 8). The topographic characteristics of the valley, with a concave shape and steep slopes that favored strong winds and fire spread {Coen, 2018 #62}, explained the high severity observed. Our results show good agreement with the Monitoring Trends in Burn Severity (MTBS) product (Fig. S10, supporting information), downloaded from https://mtbs.gov (last access on 20th February 2020). The MTBS product showed lower severity at the edge of the fire, as well as some larger patches of moderate severity in the north west Rubicon Valley than our LiDAR-based estimates.

4. Discussion

LiDAR metrics showed different degrees of sensitivity to the severity of fires. Our simulation approach represents the first attempt to evaluate the combined effect of different fire impacts, i.e. changes in color and changes in structure, on the LiDAR signal. The relative change of commonly LiDAR derived metrics showed moderate correlation ~~to~~with CBI values. These metrics were proposed for the estimation of important forest structural variables, such as biomass or wood volume (Bouvier et al. 2015; Drake et al. 2002). Therefore, they are more sensitive to fuel consumed~~, but failed to capture~~ than to color changes associated with ~~leaf color of~~charred soil and scorched vegetation, ~~which are~~ related to vegetation mortality induced by fire (Fig. 4). The new metric proposed, ~~(~~WARC,~~)~~ showed the strongest correlation and very high consistency across the different forest plots simulated. ~~The WA~~It was computed from the energy recorded by the sensor, which in addition to the range, is affected by target reflectance, size, orientation, density and the illuminated area (Korpela et al. 2010). Therefore, the WARC considers not only structural, but also foliage alteration (change in color), although PCC ~~had~~ has a higher impact on the signal than the PFA. Despite geometric variables may have a larger influence on intensity than reflectance (Korpela et al. 2010), these variables can also be modified as result of tree scorching, thus affecting the recorded intensity over burned areas. The effect on the LiDAR signal of the change in soil color, as result of charcoal and ash deposition, was evident in the amplitude of the ground peak, showing a clear reduction as the proportion of change in soil color increased. In our simulations the proportion of charcoal, with lower reflectance than the unburned substrate, was much higher than ash, with higher reflectance than the unburned substrate but rather ephemeral, thus reducing the substrate reflectance.~~The effect of the change in soil color as result of charcoal and ash deposition, with lower reflectance than the unburned soil, was evident in the amplitude of the ground peak, showing a clear reduction as the proportion of charcoal and ash on the substrate increased.~~

In addition to accounting for the changes in structure and leaf and soil color, the WARC considered all plot strata, computing the changes from the substrate to the upper canopy and averaging at the plot level, in the same way the CBI does. Therefore, the severity estimation based on WARC provides a more comprehensive evaluation ~~of severity~~ than other approaches previously published. For instance, Klauberg et al., (2019) derived a set of crown metrics from airborne LiDAR to classify crown fire severity in a conifer forest~~; h~~. However, they did not assess the damage caused in the understory and substrate layers. Montealegre et al. (2014) found good correlation between field measured CBI values and a set of post-fire LiDAR metrics, which were used to classify burn severity levels. Despite reporting a global accuracy of 85.5%, their results are not comparable to ours since they did not estimate CBI, but classified severity levels into three broad classes. Likewise, Wang and Glenn (2009) classified burn severity levels in sagebrush steppe rangelands based on vegetation height changes obtaining a global accuracy of 84%. While ~~the use of~~calculating height differences can be useful for sagebrush ecosystems, this metric may not be the most adequate to evaluate severity in forested areas, for instance due to the presence of snags, as suggested by Goetz et al. (2010), and confirmed by our simulation results.

The separation of the strata in the computation of WARC can impact the results and need to be adjusted to the study area. The separation between understory and overstory vegetation was set to 2m for our simulations given the relatively short trees of the simulated plots. For the King Fire with much taller trees, the original 5m thresholds established for the CBI protocol (Key and Benson 2006) yielded better results. Regarding the separation between understory and substrate layers, the 0.45 m threshold worked well for the simulated and the King Fire study site~~; h~~. However, the convolution of the signal is expected to be higher in low severity areas as well as in steep terrain (Harding and Carabajal 2005; Huang et al. 2017). Our simulations considered relatively flat terrain, with slope <5º, reducing the impact of slope on the signal. Therefore, further research is needed to assess the influence of this parameter in the results. In the case of pseudo-waveforms created from discrete return data, although slope can affect ground filtering algorithms {Montealegre, 2015 #82}, the convolution of ground and understory over steep terrain would be less problematic. Additionally, we assumed the same species for the understory and the overstory layers. This assumption should not significantly affect the results since our approach to estimate severity is based on the relative change of the waveform, this assumption should not affect the results. Lamelas et al., {, 2019 #83} reported the impact of scan angle on fuel type classification using the spectral angle mapper (SAM) classifier over an LVIS LiDAR signature library created from simulated waveforms. Although these authors found scan angle an important source of error in the classification, it was probably due to the large scan angles tested up to 20º, beyond the scan-angle limit of the LVIS sensor (https://lvis.gsfc.nasa.gov/Home/instrumentdetails.html; last access on 14th March 2020), and the sensitivity of the SAM algorithm to even small changes in the shape of the waveform. We tested the impact of off-nadir observations, up to 8 º {Hancock, 2019 #84; table 1}, on the metrics and found no consistent bias on most of them. Correlation between the nadir and off-nadir metrics remained above 0.9 for all metrics but RH25, RH20, RH10 and HTRT. In the case of WARC, correlation was higher than 0.99. These results agrees with Hancock et. {, 2019 #84}, who also found no impact of scan angles less than 8º on the metrics derived from simulated LVIS waveforms.

We run the FLIGHT model in forward mode to evaluate the sensitivity of full waveform LiDAR to a wide range of severity levels (Fig. 5). Inversion of the FLIGHT radiative transfer model has been applied for the estimation of forest structural parameters from LiDAR waveforms (Bye et al. 2017), so a similar approach should be possible for the retrieval of severity. Other studies already applied an RTM inversion to directly retrieve CBI values but from multispectral data (Chuvieco et al. 2007; De Santis et al. 2010).

~~The application of the WARC metric to the King Fire, with different vegetation characteristics than those of our simulated plots, proved the robustness and generalization capabilities of this metric to estimate severity.~~ The King Fire case study has its limitations to test the robustness of the metrics since the LiDAR data has different pre- and post-fire survey configurations and sensors and the data were not full waveform. This issues require further research to draw more definitive conclusions. Nevertheless, the application of the WARC metric to the King Fire, with different vegetation characteristics than those of our simulated plots, showed the robustness and generalization capabilities of this metric to estimate severity. The availability of pre- and post-fire LiDAR data along with concomitant field measures of the GeoCBI, makes it a unique dataset to evaluate the potential of LiDAR data for the assessment of fire severity. Furthermore, it also allows to demonstrate the possibility of applying the method to the more frequent airborne LiDAR discrete return data by generating pseudo-waveforms.

Contrary to the simulation results, structural metrics showed almost the same sensitivity as the WARC for the King Fire, most probably due to large fuel amounts consumed by the fire (Coen et al. 2018). Although structural metrics have shown significant differences between burned and unburned areas in boreal forests (Goetz et al. 2010; Wulder et al. 2009), and can be useful to evaluate specific impacts of fires, such as biomass consumed, the ability of these metrics to provide an integrated measure of severity, such as the CBI or the GeoCBI, which also accounts for tree mortality, may be limited. Moreover, our approach is based on a single simple metric, increasing its generalization capability, as opposed to previous studies that included multiple metrics~~, reducing their generalization capability~~. The WARC consistency for both, the simulated data as well as the King Fire case study, indicate the potential for the broad applicability of this metric. Recently, Hu et al. (2019) also proposed a single metric to estimate burn severity from LiDAR data. The performance of this metric was evaluated against changes in LAI, canopy cover and tree height, but not against field measures of CBI or GeoCBI. Their metric shows similarities to WARC, as it is based on the change in the area of the height percentile profile (PAC), but their metric is computed from the height distribution of returns and thus only account for changes in structure. ~~Instead~~ Contrary, WARC is derived from the intensity, which is affected by the radiometric changes resulting from ~~capturing changes~~ the modification in soil and leaf color. ~~Moreover,~~A comprehensive comparison between -PAC and WARC was not feasible over our simulated scenarios since PAC can only be derived from discrete return data. However, we tested PAC over the King Fire and found poorer performance compared to WARC, with R^2= 0.55 and RMSE= 0.53.~~the performance of PAC was evaluated against changes in LAI, canopy cover and tree height. Therefore, its ability to capture changes in the understory and the substrate is uncertain yet.~~

The capabilities of the WARC were evaluated against integrated measures of severity, the CBI and the GeoCBI~~; h~~. However, it has the potential for evaluating specific fire effects, for instance biomass consumption (Garcia et al. 2017a), to be later introduced into a single integrated severity index as Morgan et al. (2014) propose.

The model fitted to estimate GeoCBI values from the WARC offered good performance (R^2=0.78 and RMSE=0.37) but there is still room for improvement. The use of the same sensor with identical system settings and the same survey configuration for the pre- and post-fire acquisitions would ~~also~~ reduce the noise in the intensity data.~~First, by improving the radiometric normalization of the intensity data. W~~ In addition, we used a simple radiometric normalization of the intensity data to remove the effect of range variation across the study area produced by rough topography and the different flight height of the two LiDAR datasets. Better intensity normalization would help to improve our results reducing the noise of the intensity values used to generate the pseudo-waveforms. More robust normalization approaches have been proposed in the literature including an exponent factor to the range ratio to account for energy attenuation through the canopy, as well as a parameter to account for the automatic gain control (Gatziolis 2011; Korpela et al. 2010).~~ Better intensity normalization would help to improve our results reducing the noise of the intensity values used to generate the pseudo-waveforms; h~~ However, the available data did not allow the application of such normalization methods. Moreover, our between-sensor calibration model was derived from non-vegetated surfaces characterized by single returns. Therefore, its application to other types of returns (2^{th} – 4^{th}) may not be optimum. Despite this, the noise introduced in this group of returns by our between-sensor calibration is expected to be small, since the improvement in consistency of intensity values after normalization is less substantial in 2^{nd} and subsequent returns than for 1^{st} and single returns (Gatziolis 2011). ~~The use of the same sensor with identical system settings and the same survey configuration for the pre- and post-fire acquisitions would also reduce the noise in the intensity data.~~

The severity map derived using the WARC metric showed good agreement with the MTBS Landsat-based map, but showed some overestimation over the north west part of the Rubicon Valley. Although a thorough comparison between the LiDAR and Landsat-products is out of the scope of our study, differences between the two products could be explained by the different acquisition time of the post-fire LiDAR and Landsat data. The LiDAR data was collected shortly after the fire, thus representing an initial severity assessment. Meanwhile, the Landsat image was acquired nearly a year after the fire and so, it corresponded to an extended assessment, which could be influenced by vegetation recovery processes. Moreover, the inability of Landsat data to capture fire damage to the understory and substrate, particularly under unaffected dense canopies, can result in higher uncertainties in moderate severity areas {Chuvieco, 2007 #34;Miller, 2015 #36}, contributing also to the differences between the two products.

Our method requires having pre- and post-fire LiDAR data, which is a constraint given the limited spatial and temporal coverage of airborne LiDAR sensors. The method is potentially applicable to the recently launched Global Ecosystem Dynamics Investigation (GEDI) sensor onboard the International Space Station (Dubayah et al. 2014; Stysley et al. 2016). The sampling scheme should be taken into account, as it will not provide co-registered footprints. In such a case, an object-based approach could~~can~~ be applied by comparing typical average pre- and post-fire waveforms for each object. Additionally, integration of LiDAR and optical data (Klauberg et al. 2019; Kwak et al. 2010) could improve the assessment of fire caused damage by exploiting the synergy of the structural and the functional information derived from LiDAR and multispectral data, respectively.

5. Conclusions

~~A new method proved t~~The potential of LiDAR data to perform comprehensive evaluations of the severity of wildfires has been evaluated. ~~It relies on a simple single~~A new metric is proposed, WARC, ~~that~~ which accounts for the changes in all strata. Whereas previous studies using LiDAR just focused on the structural changes caused by fires in vegetation, we have demonstrated that LiDAR was ~~Moreover, the metric proved to be~~ able to capture severity beyond structural changes, as it is also sensitive to leaf scorching, which is related to tree mortality, and soil color changes.

The 3D FLIGHT radiative transfer model run in a forward mode enabled the evaluation of the sensitivity of LiDAR metrics to the severity of fires over a large range of severity levels. Our results demonstrated that common LiDAR metrics, which were developed for vegetation modeling, are less appropriate to estimate the fire severity than WARC.

Application of the WARC metric to the real case study of the King Fire, California, with very different vegetation characteristics of those of our simulated plots, ~~proved~~ revealed the robustness and generalization capability of this metric. Although ~~differences with~~improvement over the best performing common LiDAR metrics ~~were~~ was ~~very~~ small in this case, the WARC still outperformed ~~all other metrics~~them.

~~In this study we have proved t~~The potential of LiDAR data to estimate severity as measured by integrated indices such as the CBI and the GeoCBI was evaluated; yet, it can also be applied to assess specific fire effects that can be subsequently used in integrated evaluations of severity of wildfires.

Acknowledgements

This work was partially supported by the Marie Curie International Outgoing Fellowship within the 7th European Community Framework Programme (ForeStMap—3D Forest

Structure Monitoring and Mapping, Project Reference: 629376). The contents of this paper reflect solely the authors' views and not those of the European Commission. LiDAR data for the King Fire was provided by the JPL Airborne Snow Observatory. We greatly appreciate the constructive comments by the four anonymous reviewers, who greatly helped improve the manuscript.

References

Alonzo, M., Morton, D.C., Cook, B.D., Andersen, H.-E., Babcock, C., & Pattison, R. (2017). Patterns of canopy and surface layer consumption in a boreal forest fire from repeat airborne LiDAR. *Environmental Research Letters, 12*, 065004

Blair, J.B., Rabine, D.L., & Hofton, M.A. (1999). The laser vegetation imaging sensor: A medium-altitude, digitisation-only, airborne laser altimeter for mapping vegetation and topography. *ISPRS Journal of Photogrammetry and Remote Sensing, 54,* 115-122

Boer, M.M., Macfarlane, C., Norris, J., Sadler, R.J., Wallace, J., & Grierson, P.F. (2008). Mapping burned areas and burn severity patterns in SW Australian eucalypt forest using remotely-sensed changes in leaf area index. *Remote Sensing of Environment, 112*, 4358-4369

Bond, W.J., Woodward, F.I., & Midgley, G.F. (2005). The global distribution of ecosystems in a world without fire. *New Phytologist, 165*, 525-538

Bouvier, M., Durrieu, S., Fournier, R.A., & Renaud, J.-P. (2015). Generalizing predictive models of forest inventory attributes using an area-based approach with airborne LiDAR data. *Remote Sensing of Environment, 156*, 322-334

Bye, I.J., North, P.R.J., Los, S.O., Kljun, N., Rosette, J.A.B., Hopkinson, C., Chasmer, L., & Mahoney, C. (2017). Estimating forest canopy parameters from satellite waveform LiDAR by inversion of the FLIGHT three-dimensional radiative transfer model. *Remote Sensing of Environment, 188*, 177-189

Casas, Á., García, M., Siegel, R.B., Koltunov, A., Ramírez, C., & Ustin, S. (2016). Burned forest characterization at single-tree level with airborne laser scanning for assessing wildlife habitat. *Remote Sensing of Environment, 175*, 231-241

Coen, J.L., Stavros, E.N., & Fites-Kaufman, J.A. (2018). Deconstructing the King megafire. *Ecological Applications*, *28*, 1565-1580

Chen, B., Pang, Y., Li, Z., Lu, H., North, M.P., Rosette, J.A.B., & Yan, M. (2020). Forest signal detection for photon counting LiDAR using Random Forest. *Remote Sensing Letters*, *11*, 37-46

Chuvieco, E., De Santis, A., Riaño, D., & Halligan, K. (2007). Simulation Approaches for Burn Severity Estimation Using Remotely Sensed Images. *Fire Ecology, 3*, 129-150

Chuvieco, E., Martínez, S., Román, M.V., Hantson, S., & Pettinari, M.L. (2014). Integration of ecological and socio-economic factors to assess global vulnerability to wildfire. *Global Ecology and Biogeography, 23*, 245-258

Chuvieco, E., Riaño, D., Danson, F.M., & Martin, P. (2006). Use of a radiative transfer model to simulate the postfire spectral response to burn severity. *Journal of Geophysical Research: Biogeosciences, 111*

Dawson, T.P., Curran, P.J., & Plummer, S.E. (1998). LIBERTY—Modeling the Effects of Leaf Biochemical Concentration on Reflectance Spectra. *Remote Sensing of Environment, 65*, 50-60

De Santis, A., Asner, G.P., Vaughan, P.J., & Knapp, D.E. (2010). Mapping burn severity and burning efficiency in California using simulation models and Landsat imagery. *Remote Sensing of Environment*, *114*, 1535-1545

De Santis, A., & Chuvieco, E. (2007). Burn severity estimation from remotely sensed data: Performance of simulation versus empirical models. *Remote Sensing of Environment, 108*, 422-435

De Santis, A., & Chuvieco, E. (2009). GeoCBI: A modified version of the Composite Burn Index for the initial assessment of the short-term burn severity from remotely sensed data. *Remote Sensing of Environment, 113*, 554-562

Disney, M.I., Lewis, P., Gomez-Dans, J., Roy, D., Wooster, M.J., & Lajas, D. (2011). 3D radiative transfer modelling of fire impacts on a two-layer savanna system. *Remote Sensing of Environment*, *115*, 1866-1881

Drake, J.B., Dubayah, R.O., Knox, R.G., Clark, D.B., & Blair, J.B. (2002). Sensitivity of large-footprint lidar to canopy structure and biomass in a neotropical rainforest. *Remote Sensing of Environment*, *81*, 378-392

Dubayah, R., Goetz, S.J., Blair, J.B., Fatoyinbo, T., Hansen, M., Healey, S., Hofton, M.A., Hurtt, G., Kellner, J., luthcke, S., & Swatantran, A. (2014). The global ecosystem dynamics investigation. In. AGU Fall Meeting, San Francisco, California, U.S.

Féret, J.B., Gitelson, A.A., Noble, S.D., & Jacquemoud, S. (2017). PROSPECT-D: Towards modeling leaf optical properties through a complete lifecycle. *Remote Sensing of Environment, 193*, 204-215

Fowler, C.T. (2003). Human Health Impacts of Forest Fires in the Southern United States: A Literature Review. *Journal of Ecological Anthropology, 7*, 39-63

French, N.H.F., Kasischke, E.S., Hall, R.J., Murphy, K.A., Verbyla, D.L., Hoy, E.E., & Allen, J.L. (2008). Using Landsat data to assess fire and burn severity in the North American boreal forest region: an overview and summary of results. *International Journal of Wildland Fire, 17*, 443-462

García, M., Riaño, D., Chuvieco, E., & Danson, F.M. (2010). Estimating biomass carbon stocks for a Mediterranean forest in Spain using height and intensity LiDAR data. *Remote Sensing of Environment*, *114*, 816-830

Garcia, M., Saatchi, S., Casas, A., Koltunov, A., Ustin, S., Ramirez, C., Garcia-Gutierrez, J., & Balzter, H. (2017a). Quantifying biomass consumption and carbon release from the California Rim fire by integrating airborne LiDAR and Landsat OLI data. *Journal of Geophysical Research: Biogeosciences*, n/a-n/a

García, M., Saatchi, S., Casas, A., Koltunov, A., Ustin, S.L., Ramirez, C., & Balzter, H. (2017b). Extrapolating Forest Canopy Fuel Properties in the California Rim Fire by Combining Airborne LiDAR and Landsat OLI Data. *Remote Sensing*, *9*, 394

Gatziolis, D. (2011). Dynamic Range-based Intensity Normalization for Airborne, Discrete Return Lidar Data of Forest Canopies. *Photogrammetric Engineering & Remote Sensing*, *77*, 251-259

Goetz, S.J., Sun, M., Baccini, A., & Beck, P.S.A. (2010). Synergistic use of spaceborne lidar and optical imagery for assessing forest disturbance: An Alaska case study. *Journal of Geophysical Research: Biogeosciences*, *115*

Harding, D.J., & Carabajal, C.C. (2005). ICESat waveform measurements of within-footprint topographic relief and vegetation vertical structure. *Geophysical Research Letters*, *32*

Hood, S.M., Varner, J.M., van Mantgem, P., & Cansler, C.A. (2018). Fire and tree death: understanding and improving modeling of fire-induced tree mortality. *Environmental Research Letters*, *13*, 113004

Hu, T., Ma, Q., Su, Y., Battles, J.J., Collins, B.M., Stephens, S.L., Kelly, M., & Guo, Q. (2019). A simple and integrated approach for fire severity assessment using bi-temporal airborne LiDAR data. *International Journal of Applied Earth Observation and Geoinformation, 78*, 25-38

Huang, H., Liu, C., Wang, X., Biging, G.S., Chen, Y., Yang, J., & Gong, P. (2017). Mapping vegetation heights in China using slope correction ICESat data, SRTM, MODIS-derived and climate data. *ISPRS Journal of Photogrammetry and Remote Sensing, 129*, 189-199

Jain, T., Graham, R., & Pilliod, D. (2004). Tongue-tied: confused meanings for common fire terminology can lead to fuels mismanagement. *Wildfire, July/August*, 22-26

Jakubuaskas, M.E., Lulla, K.P., & Mausel, P.W. (1990). Assessment of vegetation change in a fire-altered forest landscapes. *Photogrammetric Engineering and Remote Sensing, 56*, 371-377

Keeley, J.E. (2009). Fire intensity, fire severity and burn severity: a brief review and suggested usage. *International Journal of Wildland Fire, 18*, 116-126

Key, C.H., & Benson, N.C. (2006). Landscape Assessment: Ground measure of severity, the Composite Burn Index; and Remote sensing of severity, the Normalized Burn Ratio. In D.C. Lutes, R.E. Keane, J.F. Caratti, C.H. Key, N.C. Benson, S. Sutherland, & L.J. Gangi (Eds.). In D.C. Lutes; R.E. Keane; J.F. Caratti; C.H. Key; N.C. Benson; S. Sutherland; and L.J. Gangi. 2006. FIREMON: Fire Effects Monitoring and Inventory System. USDA Forest Service, Rocky Mountain Research Station, Ogden, UT. Gen. Tech. Rep. RMRS-GTR-164-CD: LA 1-51.

Klauberg, C., Hudak, A.T., Silva, C.A., Lewis, S.A., Robichaud, P.R., & Jain, T.B. (2019). Characterizing fire effects on conifers at tree level from airborne laser scanning and high-resolution, multispectral satellite data. *Ecological Modelling, 412*, 108820

Korpela, I., Ørka, H.O., Hyyppä, J., Heikkinen, V., & Tokola, T. (2010). Range and AGC normalization in airborne discrete-return LiDAR intensity data for forest canopies. *ISPRS Journal of Photogrammetry and Remote Sensing, 65*, 369-379

Kwak, D.A., Chung, J., Lee, W.K., Kafatos, M., Lee, S.Y., Cho, H.K., & Lee, S.H. (2010). Evaluation for Damaged Degree of Vegetation by Forest Fire using LiDAR and Digital Aerial Photograph. *Photogrammetric Engineering and Remote Sensing*, *76*, 277-287

Landmann, T. (2003). Characterizing sub-pixel Landsat ETM+ fire severity on experimental fires in the Kruger National Park, South Africa : research letter. *South African Journal of Science, 99*, 357-360

Lefsky, M.A., Cohen, W.B., Acker, S.A., Parker, G.G., Spies, T.A., & Harding, D. (1999). Lidar Remote Sensing of the Canopy Structure and Biophysical Properties of Douglas-Fir Western Hemlock Forests. *Remote Sensing of Environment, 70*, 339-361

Lentile, L.B., Holden, Z.A., Smith, A.M.S., Falkowski, M.J., Hudak, A.T., Morgan, P., Lewis, S.A., Gessler, P.E., & Benson, N.C. (2006). Remote sensing techniques to assess active fire characteristics and post-fire effects. *International Journal of Wildland Fire, 15*, 319-345

Lewis, S.A., Wu, J.Q., & Robichaud, P.R. (2006). Assessing burn severity and comparing soil water repellency, Hayman Fire, Colorado. *Hydrological Processes, 20*, 1-16

McCarley, T.R., Kolden, C.A., Vaillant, N.M., Hudak, A.T., Smith, A.M.S., Wing, B.M., Kellogg, B.S., & Kreitler, J. (2017). Multi-temporal LiDAR and Landsat quantification of fire-induced changes to forest structure. *Remote Sensing of Environment*, *191*, 419-432

Melendo-Vega, J.R., Martín, M.P., Pacheco-Labrador, J., González-Cascón, R., Moreno, G., Pérez, F., Migliavacca, M., García, M., North, P., & Riaño, D. (2018). Improving the

Performance of 3-D Radiative Transfer Model FLIGHT to Simulate Optical Properties of a Tree-Grass Ecosystem. *Remote Sensing*, *10*, 2061

Miller, J.D., Knapp, E.E., Key, C.H., Skinner, C.N., Isbell, C.J., Creasy, R.M., & Sherlock, J.W. (2009). Calibration and validation of the relative differenced Normalized Burn Ratio (RdNBR) to three measures of fire severity in the Sierra Nevada and Klamath Mountains, California, USA. *Remote Sensing of Environment*, *113*, 645-656

Miller, J.D., & Quayle, B. (2015). Calibration and validation of inmediate post-fire satellite-derived data to three severity metrics. *Fire Ecology*, *11*, 12-30

Miller, J.D., & Thode, A.E. (2007). Quantifying burn severity in a heterogeneous landscape with a relative version of the delta Normalized Burn Ratio (dNBR). *Remote Sensing of Environment*, *109*, 66-80

Montealegre, A., Lamelas, M., Tanase, M., & de la Riva, J. (2014). Forest Fire Severity Assessment Using ALS Data in a Mediterranean Environment. *Remote Sensing*, *6*, 4240

Montesano, P.M., Rosette, J.A.B., Sun, G., North, M.P., Nelson, R.F., Dubayah, R.O., Ranson, K.J., & Kharuk, V. (2015). The uncertainty of biomass estimates from modeled ICESat-2 returns across a boreal forest gradient. *Remote Sensing of Environment*, *158*, 95-109

Morgan, P., Keane, R.E., Dillon, G.K., Jain, T.B., Hudak, A.T., Karau, E.C., Sikkink, P.G., Holden, Z.A., & Strand, E.K. (2014). Challenges of assessing fire and burn severity using field measures, remote sensing and modelling. *International Journal of Wildland Fire, 23*, 1045-1060

Neary, D.G., Klopatek, C.C., DeBano, L.F., & Ffolliott, P.F. (1999). Fire effects on belowground sustainability: a review and synthesis. *Forest Ecology and Management, 122*, 51-71

Nikonovas, T., North, P.R.J., & Doerr, S.H. (2017). Particulate emissions from large North American wildfires estimated using a new top-down method. *Atmospheric Chemistry and Physics*, *17*, 6423-6434

North, P.R.J. (1996). Three-dimensional forest light interaction model using a Monte Carlo method. *IEEE Transactions on Geoscience and Remote Sensing*, *34*, 946-956

North, P.R.J., Rosette, J.A.B., Suárez, J.C., & Los, S.O. (2010). A Monte Carlo radiative transfer model of satellite waveform LiDAR. *International Journal of Remote Sensing*, *31*, 1343-1358

Reddy, A.D., Hawbaker, T.J., Wurster, F., Zhu, Z., Ward, S., Newcomb, D., & Murray, R. (2015). Quantifying soil carbon loss and uncertainty from a peatland wildfire using multi-temporal LiDAR. *Remote Sensing of Environment*, *170*, 306-316

Stavros, E., Tane, Z., Kane, V., Veraverbeke, S.S.N., McGaughey, R., Lutz, J., Ramirez, C., & Schimel, D. (2016). Unprecedented remote sensing data over the King and Rim fires megafires in the Sierra Nevada mountains of California. *Ecology*

Stephens, S.L., Agee, J.K., Fulé, P.Z., North, M.P., Romme, W.H., Swetnam, T.W., & Turner, M.G. (2013). Managing Forests and Fire in Changing Climates. *Science*, *342*, 41-42

Stysley, P.R., Coyle, D.B., Clarke, G.B., Frese, E., Blalock, G., Morey, P., Kay, R.B., Poulios, D., & Hersh, M. (2016). *Laser production for NASA's Global Ecosystem Dynamics Investigation (GEDI) lidar*. SPIE

van der Werf, G.R., Randerson, J.T., Giglio, L., Collatz, G.J., Mu, M., Kasibhatla, P.S., Morton, D.C., DeFries, R.S., Jin, Y., & van Leeuwen, T.T. (2010). Global fire emissions and the contribution of deforestation, savanna, forest, agricultural, and peat fires (1997–2009). *Atmospheric Chemistry and Physics*, *10*, 11707-11735

Viana-Soto, A., Aguado, I., & Martínez, S. (2017). Assessment of Post-Fire Vegetation Recovery Using Fire Severity and Geographical Data in the Mediterranean Region (Spain). *Environments, 4*

Wang, C., & Glenn, N.F. (2009). Estimation of fire severity using pre- and post-fire LiDAR data in sagebrush steppe rangelands. *International Journal of Wildland Fire, 18*, 848-856

Whitman, E., Parisien, M.-A., Thompson, D.K., Hall, R.J., Skakun, R.S., & Flannigan, M.D. (2018). Variability and drivers of burn severity in the northwestern Canadian boreal forest. *Ecosphere, 9*, e02128

Whittier, T.R., & Gray, A.N. (2016). Tree mortality based fire severity classification for forest inventories: A Pacific Northwest national forests example. *Forest Ecology and Management, 359*, 199-209

Wing, B.M., Ritchie, M.W., Boston, K., Cohen, W.B., & Olsen, M.J. (2015). Individual snag detection using neighborhood attribute filtered airborne lidar data. *Remote Sensing of Environment, 163*, 165-179

Wulder, M.A., White, J.C., Alvarez, F., Han, T., Rogan, J., & Hawkes, B. (2009). Characterizing boreal forest wildfire with multi-temporal Landsat and LIDAR data. *Remote Sensing of Environment, 113*, 1540-1555

Highlights

- The potential of LiDAR to estimate fire damage is assessed using a 3D RTM approach.
- The new metric, WARC, provides a comprehensive evaluation of severity.
- The WARC outperformed common LiDAR metrics used for vegetation modeling.
- The robustness and generalization power of the method was shown over the King Fire.

EVALUATING THE POTENTIAL OF LiDAR DATA FOR FIRE DAMAGE ASSESSMENT: A RADIATIVE TRANSFER MODEL APPROACH.

Mariano García[1], Peter North[2], Alba Viana-Soto[1], Natasha E. Stavros[3], Jackie Rosette[2], M. Pilar Martín[4], Magí Franquesa[1], Rosario González-Cascón[5], David Riaño[4,6], Javier Becerra[4], Kaiguang Zhao[7,8]

[1] Environmental Remote Sensing Research Group, Department of Geology, Geography and the Environment, Universidad de Alcalá. Calle Colegios 2, Alcalá de Henares, 28801, Spain.

[2] Global Environmental Modelling and Earth Observation (GEMEO), Department of Geography, Swansea University, SA2 8PP, United Kingdom.

[3] Jet Propulsion Laboratory, California Institute of Technology, 4800 Oak Grove Drive, Pasadena, CA 91109, USA.

[4] Environmental Remote Sensing and Spectroscopy Laboratory (SpecLab), Spanish National Research Council (CSIC), Albasanz 26-28, 28037, Madrid, Spain.

[5] Department of Environment, National Institute for Agriculture and Food Research and Technology (INIA), Ctra. Coruña, Km. 7,5, Madrid, 28040, Spain.

[6] Center for Spatial Technologies and Remote Sensing (CSTARS), University of California, 139 Veihmeyer Hall, One Shields Avenue, Davis, CA 95616, USA.

[7] School of Environment and Natural Resources, Ohio Agricultural Research and Development Center, The Ohio State University, Wooster, OH 44691, USA.

[8] School of Environment and Natural Resources, Environmental Science Graduate Program, The Ohio State University, Columbus, OH 43210, USA.

ABSTRACT

Providing accurate information on fire effects is critical to understanding post-fire ecological processes and to design appropriate land management strategies. Multispectral imagery from optical passive sensors is commonly used to estimate fire damage, yet this type of data is only sensitive to the effects in the upper canopy. This paper evaluates the sensitivity of full waveform LiDAR data to estimate the severity of wildfires using a 3D radiative transfer model approach. The approach represents the first attempt to evaluate the effect of different fire impacts, i.e. changes in vegetation structure as well as soil and leaf color, on the LiDAR signal. The FLIGHT 3D radiative transfer model was employed to simulate full waveform data for 10 plots representative of Mediterranean ecosystems along with a wide range of post-fire scenarios characterized by different severity levels, as defined by the composite burn index (CBI). A new metric is proposed, the waveform area relative change (WARC), which provides a comprehensive severity assessment considering all strata and accounting for changes in structure and leaf and soil color. It showed a strong correlation with CBI values (Spearman's Rho = 0.9 ± 0.02), outperforming the relative change of LiDAR metrics commonly applied for vegetation modeling, such as the relative height of energy quantiles (Spearman's Rho = 0.56 ± 0.07, for the relative change of RH60, the second strongest correlation). Logarithmic models fitted for each plot based on the WARC yielded very good performance with R^2 (± standard deviation) and RMSE (± standard deviation) of 0.8 (± 0.05) and 0.22 (± 0.03), respectively. LiDAR metrics were evaluated over the King Fire, California, U.S., for which pre- and post-fire discrete return airborne LiDAR data were available. Pseudo-waveforms were computed after radiometric normalization of the intensity data. The WARC showed again the strongest correlation with field measures of GeoCBI values (Spearman's Rho = 0.91), closely followed by the relative change of

RH40 (Spearman's Rho = 0.89). The logarithmic model fitted using WARC offered an R^2 of 0.78 and a RMSE of 0.37. The accurate results obtained for the King Fire, with very different vegetation characteristics compared to our simulated data, demonstrate the robustness of the new metric proposed and its generalization capabilities to estimate the severity of fires.

Keywords: LiDAR, radiative transfer models, full waveform simulation, fire effects, severity, King Fire.

1. INTRODUCTION

The impact of fires encompasses a wide variety of effects, from environmental, such as vegetation pattern distribution, wildlife habitat quality and particulate and greenhouse gases emissions (Bond et al. 2005; Casas et al. 2016; Nikonovas et al. 2017; van der Werf et al. 2010), to socio-economic, including health issues related to air quality, property damage or even human casualties (Chuvieco et al. 2014; Fowler 2003). Fire impacts also vary spatially, from landscape (e.g. changes in vegetation composition and structure) to continental or global scales (e.g. biomass burning emissions); and over time, including the fire environment, post-fire environment and the response phases of the so-called fire continuum (Jain et al. 2004). Fire managers require information on fire effects to support strategic planning before and during fires, to establish mitigation strategies aimed at reducing soil erosion, establishment of invasive species, as well as to evaluate the results of prescribed fires (Morgan et al. 2014). Therefore, accurately quantifying fire effects is necessary to improve our understanding of the impact of fires on ecosystem processes as well as the carbon cycle. This becomes especially important as with projected climate change an increase in forest fires is expected (Stephens et al. 2013).

Fire damage is generally described in terms of its severity, which represents the ecological change caused by fire (Lentile et al. 2006). The use of an appropriate terminology to describe post-fire effects has been a subject of discussion. Some authors advocate for the use of fire severity when considering immediate fire effects as a result of the combustion process and the term burn severity when considering longer-term effects, thus including ecosystem response processes (Lentile et al. 2006). On the other hand, Keeley (2009) recommend not including ecosystem response in fire or burn severity measures since some of the ecosystems response processes are not related to the severity of the fire event, and in such a case the interchangeable use of both terms would not be problematic. Similar to French et al. (2008) and Morgan et al. (2014), hereinafter we will use the generic term severity to generally describe the ecological change produced by fires.

A plethora of field measures has been designed to quantify severity according to the particular objectives of the fire damage assessment. These measures include changes in soil characteristics such as color, structure or hydrophobicity (Lewis et al. 2006; Neary et al. 1999), tree mortality (Hood et al. 2018; Whittier and Gray 2016) or biomass consumed (Garcia et al. 2017a). Key and Benson (2006) proposed the composite burn index (CBI), which integrates different post-fire effects into a single semi-quantitative index ranging from 0 (unburned) to 3 (completely burned). The CBI was designed to serve as a field validation of remotely sensed estimations of burn severity. De Santis and Chuvieco (2009) proposed a modified version of the CBI, the GeoCBI, that improved severity estimations from remote sensing by accounting for the fractional cover and leaf area index (LAI) changes of the intermediate and upper canopy strata. Despite the generalized acceptance and application of the CBI/GeoCBI, particularly in remote sensing studies, they are highly subjective. Morgan et al. (2014) recommend to directly measure fire effects, which can be later integrated according to an objective severity measurement instead of collapsing them into a single integrated severity index, such as the CBI.

The heterogeneity of fire effects both in space and time make remote sensing techniques a suitable alternative to field measures given their comprehensive and systematic view of the Earth. Most attempts have been based on the use of multispectral imagery due to the spectral changes associated with vegetation removal, soil exposure, decrease in moisture content of soil and vegetation, or carbon and ash deposition that result from fires (Jakubuaskas et al. 1990). The potential of remotely sensing data, particularly Landsat imagery, for mapping wildfire severity has been demonstrated across the world from boreal forests to savannas (Boer et al. 2008; Landmann 2003; Viana-Soto et al. 2017; Whitman et al. 2018). The most common approach to derive severity from optical remote sensing develops empirical relations between the normalized burn ratio (NBR) (Key and Benson 2006) or some of its derivatives, namely the differenced NBR (dNBR) (Miller and Thode 2007) or the relative dNBR (RdNBR) (Miller et al. 2009), with the CBI or the GeoCBI. More recently, methods based on radiative transfer models (RTM) have been developed to improve the retrieval of severity estimates from the spectral information recorded by spaceborne sensors (Chuvieco et al. 2007; De Santis et al. 2010; Disney et al. 2011). RTM approaches can help improving our understanding of the factors modifying reflectance and offer better universality than empirical approaches, yet their performance is subject to an appropriate model parameterization. Performance of the different severity retrieval approaches using optical data varies widely in terms of R^2 and RMSE but in general, low and high severity values are accurately predicted while larger errors are found for intermediate severity values (Chuvieco et al. 2007; De Santis and Chuvieco 2007). This can be explained by the inability of

Landsat data to accurately capture the actual fire damage to under- and mid-story vegetation in low and moderate severity areas, especially under high canopy cover (Miller and Quayle 2015).

LiDAR data provide detailed 3D information on forest structure, so it can evaluate the severity on different strata. Specific fire caused damage such as changes in vegetation structure (McCarley et al. 2017; Wulder et al. 2009), biomass consumption (Garcia et al. 2017a), LAI changes (Hu et al. 2019) or habitat suitability (Casas et al. 2016), have been generally estimated from LiDAR data, rather than an integrated measure of severity as that provided by CBI. While only changes in the overstory layer are generally assessed, LiDAR has potential to separate biomass consumption at different canopy levels (Alonzo et al. 2017). Assessments of fire impacts using LiDAR data have been based so far on empirical relationships. Although RTM approaches have been applied to LiDAR data, they focused on the retrieval of biophysical information such as LAI, canopy height or fractional cover (Bye et al. 2017), assessment of the impact of sensor and survey characteristics on canopy height estimation (Disney et al. 2010), or to generate a fuel type LiDAR library (Lamelas-Gracia et al. 2019), but no research has been done yet on the simulation of LiDAR data to assess fire impacts, which can help improving our understanding of the capabilities of LiDAR systems to assess the severity of wildfires. The simplest approach to burn assessment consists of evaluating vegetation height changes. Although this successfully correlated to field measures in a sagebrush ecosystem (Wang and Glenn 2009), over forest areas this variable alone may not capture severity appropriately due to vegetation regrowth or presence of dead standing trees, so-called snags (Goetz et al. 2010). Differences between LiDAR derived digital elevation models (DEMs) have been also utilized to estimate soil consumption in peat swamps (Reddy et al. 2015). So far, only a study in a Mediterranean forest in Spain applied LiDAR data to classify the severity of fires using a logistic regression between

LiDAR and field measured CBI values (Montealegre et al. 2014). Nevertheless, the metrics only considered returns above 1 m not completely evaluating fire effects on the ecosystem.

These previous studies were based on a set of structural metrics derived from the height distribution of returns, founded on the changes in vegetation structure produced by fires. However, they fail to provide a complete characterization of the severity, as they focus only on structural changes rather than also considering tree mortality or change in leaf color (scorched leaves) or soil (charred soil). This is particularly relevant for scorched trees that may retain leaves at the moment of the LiDAR survey, thus preserving the pre-fire structure. On the other hand, LiDAR has proved successful to detect snags using intensity data (Casas et al. 2016; Wing et al. 2015). Therefore, further research is required to assess the utility of LiDAR data for providing an integrated estimation of the severity of wildfires. The main goal of this research was to assess the potential of LiDAR data for providing a comprehensive characterization of the severity of fires, beyond structural changes, considering all layers of a forest. The specific objectives were to: 1) assess the sensitivity of LiDAR data to different severity degrees as measured by CBI using a 3D RTM; 2) develop a new integrated LiDAR metric that better captures severity of a forest plot; 3) evaluate the proposed metric over an actual fire occurrence in a fire prone environment using pre- and post-fire airborne LiDAR data.

2. Methods

2.1. LiDAR full waveform simulations

Evaluation of fire effects requires analyzing changes over different strata, from the substrate to the upper canopy. Large footprint full waveform data provide better description of the vertical vegetation volume distribution, from the top of the canopy to the ground, including the understory layer, than discrete return data (Lim et al. 2003), thus making it ideal to evaluate severity of fires.

In order to evaluate the sensitivity of LiDAR data to different degrees of severity, the FLIGHT 3D RTM was selected to simulate LiDAR waveforms under different severity levels, including an unburned scenario representing the pre-fire conditions. FLIGHT was originally developed to model vegetation bidirectional reflectance (North 1996) and later extended to model LiDAR waveforms (North et al. 2010) and photon counting LiDAR returns (Chen et al. 2020; Montesano et al. 2015). The suitability of the FLIGHT 3D RTM to simulate full waveform and photon counting LiDAR data in forest environments have been widely demonstrated (Bye et al. 2017; Montesano et al. 2015; Morton et al. 2014; North et al. 2010; Rosette et al. 2013). The model is based on Monte Carlo evaluation of photon transport within a 3D representation of the vegetation, and can be configured for both airborne and satellite instruments. Waveforms are simulated by uniformly sampling the path of photons within the instantaneous field of view of the LiDAR sensor at a given position, accumulating the path length (equivalent to the time of signal) and energy from both laser and solar sources. Multiple orders of scattering are accounted for and the contribution of successive orders of scattering is reduced using an exponential function until contributions approach zero. The energy is binned into m bins, the width of which is defined by the sensor model temporal sampling. For this study the set of parameters defining the LiDAR sensor corresponded to the Land, Vegetation and Ice Sensor (LVIS) (Blair et al. 1999), listed in Table 1.

Insert Table 1

A forest plot or stand representation in FLIGHT can be generated statistically using fractional cover and crown size range values. Alternatively, if field measurements or airborne LiDAR data enabling tree delineation are available, a more realistic representation can be realized. Tree crowns are modeled using ellipsoidal or conical geometric primitives of given horizontal and vertical dimensions. The overlap between neighboring crowns is limited using a simple growth model. Within each crown, vegetation is represented as a turbid medium described by leaf area density, leaf-angle distribution, and the optical properties of the scene components, namely leaves, branch, shoot and ground. The ground is approximated using a planar surface with defined slope angle. In order to be able to simulate post-fire effects on different forest strata, including cases in which there is a tree canopy and understory vegetation both with various levels of fire damage, the FLIGHT model was modified to allow definition of different properties for understory and overstory vegetation.

2.2. Definition of post-fire effects scenarios

Simulation of fire effects first required the selection of a reference measure of fire damage. We used the CBI, which has been previously applied in other remote sensing simulation approaches for burn severity estimation from passive optical data (Chuvieco et al. 2007; Chuvieco et al. 2006; De Santis et al. 2010). The CBI consists of a visual assessment of fire effects on up to five vertical strata of the field plot under consideration. These strata are: A) substrate (rock and soil, duff, litter, and downed woody fuels); B) herbs, low shrubs and trees ≤ 1 m tall; C) tall shrubs and trees ≤ 5 m; D) suppressed and intermediate trees (10 ≤ DBH ≤ 25 cm; 8 ≤ canopy height ≤20 m); and E) dominant and co-dominant trees (DBH > 25 cm; canopy height >20 m). Fire effects are evaluated by analyzing soil charring, organic matter consumption, proportion of fuel consumed (change in cover), altered foliage (proportion of brown leaves), canopy mortality and char height. CBI also accounts for ecosystem response processes such as presence of colonizers or percentage of resprouting. All these changes are expressed relative (%) to the pre-fire situation (Key and Benson 2006). Each stratum is evaluated individually and rated between 0 and 3, and finally averaged to provide an estimate of the burn severity at the plot level. Although the CBI was initially designed to validate severity estimates derived from Landsat imagery, the variables considered to assess the ecological change caused by the fire makes it suitable also for LiDAR data.

With the purpose of simulating scenarios showing diverse degrees of post-fire severity using FLIGHT, we made some simplifications of the CBI taking into account those variables that LiDAR can actually measure. Similarly to Chuvieco et al. (2007), the first simplification consisted in reducing the five strata of the CBI to three by grouping strata B and C into the understory vegetation stratum, and strata D and E into the overstory stratum. The CBI variables considered for the simulations included charcoal and ash proportion for the substrate (soil charring); whereas for the understory and overstory layers, the percentage of foliage altered (PFA), i.e. change in leaf color; and percentage of cover change (PCC) were evaluated. In order to use remote sensing data, and more specifically LiDAR data, to evaluate the severity of fires, it is important to have in mind how the ecological changes observed in the field translate into the remotely sensed signal. Hence, changes in cover represent structural changes that LiDAR data can accurately capture. On the other hand, variation in color of scorched leaves results in changes in the spectral reflectance, affecting the returned LiDAR signal.

Because severity is measured in relation to the vegetation conditions before the fire event, a pre-fire scenario was simulated for 10 plots representing typical Mediterranean vegetation (Table 2). Further details about vegetation in these plots can be found in Garcia et al. (2010).

Insert Table 2

Field measurements of tree height, diameter at breast height (DBH), crown size and LAI defined the structural characteristics of the overstory vegetation. Likewise, measurements of LAI, height and diameter of shrubs described the understory vegetation. Because tree location was not measured in the field, each individual was randomly set within the plot of 25 m diameter, equivalent to the LVIS footprint. Regarding the optical properties of leaves, reflectance was measured using an ASD Fieldspec® 3 spectroradiometer (Analytical Spectral Devices Inc., Boulder, CO, USA), with a spectral resolution of 2–10 nm in the range of 400–2500 nm. Transmittance values were estimated using Prospect-5D (Féret et al. 2017) for oak leaves and the LIBERTY model (Dawson et al. 1998) for pine needles (see supporting information). For this study we assumed that understory was composed of the same species as the overstory; therefore, the optical properties of the overstory were applied. In addition to leaf properties, FLIGHT requires tree-bark reflectance factor which was measured in the field using an ASD Fieldspec® 3attached to an ASD Plant Probe based on 25 measurements collected over three different individuals (Melendo-Vega et al. 2018). The substrate stratum was modeled as a plane with slope <5° and its optical properties defined by a mixture of soil (≤10%), grass (20-30%) and leaf litter (60-40%). The proportion of soil, grass and litter was set based on our knowledge of the study area of the reference plots used to create the scenarios. Grass and soil reflectance values, measured over a medium-moisture sandy soil, were provided by Melendo-Vega (personal communication, 2019). Leaf litter corresponding to dry leaves and needles of holm oak (*Quercus ilex* L.) and black pine (*Pinus nigra* Arn.) were measured using an ASD FieldSpec® 3 spectroradiometer (see supporting information for more details). Despite measuring the reflectance of each cover in the range of 400-2500 nm, we use here only the 1064 nm wavelength, at which the LVIS sensor operates.

In order to simulate post-fire scenarios representing a wide range of severity levels, CBI values resulting from changes in color and cover for each of the three strata considered were combined in the range [0, 3] at 0.5 step values. Tables 3 and 4 show the relative change of each variable and stratum associated with each CBI value, and their combination to yield the CBI of the understory and overstory strata.

Insert Table 3

Insert Table 4

The substrate stratum of the post-fire scenarios was comprised of soil, charcoal and ash. Bearing in mind the low persistence of the ash signal, which is usually blown away by the wind shortly after the fire, the ash cover was limited to a maximum of 15% of the plot. This would represent a situation of up to a few weeks after a fire, i.e. an initial assessment (Key and Benson 2006). Soil reflectance values were the same for the pre-fire scenario whereas the spectra for charcoal and ash were measured in the field with a GER-2600 spectroradiometer (Geophysical & Environmental Research Corporation, Millbrook, NY) and provided by Chuvieco et al., (personal communication, 2019). The final spectrum for the post-fire substrate layer was a linear combination of the reflectance of the three components weighted by their proportion according to the CBI values as specified in Table 3.

As for the changes in understory and overstory strata the same two variables were considered, PCC and PFA. PCC was simulated as a reduction in the LAI. Based on the reference values of the CBI definition we assigned CBI values of 1, 2 and 3 to relative LAI reductions of 15%, 70% and 100% (Key and Benson 2006), whereas all intermediate values in Table 3 were linearly interpolated. With regards PFA, simulations were realized as a linear combination of green and scorched leaves/needles weighted by their proportion according to the CBI values (Table 3). Although in previous studies the spectral characteristics of scorched leaves were assimilated to senescent leaves (Chuvieco et al. 2007; Chuvieco et al. 2006), in this work we measured the spectra of scorched leaves in the laboratory using an ASD FieldSpec® 3 spectroradiometer attached to a ASD plant probe and leaf clip (Analytical Spectral Devices Inc., Boulder, CO, USA) provided with a low-intensity bulb specially designed for collecting non-destructive data from vegetation and other heat-sensitive targets. Samples of holm oak leaves and black pine needles were scorched to different degrees (see supporting information) and averaged to provide a single post-fire value for holm oak and black pine, respectively. Transmittance values were simulated using leaf level simulation models. Reference values of the CBI definition assigned CBI values of 1, 2 and 3 to relative changes in leaf color of 25%, 80% and 100% respectively (Key and Benson 2006), and intermediate values in Table 3 were obtained by linear interpolation. After the proportion of green and brown leaves was set, FLIGHT distributed them randomly within each tree crown.

Once the variables for each CBI scenario and stratum were defined, they were all combined to represent the CBI at the plot level. Considering the seven scenarios for the substrate and the 49 possibilities for each of the vegetation strata (Tables 3 and 4), 16807 simulated scenarios were possible. However, in order to avoid unrealistic simulations such as high overstory CBI with low understory CBI values, we applied the same set of filters as Chuvieco et al., (2007, 2006 #48): 1) CBI (understory) > CBI (substrate); 2) CBI (understory) > CBI (overstory); 3) CBI (understory) < 4 * CBI (substrate); 4) (PCC-PCC_e) ≤ PCC ≤ (PCC+PCC_e). The last filter was applied to avoid unrealistic combinations of PCC and PFA. PCCe was calculated applying the following equations (Chuvieco et al. 2007):

$$PCC_e = 0.2858 + 0.9188 * PFA, \text{ for the understory} \quad (1)$$

$$PCC_e = 0.0008 + 0.8912 * PFA, \text{ for the overstory} \quad (2)$$

These filters were considered adequate for this study since they were based on field observations carried out in the same study area as the field data used to characterize our plots. After filtering out unrealistic scenarios, 1348 simulations were run for each of the 10 plots considered.

2.3. Derivation of LiDAR metrics to estimate severity

A common pre-processing procedure of the waveform was applied prior to computing the LiDAR metrics from the simulated waveforms for each of the pre- and post-fire scenarios. First, the waveform was smoothed by applying a Gaussian filter with a width size of 5 bins. Second, a background noise threshold was applied to identify the signal beginning and end, that is, the first and last height bins where the returned energy is detected above the noise threshold, thus representing the interaction of the laser with surface elements. Subsequently, we derived a set of metrics previously applied for the estimation of structural attributes of vegetation and to assess forest disturbances and therefore, were expected to capture the changes caused by fire on vegetation. From the total waveform energy, the 1^{st} to 9^{th} deciles of the energy relative to the ground elevation, identified as the last Gaussian peak fitted to the waveform, were computed as well as the 25^{th} and 75^{th} percentiles. The height/median ratio (Drake et al. 2002) was computed and from the canopy height profile (CHP) we derived the quadratic mean canopy height (QMCH), the mean canopy height (MCH), representing the average height of the CHP (Lefsky et al. 1999), and the coefficient of variation of the CHP (Bouvier et al. 2015). García et al., (Garcia et al. 2017a) calculated the canopy waveform from a post-fire LiDAR campaign, and based on a qualitative analysis they observed a very good agreement between this metric and a severity map derived from Landsat data. Nevertheless, they only used the energy reflected by the canopy to compute the metric, thus missing the information from the ground and the vegetation below the height threshold used to separate the canopy. Therefore, in this study we modified the metric to account for the total energy of the waveform to compute the waveform area in order to include all vertical strata affected by the fire. Moreover, since the plot CBI is the average of the CBI values of the strata considered, three in our simulations, we divided the waveform into three parts corresponding to the substrate, the understory and the overstory strata, and the area of each part was calculated. Because the ground signal is convolved with the energy reflected from low vegetation, even for flat surfaces, we applied different height thresholds from 0.3 to 1.2 m at 0.15 intervals, to separate the ground and the understory parts of the signal. Regarding the separation of understory and overstory vegetation, although the CBI establishes a threshold of 5 m, we reduced this threshold to 2 m, based on the characteristics of the vegetation used to model the 10 simulated plots.

2.4. Modeling severity from LiDAR

Severity is estimated as the change occurred relative to the pre-fire conditions, therefore it was estimated from LiDAR data as the relative change of the metrics computed from the pre-fire and post-fire simulated waveforms. Since the post-fire magnitude of the metrics was generally smaller than the pre-fire magnitude, we computed the absolute value of the difference to avoid negative values (eq.3):

$$RC_{LM} = \frac{\left|LM_{post-fire} - LM_{pre-fire}\right|}{LM_{pre-fire}}, \quad (3)$$

where RC_{LM} is the relative change of a given LiDAR metric, and $LM_{pre\text{-}fire}$ and $LM_{post\text{-}fire}$ represent the value of the metric before and after the fire, respectively. In the case of the waveform area relative change (WARC) metric, the relative change of each stratum was derived and the average of the three was computed to provide a plot value; the CBI at the plot level is computed in the same way.

To assess the sensitivity of each metric to severity we computed the Spearman's rank correlation between the relative change of the metrics and the CBI since the variables did not fulfil the assumptions to compute Pearson's correlation coefficient.

2.5. The King Fire case study

The King Fire served to evaluate the potential of the LiDAR metrics to estimate severity over a real scenario. The King Fire started in July 2014 and was controlled in October 2014 burning over 50000 ha in Eldorado National Forest located in the Sierra Nevada Mountain Range, California, U.S. For this site an exceptional set of airborne data were collected (see Stavros et al., (2016) for detailed information on the available dataset) including pre- and post-fire LiDAR. In addition, a field assessment of severity was carried out between November 2014 and January 2015 over 52 plots, 22 of which were located within the pre- and post-fire LiDAR surveys. Plots were positioned using GPS measurements and the ecological damage caused by the fire was assessed using the GeoCBI index. Table 5 shows the characteristics of the available LiDAR data and Fig. 1 shows the study area.

Insert Table 5

Insert Figure 1

Based on the intensity of the returns, the discrete return data was converted into a pseudo-waveform as described in García et al., (2017b). Previously, the intensity was normalized to eliminate the impact of the range on the intensity values as follows (García et al. 2010):

$$I_n = I_{raw} \frac{R}{R_{std}}, \tag{4}$$

where I_n is the normalized intensity, I_{raw} is the intensity value before normalization, R is the range (sensor-target distance) and R_s is the standard range, which was set to 1000 m. This normalization removed the dependence of intensity on the sensor-target distance. However, due to the differences in the sensors used for the pre- and post-fire surveys, such as the radiometric resolution, it was necessary to carry out a between-sensors normalization. We selected 500+ plots over pseudo-invariant features encompassing roads and bare-soil across the study site. The radius of these plots was set to 2 m to avoid including other covers, particularly at the edge of the roads. Consequently, a linear model was fit (Fig. 2) and the pre-fire intensity values were normalized by applying the following equation:

$$I_{sensor\_n} = 1373.6 + 14.479 * I_n, \tag{5}$$

where I_{sensor_n} is the pre-fire sensor intensity normalized to the post-fire sensor and I_n is the range normalized intensity values of the pre-fire data.

Insert Figure 2

After generating the pseudo-waveforms, the set of metrics previously described were derived and their relative change computed. Due to the signal attenuation through the canopy, particularly in areas of dense cover, ground returns can be missed if the amount of energy reflected is lower than the triggering threshold of the sensor, resulting in a smaller amplitude of the ground and understory signal in the pseudo-waveform. After the fire, when the canopy is removed and most of the returns come from the ground, the amplitude of the ground peak can be much larger than that of the pre-fire waveform, despite the lower reflectance of the charcoal. This can result in a relative change > 1, which could result in an overestimation of severity at the plot level; therefore, in these cases the relative change was constrained to 1.

The Spearman's rank correlation between the derived variables and the field measured GeoCBI was computed, and a model was calibrated using a jackknife approach, based on the variable showing the strongest correlation. The model fit was evaluated in terms of its R^2 and the RMSE, and subsequently applied to the part of the study area covered by the pre- and post-fire LiDAR data to generate a LiDAR severity map.

3. Results

3.1. Sensitivity of full waveform LiDAR to severity

The sensitivity of LiDAR waveforms to different degrees of severity was first qualitatively evaluated according to the changes observed in the post-fire waveform relative to the pre-fire one for the different scenarios simulated (Fig. 3).

Insert figure 3.

For the low severity scenario (CBI=1.0; Fig. 3A), only the understory and the substrate are affected. The waveforms show a reduction in the amplitude of the lowest peak as well as a reduction for the understory part of the waveform (enlarged window). It should be noted that part of the effect of the understory change is reflected in the substrate section of the waveform due to the convolution of the ground and the low vegetation energy. The overstory part of the waveform remains unchanged since this stratum was unburned in this scenario. For the first moderate severity scenario (CBI= 2.0; Fig. 3B) a greater difference can be observed between the unburned and the burned signals. The largest effect occurs in the substrate and understory strata, which had a large proportion of charcoal on the ground as well as a large reduction of the understory LAI, with the remaining leaves totally scorched. A smaller change occurred in the overstory given the lower severity of this stratum, with only a small reduction in LAI and partial scorching of the leaves. As expected, the high severity scenario (CBI=2.42; Fig. 3C) showed the largest change in the waveform given the large proportion of charcoal in the substrate as well as the large reduction in LAI for both vegetation strata. The second moderate severity scenario (CBI=1.83; Fig. 3D) demonstrates the sensitivity of the LiDAR waveform to damage due to changes in color, resulting in changes in the spectral reflectance, rather than changes in the vegetation structure. Thus, a smaller amplitude is observed in the upper part of the waveform of the burned scenario, which is the result of a canopy that has been scorched but retains most of its leaves. Likewise, the lower part of waveform showed a significant reduction as result of the substrate charring and the scorching of the understory vegetation.

3.2. LiDAR metrics assessment

LiDAR metrics were computed using different height thresholds to separate the understory from the substrate part of the waveform. The best results were obtained for a 0.45 m height threshold, although differences with a 0.6 m threshold were negligible. Therefore, the results shown throughout the rest of the text correspond to the former threshold. Fig. 4 shows the Spearman's rank correlation coefficient values between the relative change of the metrics derived from the waveforms and the CBI of the simulated scenarios.

Insert figure 4.

The WARC presented the strongest correlation with the CBI values, with a mean Spearman's Rho value of 0.9. This metric also showed a very good consistency among the 10 different simulated plots, with a standard deviation of 0.02 and a range of variation comprised between 0.86 and 0.93. The relative change of the structural metrics commonly derived from LiDAR data showed a moderate correlation with the CBI, with a mean value of approximately 0.55 and a much larger dispersion than the WARC. For instance, the relative height of the 60th percentile of the energy, which was ranked second, showed a mean Spearman's Rho value of 0.56, with a standard deviation of 0.07 and a range of variation between 0.49 and 0.69. A similar behavior was observed for the other structural metrics although negative correlations were found for the lower percentiles, since they just represent the lower part of the signal, i.e. the substrate and the understory layers.

After identifying the best LiDAR-based metric to estimate CBI we fitted a logarithmic model for each of the forest plots simulated (Fig. 5).

Insert figure 5.

The models showed very good performance with a mean R^2 of 0.8 (± 0.05) and values ranging between 0.73 and 0.86. The mean RMSE was 0.22 (± 0.03) and values that varied between 0.18 and 0.26.

3.3. The King Fire case study

Pseudo-waveforms generated from discrete return intensity data also showed ability to discriminate different degrees of severity (Fig. S6-S9, supporting information). Nevertheless, the sensitivity analysis of the LiDAR metrics to the burn severity of the King Fire showed important differences with our previous simulations (Fig. 6). The WARC once again showed the strongest correlation with field measured GeoCBI values (Spearman's Rho = 0.91); however, the structural metrics derived from the pseudo-waveforms showed much stronger correlation than that obtained for the simulated data. Thus, the RH40, the relchp_cv, the RH90, the MCHP and the QMCH yielded a Spearman's Rho value of 0.89, 0.87, 0.86, 0.81 and 0.8, respectively. The weakest correlation was obtained for the HTRT variable, with a Spearman's Rho correlation of 0.19.

Insert figure 6.

The height thresholds used to separate the three strata considered had a significant impact on the estimation of severity from the LiDAR data, obtaining the best results using a height threshold of 0.45 m to separate the understory from the substrate, and a height threshold of 5 m to separate the overstory from the understory strata.

The model fitted (Fig. 7) to the estimate GeoCBI values from the WARC using the jackknife approach was: $GeoCBI = 1.6 * \ln(WARC) + 3.03$, with a standard deviation of the parameters of 0.05 and 0.02, respectively. This model offered an R^2 of 0.78 and a RMSE of 0.37. This model was subsequently applied to the part of the King Fire for which pre- and post-fire LiDAR data were available to produce the LiDAR-based severity map shown in Fig. 8.

Insert figure 7.

Insert figure 8.

The LiDAR data covered the Rubicon Valley, which was characterized by high severity levels (estimated GeoCBI ≥2.25). Moderate severity is observed near the edge of the burn area, as well as the bottom of the valley, and a low severity patch at the north east part of the fire (Fig. 8). The topographic characteristics of the valley, with a concave shape and steep slopes that favored strong winds and fire spread (Coen et al. 2018), explained the high severity observed. Our results show good agreement with the Monitoring Trends in Burn Severity (MTBS) product (Fig. S10, supporting information), downloaded from https://mtbs.gov (last access on 20th February 2020). The MTBS product showed lower severity at the edge of the fire, as well as some larger patches of moderate severity in the north west Rubicon Valley than our LiDAR-based estimates.

4. Discussion

LiDAR metrics showed different degrees of sensitivity to the severity of fires. Our simulation approach represents the first attempt to evaluate the combined effect of different fire impacts, i.e. changes in color and changes in structure, on the LiDAR signal. The relative change of commonly LiDAR derived metrics showed moderate correlation with CBI values. These metrics were proposed for the estimation of important forest structural variables, such as biomass or wood volume (Bouvier et al. 2015; Drake et al. 2002). Therefore, they are more sensitive to fuel consumed than to color changes associated with charred soil and scorched vegetation, related to vegetation mortality induced by fire (Fig. 4). The new metric proposed, WARC, showed the strongest correlation and very high consistency across the different forest plots simulated. It was computed from the energy recorded by the sensor, which in addition to the range, is affected by target reflectance, size, orientation, density and the illuminated area (Korpela et al. 2010). Therefore, the WARC considers not only structural, but also foliage alteration (change in color), although PCC has a higher impact on the signal than the PFA. Despite geometric variables may have a larger influence on intensity than reflectance (Korpela et al. 2010), these variables can also be modified as result of tree scorching, thus affecting the recorded intensity over burned areas. The effect on the LiDAR signal of the change in soil color, as result of charcoal and ash deposition, was evident in the amplitude of the ground peak, showing a clear reduction as the proportion of change in soil color increased. In our simulations the proportion of charcoal, with lower reflectance than the unburned substrate, was much higher than ash, with higher reflectance than the unburned substrate but rather ephemeral, thus reducing the substrate reflectance.

In addition to accounting for the changes in structure and leaf and soil color, the WARC considered all plot strata, computing the changes from the substrate to the upper canopy and averaging at the plot level, in the same way the CBI does. Therefore, the severity estimation based on WARC provides a more comprehensive evaluation than other approaches previously published. For instance, Klauberg et al., (2019) derived a set of crown metrics from airborne LiDAR to classify crown fire severity in a conifer forest. However, they did not assess the damage caused in the understory and substrate layers. Montealegre et al. (2014) found good correlation between field measured CBI values and a set of post-fire LiDAR metrics, which were used to classify burn severity levels. Despite reporting a global accuracy of 85.5%, their results are not comparable to ours since they did not estimate CBI, but classified severity levels into three broad classes. Likewise, Wang and Glenn (2009) classified burn severity levels in sagebrush steppe rangelands based on vegetation height changes obtaining a global accuracy of 84%. While calculating height differences can be useful for sagebrush ecosystems, this metric may not be the most adequate to evaluate severity in forested areas, for instance due to the presence of snags, as suggested by Goetz et al. (2010), and confirmed by our simulation results.

The separation of the strata in the computation of WARC can impact the results and need to be adjusted to the study area. The separation between understory and overstory vegetation was set to 2m for our simulations given the relatively short trees of the simulated plots. For the King Fire with much taller trees, the original 5m thresholds established for the CBI protocol (Key and Benson 2006) yielded better results. Regarding the separation between understory and substrate layers, the 0.45 m threshold worked well for the simulated and the King Fire study site. However, the convolution of the signal is expected to be higher in low severity areas as well as in steep terrain (Harding and Carabajal 2005; Huang et al. 2017). Our simulations considered relatively flat terrain, with slope <5º, reducing the impact of slope on the signal. Therefore, further research is needed to assess the influence of this parameter in the results. In the case of pseudo-waveforms created from discrete return data, although slope can affect ground filtering algorithms (Montealegre et al. 2015), the convolution of ground and understory over steep terrain would be less problematic. Additionally, we assumed the same species for the understory and the overstory layers. This assumption should not significantly affect the results since our approach to estimate severity is based on the relative change of the waveform, this assumption should not affect the results. Lamelas et al., (2019) reported the impact of scan angle on fuel type classification using the spectral angle mapper (SAM) classifier over an LVIS LiDAR signature library created from simulated waveforms. Although these authors found scan angle an important source of error in the classification, it was probably due to the large scan angles tested up to 20º, beyond the scan-angle limit of the LVIS sensor (https://lvis.gsfc.nasa.gov/Home/instrumentdetails.html; last access on 14th March 2020), and the sensitivity of the SAM algorithm to even small changes in the shape of the waveform. We tested the impact of off-nadir observations, up to 8º (Hancock et al. 2019; table 1), on the metrics and found no consistent bias on most of them. Correlation between the nadir and off-nadir metrics remained above 0.9 for all metrics but RH25, RH20, RH10 and HTRT. In the case of WARC, correlation was higher than 0.99. These results agrees with Hancock et al. (2019), who also found no impact of scan angles less than 8º on the metrics derived from simulated LVIS waveforms.

We run the FLIGHT model in forward mode to evaluate the sensitivity of full waveform LiDAR to a wide range of severity levels (Fig. 5). Inversion of the FLIGHT radiative transfer model has been applied for the estimation of forest structural parameters from LiDAR waveforms (Bye et al. 2017), so a similar approach should be possible for the retrieval of severity. Other studies already applied an RTM inversion to directly retrieve CBI values but from multispectral data (Chuvieco et al. 2007; De Santis et al. 2010).

The King Fire case study has its limitations to test the robustness of the metrics since the LiDAR data has different pre- and post-fire survey configurations and sensors and the data were not full waveform. This issues require further research to draw more definitive conclusions. Nevertheless, the application of the WARC metric to the King Fire, with different vegetation characteristics than those of our simulated plots, showed the robustness and generalization capabilities of this metric to estimate severity. The availability of pre- and post-fire LiDAR data along with concomitant field measures of the GeoCBI, makes it a unique dataset to evaluate the potential of LiDAR data for the assessment of fire severity.

Furthermore, it also allows to demonstrate the possibility of applying the method to the more frequent airborne LiDAR discrete return data by generating pseudo-waveforms.

Contrary to the simulation results, structural metrics showed almost the same sensitivity as the WARC for the King Fire, most probably due to large fuel amounts consumed by the fire (Coen et al. 2018). Although structural metrics have shown significant differences between burned and unburned areas in boreal forests (Goetz et al. 2010; Wulder et al. 2009), and can be useful to evaluate specific impacts of fires, such as biomass consumed, the ability of these metrics to provide an integrated measure of severity, such as the CBI or the GeoCBI, which also accounts for tree mortality, may be limited. Moreover, our approach is based on a single simple metric, increasing its generalization capability, as opposed to previous studies that included multiple metrics. The WARC consistency for both, the simulated data as well as the King Fire case study, indicate the potential for the broad applicability of this metric. Recently, Hu et al. (2019) also proposed a single metric to estimate burn severity from LiDAR data. The performance of this metric was evaluated against changes in LAI, canopy cover and tree height, but not against field measures of CBI or GeoCBI. Their metric shows similarities to WARC, as it is based on the change in the area of the height percentile profile (PAC), but their metric is computed from the height distribution of returns and thus only account for changes in structure. Contrary, WARC is derived from the intensity, which is affected by the radiometric changes resulting from the modification in soil and leaf color. A comprehensive comparison between PAC and WARC was not feasible over our simulated scenarios since PAC can only be derived from discrete return data. However, we tested PAC over the King Fire and found poorer performance compared to WARC, with R^2= 0.55 and RMSE= 0.53.

The capabilities of the WARC were evaluated against integrated measures of severity, the CBI and the GeoCBI. However, it has the potential for evaluating specific fire effects, for instance biomass consumption (Garcia et al. 2017a), to be later introduced into a single integrated severity index as Morgan et al. (2014) propose.

The model fitted to estimate GeoCBI values from the WARC offered good performance (R^2=0.78 and RMSE=0.37) but there is still room for improvement. The use of the same sensor with identical system settings and the same survey configuration for the pre- and post-fire acquisitions would reduce the noise in the intensity data. In addition, we used a simple radiometric normalization of the intensity data to remove the effect of range variation across the study area produced by rough topography and the different flight height of the two LiDAR datasets. Better intensity normalization would help to improve our results reducing the noise of the intensity values used to generate the pseudo-waveforms. More robust normalization approaches have been proposed in the literature including an exponent factor to the range ratio to account for energy attenuation through the canopy, as well as a parameter to account for the automatic gain control (Gatziolis 2011; Korpela et al. 2010). However, the available data did not allow the application of such normalization methods. Moreover, our between-sensor calibration model was derived from non-vegetated surfaces characterized by single returns. Therefore, its application to other types of returns (2^{th} – 4^{th}) may not be optimum. Despite this, the noise introduced in this group of returns by our between-sensor calibration is expected to be small, since the improvement in consistency of intensity values after normalization is less substantial in 2^{nd} and subsequent returns than for 1^{st} and single returns (Gatziolis 2011).

The severity map derived using the WARC metric showed good agreement with the MTBS Landsat-based map, but showed some overestimation over the north west part of the Rubicon Valley. Although a thorough comparison between the LiDAR and Landsat-products is out of the scope of our study, differences between the two products could be explained by the different acquisition time of the post-fire LiDAR and Landsat data. The LiDAR data was collected shortly after the fire, thus representing an initial severity assessment. Meanwhile, the Landsat image was acquired nearly a year after the fire and so, it corresponded to an extended assessment, which could be influenced by vegetation recovery processes. Moreover, the inability of Landsat data to capture fire damage to the understory and substrate, particularly under unaffected dense canopies, can result in higher uncertainties in moderate severity areas (Chuvieco et al. 2007; Miller and Quayle 2015), contributing also to the differences between the two products.

Our method requires having pre- and post-fire LiDAR data, which is a constraint given the limited spatial and temporal coverage of airborne LiDAR sensors. The method is potentially applicable to the recently launched Global Ecosystem Dynamics Investigation (GEDI) sensor onboard the International Space Station (Dubayah et al. 2014; Stysley et al. 2016). The sampling scheme should be taken into account, as it will not provide co-registered footprints. In such a case, an object-based approach could be applied by comparing typical average pre- and post-fire waveforms for each object. Additionally, integration of LiDAR and optical data (Klauberg et al. 2019; Kwak et al. 2010) could improve the assessment of fire caused damage by exploiting the synergy of the structural and the functional information derived from LiDAR and multispectral data, respectively.

5. Conclusions

The potential of LiDAR data to perform comprehensive evaluations of the severity of wildfires has been evaluated. A new metric is proposed, WARC, which accounts for the changes in all strata. Whereas previous studies using LiDAR just focused on the structural changes caused by fires in vegetation, we have demonstrated that LiDAR was able to capture severity beyond structural changes, as it is also sensitive to leaf scorching, which is related to tree mortality, and soil color changes.

The 3D FLIGHT radiative transfer model run in a forward mode enabled the evaluation of the sensitivity of LiDAR metrics to the severity of fires over a large range of severity levels. Our results demonstrated that common LiDAR metrics, which were developed for vegetation modeling, are less appropriate to estimate the fire severity than WARC.

Application of the WARC metric to the real case study of the King Fire, California, with very different vegetation characteristics of those of our simulated plots, revealed the robustness and generalization capability of this metric. Although improvement over the best performing common LiDAR metrics was small in this case, the WARC still outperformed them.

The potential of LiDAR data to estimate severity as measured by integrated indices such as the CBI and the GeoCBI was evaluated; yet, it can also be applied to assess specific fire effects that can be subsequently used in integrated evaluations of severity of wildfires.

Acknowledgements

This work was partially supported by the Marie Curie International Outgoing Fellowship within the 7th European Community Framework Programme (ForeStMap—3D Forest Structure Monitoring and Mapping, Project Reference: 629376). The contents of this paper reflect solely the authors' views and not those of the European Commission. LiDAR data for the King Fire was provided by the JPL Airborne Snow Observatory. We greatly appreciate the constructive comments by the four anonymous reviewers, who greatly helped improve the manuscript.

References

Alonzo, M., Morton, D.C., Cook, B.D., Andersen, H.-E., Babcock, C., & Pattison, R. (2017). Patterns of canopy and surface layer consumption in a boreal forest fire from repeat airborne LiDAR. *Environmental Research Letters, 12*, 065004

Blair, J.B., Rabine, D.L., & Hofton, M.A. (1999). The laser vegetation imaging sensor: A medium-altitude, digitisation-only, airborne laser altimeter for mapping vegetation and topography. *ISPRS Journal of Photogrammetry and Remote Sensing, 54,* 115-122

Boer, M.M., Macfarlane, C., Norris, J., Sadler, R.J., Wallace, J., & Grierson, P.F. (2008). Mapping burned areas and burn severity patterns in SW Australian eucalypt forest using remotely-sensed changes in leaf area index. *Remote Sensing of Environment, 112*, 4358-4369

Bond, W.J., Woodward, F.I., & Midgley, G.F. (2005). The global distribution of ecosystems in a world without fire. *New Phytologist, 165,* 525-538

Bouvier, M., Durrieu, S., Fournier, R.A., & Renaud, J.-P. (2015). Generalizing predictive models of forest inventory attributes using an area-based approach with airborne LiDAR data. *Remote Sensing of Environment, 156*, 322-334

Bye, I.J., North, P.R.J., Los, S.O., Kljun, N., Rosette, J.A.B., Hopkinson, C., Chasmer, L., & Mahoney, C. (2017). Estimating forest canopy parameters from satellite waveform LiDAR by inversion of the FLIGHT three-dimensional radiative transfer model. *Remote Sensing of Environment, 188*, 177-189

Casas, Á., García, M., Siegel, R.B., Koltunov, A., Ramírez, C., & Ustin, S. (2016). Burned forest characterization at single-tree level with airborne laser scanning for assessing wildlife habitat. *Remote Sensing of Environment, 175*, 231-241

Coen, J.L., Stavros, E.N., & Fites-Kaufman, J.A. (2018). Deconstructing the King megafire. *Ecological Applications, 28*, 1565-1580

Chen, B., Pang, Y., Li, Z., Lu, H., North, M.P., Rosette, J.A.B., & Yan, M. (2020). Forest signal detection for photon counting LiDAR using Random Forest. *Remote Sensing Letters, 11*, 37-46

Chuvieco, E., De Santis, A., Riaño, D., & Halligan, K. (2007). Simulation Approaches for Burn Severity Estimation Using Remotely Sensed Images. *Fire Ecology, 3*, 129-150

Chuvieco, E., Martínez, S., Román, M.V., Hantson, S., & Pettinari, M.L. (2014). Integration of ecological and socio-economic factors to assess global vulnerability to wildfire. *Global Ecology and Biogeography, 23*, 245-258

Chuvieco, E., Riaño, D., Danson, F.M., & Martin, P. (2006). Use of a radiative transfer model to simulate the postfire spectral response to burn severity. *Journal of Geophysical Research: Biogeosciences, 111*

Dawson, T.P., Curran, P.J., & Plummer, S.E. (1998). LIBERTY—Modeling the Effects of Leaf Biochemical Concentration on Reflectance Spectra. *Remote Sensing of Environment*, *65*, 50-60

De Santis, A., Asner, G.P., Vaughan, P.J., & Knapp, D.E. (2010). Mapping burn severity and burning efficiency in California using simulation models and Landsat imagery. *Remote Sensing of Environment*, *114*, 1535-1545

De Santis, A., & Chuvieco, E. (2007). Burn severity estimation from remotely sensed data: Performance of simulation versus empirical models. *Remote Sensing of Environment, 108*, 422-435

De Santis, A., & Chuvieco, E. (2009). GeoCBI: A modified version of the Composite Burn Index for the initial assessment of the short-term burn severity from remotely sensed data. *Remote Sensing of Environment*, *113*, 554-562

Disney, M.I., Kalogirou, V., Lewis, P., Prieto-Blanco, A., Hancock, S., & Pfeifer, M. (2010). Simulating the impact of discrete-return lidar system and survey characteristics over young conifer and broadleaf forests. *Remote Sensing of Environment*, *114*, 1546-1560

Disney, M.I., Lewis, P., Gomez-Dans, J., Roy, D., Wooster, M.J., & Lajas, D. (2011). 3D radiative transfer modelling of fire impacts on a two-layer savanna system. *Remote Sensing of Environment, 115*, 1866-1881

Drake, J.B., Dubayah, R.O., Knox, R.G., Clark, D.B., & Blair, J.B. (2002). Sensitivity of large-footprint lidar to canopy structure and biomass in a neotropical rainforest. *Remote Sensing of Environment*, *81*, 378-392

Dubayah, R., Goetz, S.J., Blair, J.B., Fatoyinbo, T., Hansen, M., Healey, S., Hofton, M.A., Hurtt, G., Kellner, J., luthcke, S., & Swatantran, A. (2014). The global ecosystem dynamics investigation. In. AGU Fall Meeting, San Francisco, California, U.S.

Féret, J.B., Gitelson, A.A., Noble, S.D., & Jacquemoud, S. (2017). PROSPECT-D: Towards modeling leaf optical properties through a complete lifecycle. *Remote Sensing of Environment, 193*, 204-215

Fowler, C.T. (2003). Human Health Impacts of Forest Fires in the Southern United States: A Literature Review. *Journal of Ecological Anthropology, 7*, 39-63

French, N.H.F., Kasischke, E.S., Hall, R.J., Murphy, K.A., Verbyla, D.L., Hoy, E.E., & Allen, J.L. (2008). Using Landsat data to assess fire and burn severity in the North American boreal forest region: an overview and summary of results. *International Journal of Wildland Fire, 17*, 443-462

García, M., Riaño, D., Chuvieco, E., & Danson, F.M. (2010). Estimating biomass carbon stocks for a Mediterranean forest in Spain using height and intensity LiDAR data. *Remote Sensing of Environment, 114*, 816-830

Garcia, M., Saatchi, S., Casas, A., Koltunov, A., Ustin, S., Ramirez, C., Garcia-Gutierrez, J., & Balzter, H. (2017a). Quantifying biomass consumption and carbon release from the California Rim fire by integrating airborne LiDAR and Landsat OLI data. *Journal of Geophysical Research: Biogeosciences*, n/a-n/a

García, M., Saatchi, S., Casas, A., Koltunov, A., Ustin, S.L., Ramirez, C., & Balzter, H. (2017b). Extrapolating Forest Canopy Fuel Properties in the California Rim Fire by Combining Airborne LiDAR and Landsat OLI Data. *Remote Sensing, 9*, 394

Gatziolis, D. (2011). Dynamic Range-based Intensity Normalization for Airborne, Discrete Return Lidar Data of Forest Canopies. *Photogrammetric Engineering & Remote Sensing, 77*, 251-259

Goetz, S.J., Sun, M., Baccini, A., & Beck, P.S.A. (2010). Synergistic use of spaceborne lidar and optical imagery for assessing forest disturbance: An Alaska case study. *Journal of Geophysical Research: Biogeosciences, 115*

Hancock, S., Armston, J., Hofton, M., Sun, X., Tang, H., Duncanson, L.I., Kellner, J.R., & Dubayah, R. (2019). The GEDI Simulator: A Large-Footprint Waveform Lidar Simulator for Calibration and Validation of Spaceborne Missions. *Earth and Space Science, 6*, 294-310

Harding, D.J., & Carabajal, C.C. (2005). ICESat waveform measurements of within-footprint topographic relief and vegetation vertical structure. *Geophysical Research Letters, 32*

Hood, S.M., Varner, J.M., van Mantgem, P., & Cansler, C.A. (2018). Fire and tree death: understanding and improving modeling of fire-induced tree mortality. *Environmental Research Letters, 13*, 113004

Hu, T., Ma, Q., Su, Y., Battles, J.J., Collins, B.M., Stephens, S.L., Kelly, M., & Guo, Q. (2019). A simple and integrated approach for fire severity assessment using bi-temporal airborne LiDAR data. *International Journal of Applied Earth Observation and Geoinformation, 78*, 25-38

Huang, H., Liu, C., Wang, X., Biging, G.S., Chen, Y., Yang, J., & Gong, P. (2017). Mapping vegetation heights in China using slope correction ICESat data, SRTM, MODIS-derived and climate data. *ISPRS Journal of Photogrammetry and Remote Sensing, 129,* 189-199

Jain, T., Graham, R., & Pilliod, D. (2004). Tongue-tied: confused meanings for common fire terminology can lead to fuels mismanagement. *Wildfire, July/August*, 22-26

Jakubuaskas, M.E., Lulla, K.P., & Mausel, P.W. (1990). Assessment of vegetation change in a fire-altered forest landscapes. *Photogrammetric Engineering and Remote Sensing, 56*, 371-377

Keeley, J.E. (2009). Fire intensity, fire severity and burn severity: a brief review and suggested usage. *International Journal of Wildland Fire, 18,* 116-126

Key, C.H., & Benson, N.C. (2006). Landscape Assessment: Ground measure of severity, the Composite Burn Index; and Remote sensing of severity, the Normalized Burn Ratio. In D.C. Lutes, R.E. Keane, J.F. Caratti, C.H. Key, N.C. Benson, S. Sutherland, & L.J. Gangi (Eds.). In D.C. Lutes; R.E. Keane; J.F. Caratti; C.H. Key; N.C. Benson; S. Sutherland; and L.J. Gangi. 2006. FIREMON: Fire Effects Monitoring and Inventory System. USDA Forest Service, Rocky Mountain Research Station, Ogden, UT. Gen. Tech. Rep. RMRS-GTR-164-CD: LA 1-51.

Klauberg, C., Hudak, A.T., Silva, C.A., Lewis, S.A., Robichaud, P.R., & Jain, T.B. (2019). Characterizing fire effects on conifers at tree level from airborne laser scanning and high-resolution, multispectral satellite data. *Ecological Modelling, 412*, 108820

Korpela, I., Ørka, H.O., Hyyppä, J., Heikkinen, V., & Tokola, T. (2010). Range and AGC normalization in airborne discrete-return LiDAR intensity data for forest canopies. *ISPRS Journal of Photogrammetry and Remote Sensing, 65*, 369-379

Kwak, D.A., Chung, J., Lee, W.K., Kafatos, M., Lee, S.Y., Cho, H.K., & Lee, S.H. (2010). Evaluation for Damaged Degree of Vegetation by Forest Fire using LiDAR and Digital Aerial Photograph. *Photogrammetric Engineering and Remote Sensing, 76*, 277-287

Lamelas-Gracia, M.T., Riaño, D., & Ustin, S. (2019). A LiDAR signature library simulated from 3-dimensional Discrete Anisotropic Radiative Transfer (DART) model to classify fuel types using spectral matching algorithms. *GIScience & Remote Sensing, 56*, 988-1023

Landmann, T. (2003). Characterizing sub-pixel Landsat ETM+ fire severity on experimental fires in the Kruger National Park, South Africa : research letter. *South African Journal of Science, 99*, 357-360

Lefsky, M.A., Cohen, W.B., Acker, S.A., Parker, G.G., Spies, T.A., & Harding, D. (1999). Lidar Remote Sensing of the Canopy Structure and Biophysical Properties of Douglas-Fir Western Hemlock Forests. *Remote Sensing of Environment, 70*, 339-361

Lentile, L.B., Holden, Z.A., Smith, A.M.S., Falkowski, M.J., Hudak, A.T., Morgan, P., Lewis, S.A., Gessler, P.E., & Benson, N.C. (2006). Remote sensing techniques to assess active fire characteristics and post-fire effects. *International Journal of Wildland Fire, 15*, 319-345

Lewis, S.A., Wu, J.Q., & Robichaud, P.R. (2006). Assessing burn severity and comparing soil water repellency, Hayman Fire, Colorado. *Hydrological Processes, 20*, 1-16

Lim, K., Treitz, P., Wulder, M., St-Onge, B., & Flood, M. (2003). LiDAR remote sensing of forest structure. *Progress in Physical Geography, 27*, 88-106

McCarley, T.R., Kolden, C.A., Vaillant, N.M., Hudak, A.T., Smith, A.M.S., Wing, B.M., Kellogg, B.S., & Kreitler, J. (2017). Multi-temporal LiDAR and Landsat quantification of fire-induced changes to forest structure. *Remote Sensing of Environment, 191*, 419-432

Melendo-Vega, J.R., Martín, M.P., Pacheco-Labrador, J., González-Cascón, R., Moreno, G., Pérez, F., Migliavacca, M., García, M., North, P., & Riaño, D. (2018). Improving the Performance of 3-D Radiative Transfer Model FLIGHT to Simulate Optical Properties of a Tree-Grass Ecosystem. *Remote Sensing, 10*, 2061

Miller, J.D., Knapp, E.E., Key, C.H., Skinner, C.N., Isbell, C.J., Creasy, R.M., & Sherlock, J.W. (2009). Calibration and validation of the relative differenced Normalized Burn Ratio (RdNBR) to three measures of fire severity in the Sierra Nevada and Klamath Mountains, California, USA. *Remote Sensing of Environment, 113*, 645-656

Miller, J.D., & Quayle, B. (2015). Calibration and validation of inmediate post-fire satellite-derived data to three severity metrics. *Fire Ecology, 11*, 12-30

Miller, J.D., & Thode, A.E. (2007). Quantifying burn severity in a heterogeneous landscape with a relative version of the delta Normalized Burn Ratio (dNBR). *Remote Sensing of Environment, 109*, 66-80

Montealegre, A., Lamelas, M., Tanase, M., & de la Riva, J. (2014). Forest Fire Severity Assessment Using ALS Data in a Mediterranean Environment. *Remote Sensing, 6*, 4240

Montealegre, A.L., Lamelas, M.T., & Riva, J.d.l. (2015). A Comparison of Open-Source LiDAR Filtering Algorithms in a Mediterranean Forest Environment. *IEEE Journal of Selected Topics in Applied Earth Observations and Remote Sensing, 8*, 4072-4085

Montesano, P.M., Rosette, J.A.B., Sun, G., North, M.P., Nelson, R.F., Dubayah, R.O., Ranson, K.J., & Kharuk, V. (2015). The uncertainty of biomass estimates from modeled ICESat-2 returns across a boreal forest gradient. *Remote Sensing of Environment*, *158*, 95-109

Morgan, P., Keane, R.E., Dillon, G.K., Jain, T.B., Hudak, A.T., Karau, E.C., Sikkink, P.G., Holden, Z.A., & Strand, E.K. (2014). Challenges of assessing fire and burn severity using field measures, remote sensing and modelling. *International Journal of Wildland Fire, 23*, 1045-1060

Morton, D.C., Nagol, J., Carabajal, C.C., Rosette, J., Palace, M., Cook, B.D., Vermote, E.F., Harding, D.J., & North, P.R.J. (2014). Amazon forests maintain consistent canopy structure and greenness during the dry season. *Nature, 506*, 221-224

Neary, D.G., Klopatek, C.C., DeBano, L.F., & Ffolliott, P.F. (1999). Fire effects on belowground sustainability: a review and synthesis. *Forest Ecology and Management, 122*, 51-71

Nikonovas, T., North, P.R.J., & Doerr, S.H. (2017). Particulate emissions from large North American wildfires estimated using a new top-down method. *Atmospheric Chemistry and Physics, 17*, 6423-6434

North, P.R.J. (1996). Three-dimensional forest light interaction model using a Monte Carlo method. *IEEE Transactions on Geoscience and Remote Sensing, 34*, 946-956

North, P.R.J., Rosette, J.A.B., Suárez, J.C., & Los, S.O. (2010). A Monte Carlo radiative transfer model of satellite waveform LiDAR. *International Journal of Remote Sensing, 31*, 1343-1358

Reddy, A.D., Hawbaker, T.J., Wurster, F., Zhu, Z., Ward, S., Newcomb, D., & Murray, R. (2015). Quantifying soil carbon loss and uncertainty from a peatland wildfire using multi-temporal LiDAR. *Remote Sensing of Environment, 170*, 306-316

Rosette, J., North, P.R.J., Rubio-Gil, J., Cook, B., Los, S., Suarez, J., Sun, G., Ranson, J., & Blair, J.B. (2013). Evaluating Prospects for Improved Forest Parameter Retrieval From Satellite LiDAR Using a Physically-Based Radiative Transfer Model. *IEEE Journal of Selected Topics in Applied Earth Observations and Remote Sensing, 6*, 45-53

Stavros, E.N., Tane, Z., Kane, V.R., Veraverbeke, S., McGaughey, R.J., Lutz, J.A., Ramirez, C., & Schimel, D. (2016). Unprecedented remote sensing data over King and Rim megafires in the Sierra Nevada Mountains of California. *Ecology, 97*, 3244-3244

Stephens, S.L., Agee, J.K., Fulé, P.Z., North, M.P., Romme, W.H., Swetnam, T.W., & Turner, M.G. (2013). Managing Forests and Fire in Changing Climates. *Science, 342*, 41-42

Stysley, P.R., Coyle, D.B., Clarke, G.B., Frese, E., Blalock, G., Morey, P., Kay, R.B., Poulios, D., & Hersh, M. (2016). *Laser production for NASA's Global Ecosystem Dynamics Investigation (GEDI) lidar*. SPIE

van der Werf, G.R., Randerson, J.T., Giglio, L., Collatz, G.J., Mu, M., Kasibhatla, P.S., Morton, D.C., DeFries, R.S., Jin, Y., & van Leeuwen, T.T. (2010). Global fire emissions and the contribution of deforestation, savanna, forest, agricultural, and peat fires (1997–2009). *Atmospheric Chemistry and Physics, 10*, 11707-11735

Viana-Soto, A., Aguado, I., & Martínez, S. (2017). Assessment of Post-Fire Vegetation Recovery Using Fire Severity and Geographical Data in the Mediterranean Region (Spain). *Environments, 4*

Wang, C., & Glenn, N.F. (2009). Estimation of fire severity using pre- and post-fire LiDAR data in sagebrush steppe rangelands. *International Journal of Wildland Fire, 18*, 848-856

Whitman, E., Parisien, M.-A., Thompson, D.K., Hall, R.J., Skakun, R.S., & Flannigan, M.D. (2018). Variability and drivers of burn severity in the northwestern Canadian boreal forest. *Ecosphere, 9,* e02128

Whittier, T.R., & Gray, A.N. (2016). Tree mortality based fire severity classification for forest inventories: A Pacific Northwest national forests example. *Forest Ecology and Management, 359*, 199-209

Wing, B.M., Ritchie, M.W., Boston, K., Cohen, W.B., & Olsen, M.J. (2015). Individual snag detection using neighborhood attribute filtered airborne lidar data. *Remote Sensing of Environment, 163*, 165-179

Wulder, M.A., White, J.C., Alvarez, F., Han, T., Rogan, J., & Hawkes, B. (2009). Characterizing boreal forest wildfire with multi-temporal Landsat and LIDAR data. *Remote Sensing of Environment, 113,* 1540-1555

Parameter	Description	Unit	Value
X_0,Y_0,Z_0	Sensor position relative to the center of the scene	m	0, 0, 10000
θ_0,ϕ_0	Sensor azimuth and zenith angle	deg	0, 0
β	Half width angle of beam divergence	mrad	1
β_{FOV}	FOV divergence half angle	mrad	1,9
ω	Half pulse duration at relative power	ns	7
E_t	Pulse energy	mJ	5
Δ_t	Recording bin width	ns	1

Table 1. FLIGHT LiDAR sensor model parameters corresponding to the LVIS sensor.

Plot	Main vegetation type	Understory		Overstory		Stand density (trees/ha)
		mean height (m)	LAI (m^2/m^2)	mean height (m)	LAI (m^2/m^2)	
1	*Quecus ilex L.; Pinus nigra Arn.*	0.55	1.18	4.75	1.63	224
2	*Pinus nigra Arn.*	0.89	0.82	7.24	3.16	160
3	*Pinus nigra Arn.*	0.78	1.17	12.95	6.34	320
4	*Pinus nigra Arn.*	1.12	0.48	7.00	3.11	496
5	*Quecus ilex L.; Pinus nigra Arn.*	1.57	0.21	6.79	3.78	416
6	*Pinus nigra Arn.*	2.90	1.29	7.08	4.8	608
7	*Quecus ilex L.; Pinus nigra Arn.*	0.98	2.53	6.89	3.65	208
8	*Quecus ilex L.; Pinus nigra Arn.*	1.19 (0.77)	3.1	6.81	2.37	304
9	*Pinus nigra Arn.*	1.35 (1.21)	1.9	7.03	3.02	288
10	*Quecus ilex L.; Pinus nigra Arn.*	0.91 (0.48)	1.5	5.85	3.74	192

Table 2. Characteristics of the vegetation of the study area used to model the forest plots.

Substrate		Understory and Overstory	
CBI	% change in color	PFA (% of brown leaves)	PCC (% LAI reduction)
0	0	0	0
0.5	5	12.5	7.5
1	10	25	15
1.5	25	52.5	42.5
2	40	80	70
2.5	60	95	85
3	80	100	100

Table 3: Relative change of the variables assessed associated with each CBI value simulated.

		CBI-Percentage of Foliage Altered						
CBI-Percentage of Cover Change		**0**	**0.5**	**1**	**1.5**	**2**	**2.5**	**3**
	0	0	0.25	0.5	0.75	1	1.25	1.5
	0.5	0.25	0.5	0.75	1	1.25	1.5	1.75
	1	0.5	0.75	1	1.25	1.5	1.75	2
	1.5	0.75	1	1.25	1.5	1.75	2	2.25
	2	1	1.25	1.5	1.75	2	2.25	2.5
	2.5	1.25	1.5	1.75	2	2.25	2.5	2.75
	3	1.5	1.75	2	2.25	2.5	2.75	3

Table 4: CBI values resulting from the combination of the percentage of cover change and foliage altered for the vegetation strata.

Sensor	Survey Date	Flight height (m)	Scan angle (˚)	Point density (p/m^2)
Optech Gemini	1-7 November 2012	600-800	14	7.3
Riegl Q1560	13-14 January 2015	2100	30	9.9

Table 5. Characteristics of the airborne LiDAR data available for the King Fire.

Figure 1. Location of the study area. Enlarged window: King Fire perimeter. Background: Landsat-OLI post-fire image (25th January 2015) RGB: SWIR, NIR, Red.

Figure 2. Scatter plot of pre-fire intensity values after the between-sensors normalization and the post-fire intensity for the pseudo-invariant features. The black dashed line represents the fit line. The gray solid line represents the Y=X line.

Figure 3. Waveform examples for different severity scenarios. A) Low severity scenario in which only the substrate and understory layers are affected by the fire. B) Moderate severity scenario with high severity for the substrate and understory layers and a slightly affected overstory. C) High severity scenario with high fire damage for all layers. D) Moderate severity scenario in which the main effect on vegetation layers is a change in soil and leaf color.

Figure 4. Spearman's rank correlation coefficient between CBI and the relative change of the waveform derived metrics. Error bars represent ±1 standard deviation.

Figure 5. Scatter plots of CBI vs WARC values and fitted logarithmic models for each of the 10 forest plots simulated.

Figure 6. Spearman's rank correlation coefficient between field measured GeoCBI and the relative change of the pseudo-waveform derived metrics for the King Fire.

Figure 7. Scatter plot of GeoCBI vs WARC values and fitted logarithmic model for the King Fire case study.

Figure 8. Severity map of the King Fire derived from the WARC model using pre- and post-fire airborne LiDAR data.

Fig. 1

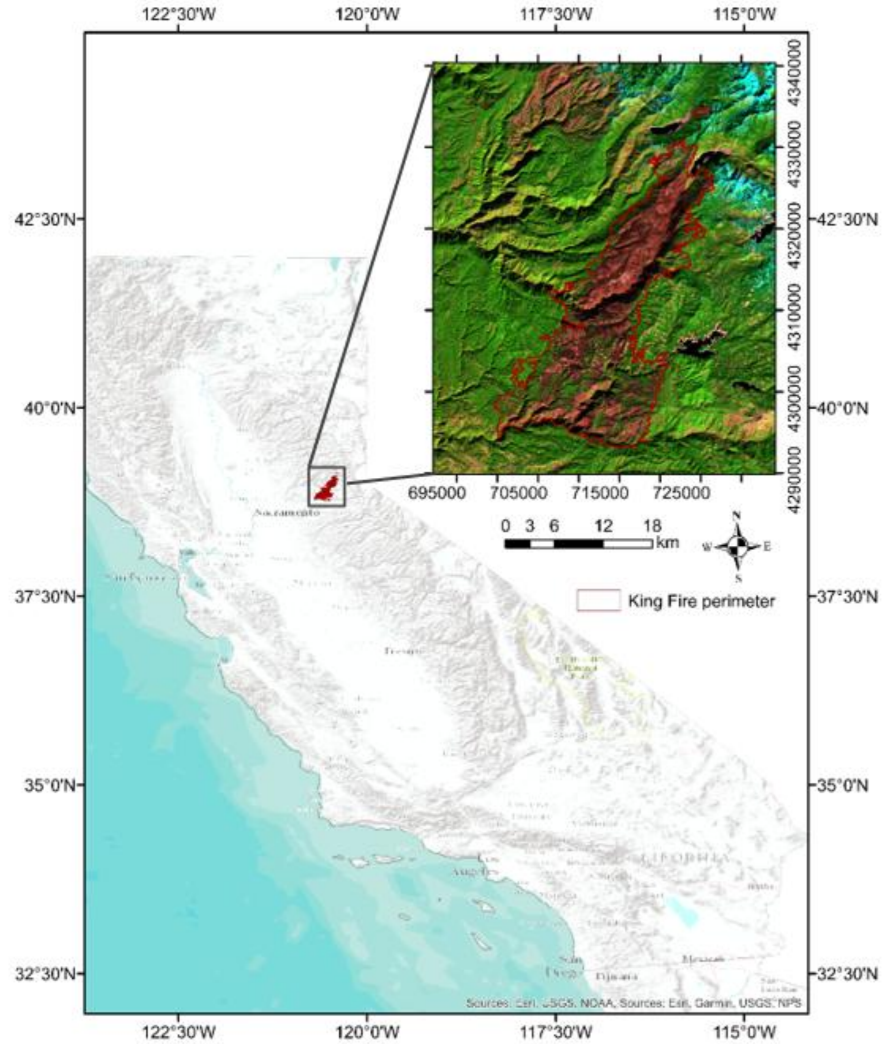
122°30'W
120°0'W
117°30'W
115°0'W
42°30'N
40°0'N
37°30'N
35°0'N
32°30'N
4340000
4330000
4320000
4310000
4300000
4290000
695000
705000
715000
725000
0 3 6 12 18
km
N
W
E
S
King Fire perimeter
Sacramento
Sources: Esri, USGS, NOAA, Sources: Esri, Garmin, USGS, NPS

Fig. 2

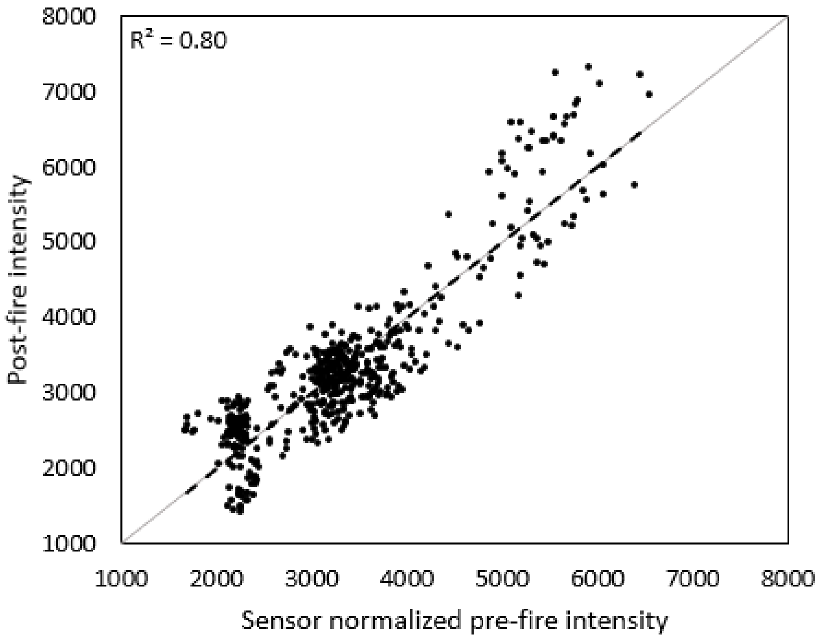

R^2 = 0.80
Post-fire intensity
Sensor normalized pre-fire intensity
8000
7000
6000
5000
4000
3000
2000
1000
1000
2000
3000
4000
5000
6000
7000
8000

Fig. 3

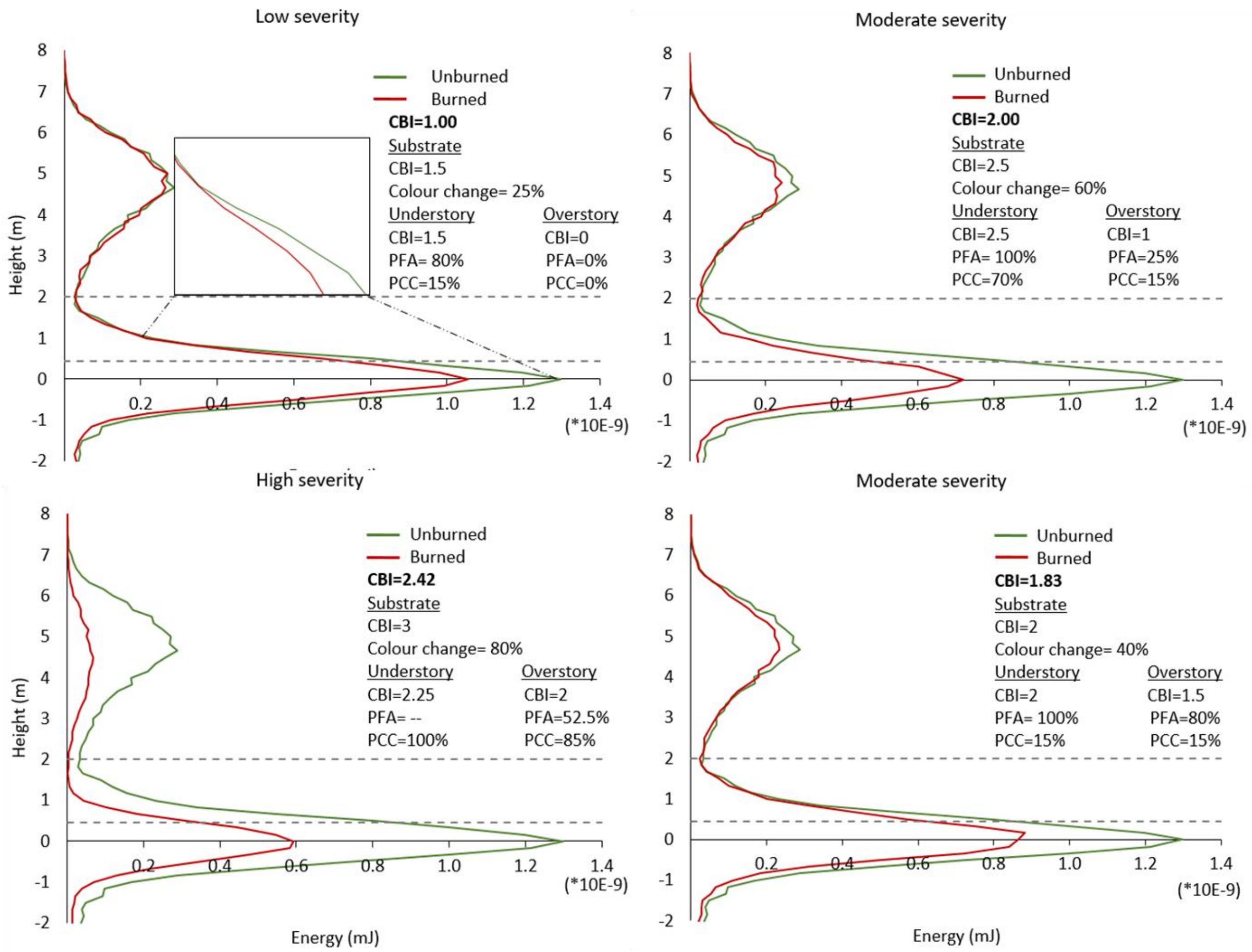
Low severity
Unburned
Burned
CBI=1.00
Substrate
CBI=1.5
Colour change= 25%
Understory
CBI=1.5
PFA= 80%
PCC=15%
Overstory
CBI=0
PFA=0%
PCC=0%
Moderate severity
Unburned
Burned
CBI=2.00
Substrate
CBI=2.5
Colour change= 60%
Understory
CBI=2.5
PFA= 100%
PCC=70%
Overstory
CBI=1
PFA=25%
PCC=15%
High severity
Unburned
Burned
CBI=2.42
Substrate
CBI=3
Colour change= 80%
Understory
CBI=2.25
PFA= --
PCC=100%
Overstory
CBI=2
PFA=52.5%
PCC=85%
Moderate severity
Unburned
Burned
CBI=1.83
Substrate
CBI=2
Colour change= 40%
Understory
CBI=2
PFA= 100%
PCC=15%
Overstory
CBI=1.5
PFA=80%
PCC=15%
Height (m)
Energy (mJ)
(*10E-9)

Fig. 4

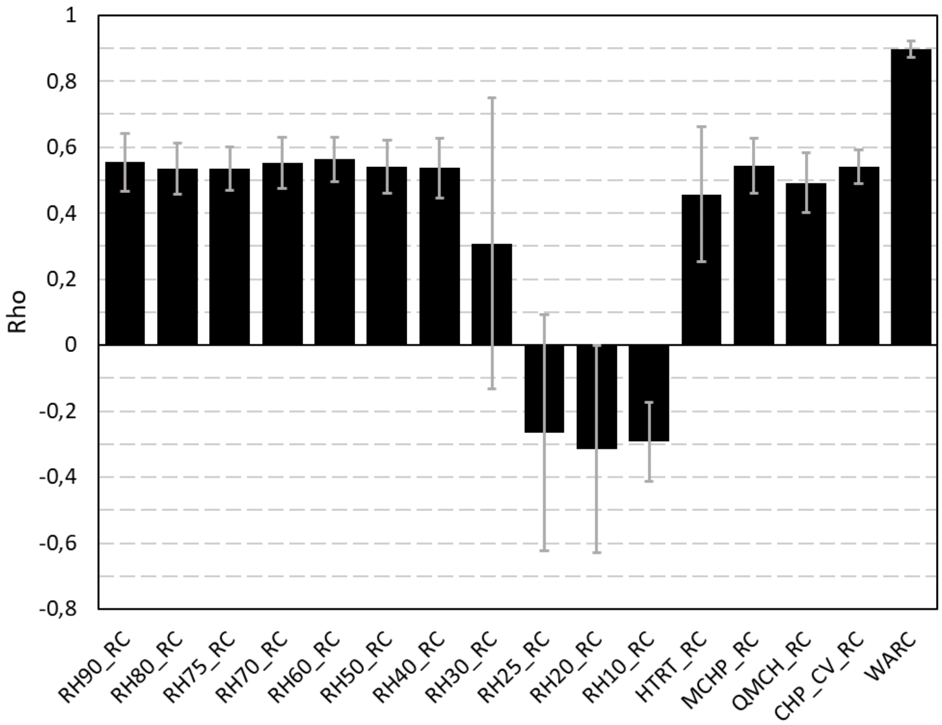

1
0,8
0,6
0,4
0,2
0
-0,2
-0,4
-0,6
-0,8
Rho
RH90_RC
RH80_RC
RH75_RC
RH70_RC
RH60_RC
RH50_RC
RH40_RC
RH30_RC
RH25_RC
RH20_RC
RH10_RC
HTRT_RC
MCHP_RC
QMCH_RC
CHP_CV_RC
WARC

Fig. 5

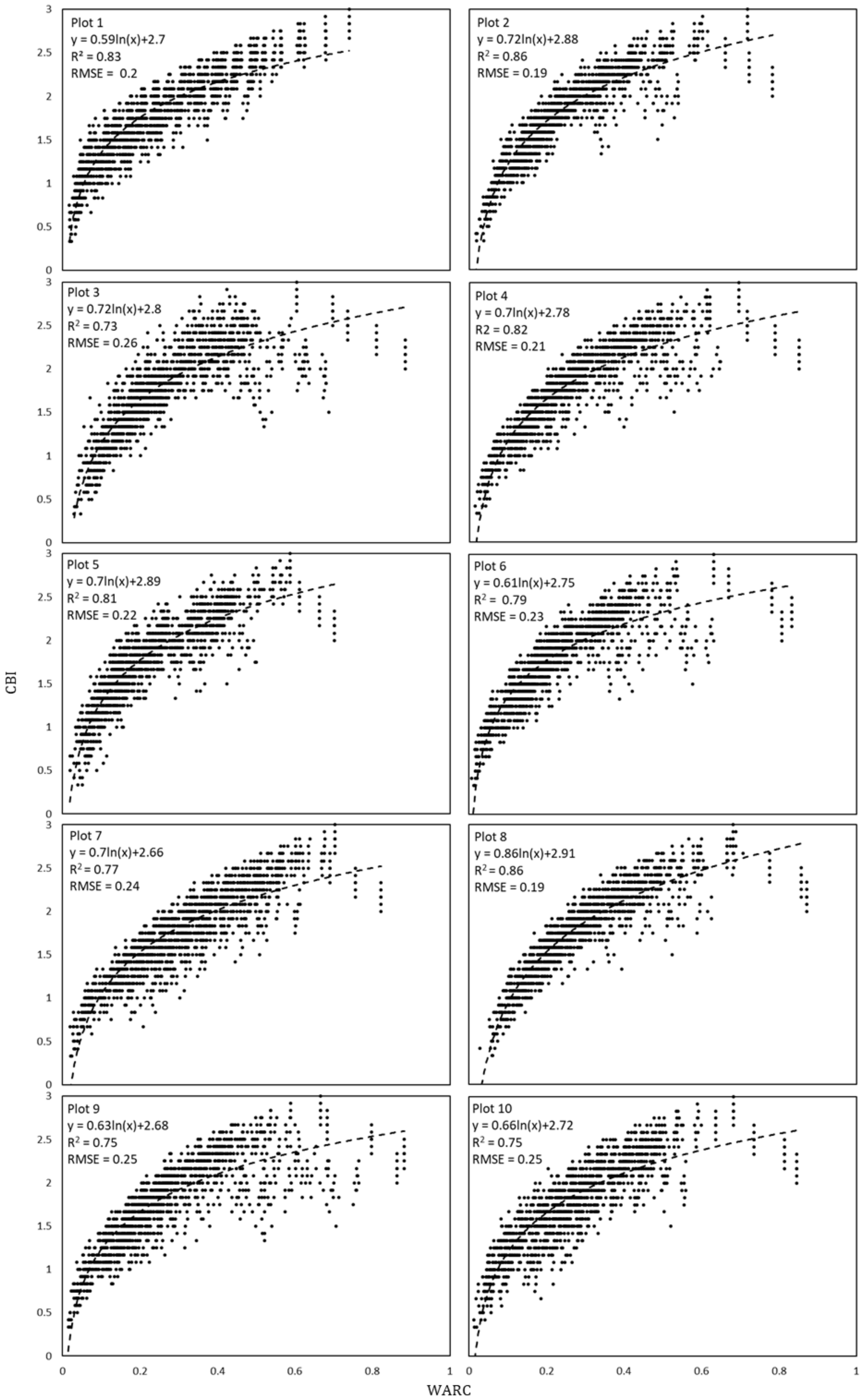

Plot 1
y = 0.59ln(x)+2.7
R² = 0.83
RMSE = 0.2
Plot 2
y = 0.72ln(x)+2.88
R² = 0.86
RMSE = 0.19
Plot 3
y = 0.72ln(x)+2.8
R² = 0.73
RMSE = 0.26
Plot 4
y = 0.7ln(x)+2.78
R2 = 0.82
RMSE = 0.21
Plot 5
y = 0.7ln(x)+2.89
R² = 0.81
RMSE = 0.22
Plot 6
y = 0.61ln(x)+2.75
R² = 0.79
RMSE = 0.23
Plot 7
y = 0.7ln(x)+2.66
R² = 0.77
RMSE = 0.24
Plot 8
y = 0.86ln(x)+2.91
R² = 0.86
RMSE = 0.19
Plot 9
y = 0.63ln(x)+2.68
R² = 0.75
RMSE = 0.25
Plot 10
y = 0.66ln(x)+2.72
R² = 0.75
RMSE = 0.25
CBI
WARC

Fig. 6

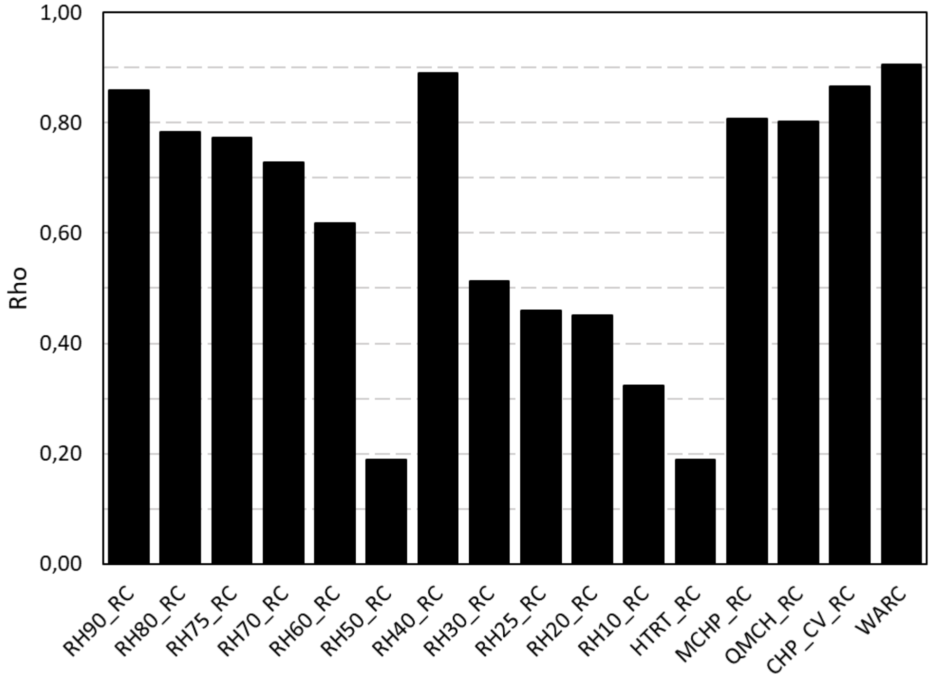

1,00
0,80
0,60
0,40
0,20
0,00
Rho
RH90_RC
RH80_RC
RH75_RC
RH70_RC
RH60_RC
RH50_RC
RH40_RC
RH30_RC
RH25_RC
RH20_RC
RH10_RC
HTRT_RC
MCHP_RC
QMCH_RC
CHP_CV_RC
WARC

Fig 7.

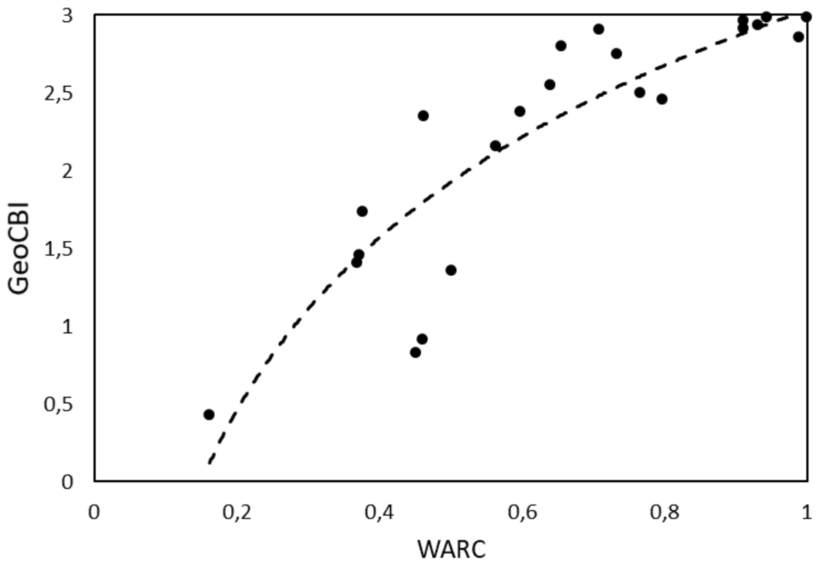

Fig. 8

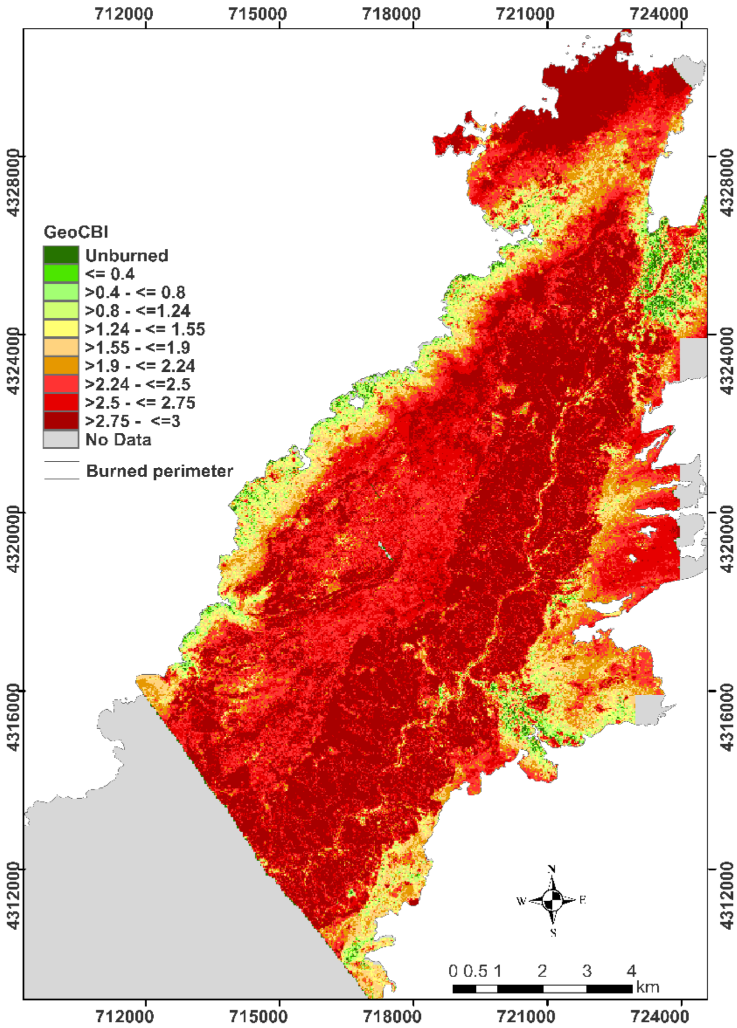
712000
715000
718000
721000
724000
4328000
4324000
4320000
4316000
4312000
GeoCBI
Unburned
<= 0.4
>0.4 - <= 0.8
>0.8 - <=1.24
>1.24 - <= 1.55
>1.55 - <=1.9
>1.9 - <= 2.24
>2.24 - <=2.5
>2.5 - <= 2.75
>2.75 - <=3
No Data
Burned perimeter
N
W
E
S
0 0.5 1 2 3 4
km

Supporting information

Click here to download Supplementary Data: Supporting_Information.pdf

***Credit Author Statement**

Mariano García: conceptualization, methodology, software, validation, formal analysis, investigation, writing - original Draft,

Peter North: methodology, software, validation, writing - review & editing

Alba Viana-Soto: validation, formal analysis, writing - review & editing

Natasha E. Stavros: investigation, resources, writing - review & editing

Jackie Rosette: validation, writing - review & editing

M. Pilar Martín: investigation, resources, validation, writing - review & editing

Magí Franquesa: investigation, writing - review & editing

Rosario González-Cascón: investigation, resources, validation, writing - review & editing

David Riaño: investigation, formal analysis, writing - review & editing

Javier Becerra: investigation, writing - review & editing

Kaiguang Zhao: writing - review & editing

***Declaration of Interest Statement**

Declaration of interests

☒ The authors declare that they have no known competing financial interests or personal relationships that could have appeared to influence the work reported in this paper.

☐The authors declare the following financial interests/personal relationships which may be considered as potential competing interests: